

Álvaro Filipe Alves Magalhães

Yicathins B and C: synthesis and *in silico* ADME properties.

Dissertation presented to the
Faculdade de Farmácia da Universidade
do Porto, to obtain the degree of Master in
Pharmaceutical Chemistry.

Work developed under the scientific supervision of Professor Carlos Afonso and
Professor Carlos Azevedo.



October, 2017

DE ACORDO COM A LEGISLAÇÃO EM VIGOR, NÃO É PERMITIDA A REPRODUÇÃO DE QUALQUER PARTE DESTA DISSERTAÇÃO.

IN ACCORDANCE WITH THE APPLICABLE LAW, IT IS NOT ALLOWED TO REPRODUCE ANY PART OF THIS THESIS.

Advisor

Carlos Afonso

Prof. Dr. Carlos Afonso

Co-advisor

Carlos Azevedo

Dr. Carlos Azevedo

Master Course Director

Madalena M.M. Pinto

Prof. Dra. Madalena Pinto

This research was developed under the project PTDC/ MAR-BIO/4694/2014 (reference POCI-01-0145-FEDER-016790) supported through national funds provided by FCT – Foundation for Science and Technology and European Regional Development Fund (ERDF) through the COMPETE – Programa Operacional Factores de Competitividade (POFC) programme and the Project 3599 – Promover a Produção Científica e Desenvolvimento Tecnológico e a Constituição de Redes Temáticas (3599-PPCDT)



AUTHOR'S DECLARATION

Under the terms of the Decree-Law n^o 216/92, of October 13th, it is hereby declared that the author afforded a major contribution to the conceptual design and technical execution of the work and interpretation of the results included in this dissertation. Under the terms of the referred Decree-Law, it is hereby declared that the following articles/communications were prepared in the scope of this dissertation.

The results presented in this thesis are part of the following scientific communications:

Poster communication:

A. F. Magalhães, J. Soares, D. Loureiro, J. Pinto, S. Cravo, C. Azevedo, C. Afonso, M. Pinto; Routes to benzophenones: exploration of two different synthetic pathways. 10th Meeting of Young Researchers of University of Porto (IJUP17), Porto, Portugal, February 8-10, **2017**.

AGRADECIMENTOS

Ao Professor Doutor Carlos Afonso, meu orientador, pela grande oportunidade de fazer parte deste trabalho e assim desenvolver a minha dissertação de mestrado. Pelo transmitir de todo o conhecimento científico, paciência e preocupação. Sem dúvida nenhuma que me orientou sempre para o melhor caminho e fico imensamente grato.

Ao Doutor Carlos Azevedo, meu co-orientador, que, apesar da distância, sempre esteve disponível para ajudar, para guiar-me e tirar dúvidas. Fico muito grato pela ótima orientação e pelo conhecimento científico que me passou durante estes últimos dois anos.

À Professora Doutora Madalena Pinto, diretora do Laboratório de Química Orgânica e Farmacêutica e diretora do Mestrado em Química Farmacêutica, do qual faço parte, pela maravilhosa oportunidade de continuar o meu percurso académico e científico nesta faculdade, num mestrado que me permite desenvolver um trabalho movido pela paixão pela área.

Ao Mestre José Soares, por toda a maravilhosa orientação durante o meu percurso neste mestrado. Por todas as conversas, debates, dúvidas tiradas, pelo enriquecimento científico que me proporcionou. Por toda a amizade desenvolvida durante este ano, pela preocupação e pela paciência, um sincero obrigado.

À Dr.^a Sara Cravo, por todo o apoio dado durante o desenvolvimento deste trabalho. Por toda a experiência transmitida, por todo o passar de conhecimento que proporcionou, por todos os debates que permitiram o meu enriquecer científico. Também por toda a amizade, paciência e preocupação demonstradas ao longo deste ano.

Ao apoio técnico dado pela Liliana e pela Gisela. Pela vontade de ajudar, pelos jogos de voleibol e, sobretudo, pela amizade criada!

Ao Professor Doutor Artur Silva e ao Dr. Hilário Tavares pela aquisição dos espetros de RMN e pelo esforço e dedicação que permitiu a caracterização dos compostos sintetizados.

Aos meus colegas e amigos do laboratório, em especial os que iniciaram o mestrado comigo, mas também os que desenvolvi amizade quando lá comecei a trabalhar. À Daniela e à Joana, pelo acompanhamento e ajuda, pelo companheirismo e sentimento de entreatajuda criado, pela nossa amizade, obrigado!

Aos meus amigos, em especial ao João, pela grande amizade já desde há 5 anos, à Mariana, que iniciou este percurso comigo, após termos partilhado também 3 anos de licenciatura, e ao Filipe, por todo o apoio, pessoal e técnico, e pela amizade.

Aos meus pais, ao meu irmão e à minha avó, por todo o carinho incondicional, todo o apoio dado, toda a preocupação e por acreditarem em mim e nas minhas capacidades.

Muito obrigado a todos!

RESUMO

Embora existam muitos fármacos disponíveis para tratar as doenças infecciosas, a realidade mostra que, com o surgimento de resistências aos quimioterápicos e o aparecimento de novos agentes infecciosos, a procura de outros agentes antimicrobianos continua a suscitar o maior interesse.

A Natureza sempre serviu como fonte de novas substâncias ativas. As plantas, que, sendo organismos terrestres se encontram mais facilmente disponíveis para os investigadores, têm sido ampla e sistematicamente estudadas. Pelo contrário, o mar, apesar de constituir o maior reservatório da Natureza, foi durante muito tempo ignorado. Contudo, com o desenvolvimento tecnológico, os produtos marinhos estão mais facilmente ao alcance dos pesquisadores, pelo que a procura de substâncias farmacologicamente ativas com origem no mar tem aumentado drasticamente, proporcionando novos *hits* e *leads* muito promissores para o desenvolvimento de novos fármacos. Além disso, é relevante o facto dos seres marinhos estarem sujeitos a condições muitas vezes extremas e distintas das dos seres terrestres, levando a processos biossintéticos diferentes, que conduzem a substâncias inovadoras e muito promissoras sob o ponto de vista terapêutico.

Em 2012, foram descobertas duas novas xantonas, as hicasinas B e C, no fungo *Aspergillus wentii*, que vive em simbiose com a alga *Gymnogongrus flabelliformis*, que mostraram possuir potencial atividade anti-infecciosa. No entanto, estas xantonas são produzidas em pequenas quantidades na natureza, sendo necessária a sua síntese laboratorial para poderem ser obtidas em quantidades significativas, de modo a serem melhor estudadas e poderem ser introduzidas num processo de planeamento e desenvolvimento de novos fármacos.

Neste trabalho apresenta-se a síntese total das hicasinas B e C, bem como de dois análogos estruturais. Todas as substâncias sintetizadas foram purificadas e as estruturas estabelecidas por métodos espectrométricos. Deste processo, resultaram ainda quatro intermediários, duas benzofenonas e duas xantonas, cujo potencial farmacológico poderá revelar-se de interesse. No total, foram obtidas oito substâncias que têm como bases moleculares estruturas privilegiadas em Química Farmacêutica.

Neste trabalho, mostram-se também as propriedades biofísico-químicas (log P e log D, pKa, solubilidade, permeabilidade e ligação às proteínas plasmáticas), obtidas *in silico*, das oito substâncias referidas.

PALAVRAS-CHAVE

Xantonas marinhas; Síntese total; Hicasinas; Atividade anti-infecciosa ; Propriedades biofísico-químicas.

ABSTRACT

Even though there are a lot of drugs available for the treatment of infectious diseases, reality shows that, in light of the emergence of resistances to chemotherapeutics and the appearance of new infectious agents, the search for other antimicrobial agents remains of great interest.

Nature has always been a source of new active substances. Being terrestrial organisms which, for that very reason, are most easily found and within reach of researchers, plants have been exhaustively studied. On the contrary, the sea was ignored for too long, in spite of the fact that it is Nature's biggest reservoir. However, as a consequence of the technological development, marine products are now much more reachable to researchers, reason why the seek for sea-based pharmacological active substances has been drastically increasing, allowing new hits and leads truly promising for the development of new drugs. Besides, it is not less important the fact that the sea life is very often subject to extreme conditions, way different from those onshore, originating different biosynthetic pathways, eventually leading to new and promising substances, from a therapeutic point of view.

In 2012, two new xanthenes were discovered, yicathins B and C, on fungus *Aspergillus wentii*, which lives in symbiosis with algae *Gymnogongrus flabelliformis*, that revealed some anti-infectious activity potential. Nevertheless, these xanthenes are produced in small quantities in Nature, making it necessary its laboratorial synthesis in order to be obtained in significant quantities and, afterwards, to be studied and then introduced in a new drugs planning and development process.

In this work, it is presented the full synthesis of yicathins B and C and also of two structural analogues. All synthesized substances were purified and their structures established by spectrometric methods. Out of this process, four intermediates stemmed too, two benzophenones and two xanthenes, whose pharmacological potential may be interesting. In total, eight substances were obtained, each one with molecular scaffold having privileged structures in Pharmaceutical Chemistry.

Also in this work, the biophysicochemical properties (log P and log D, pKa, solubility, permeation and plasma proteins binding), obtained *in silico*, of the eight abovementioned substances are shown.

KEYWORDS

Marine xanthenes; Total synthesis; Yicathins; Anti-infectious activity; Biophysicochemical properties.

INDEX:

AUTHOR'S DECLARATION	VII
AGRADECIMENTOS	IX
RESUMO	XI
PALAVRAS-CHAVE	XI
ABSTRACT	XIII
KEYWORDS	XIII
INDEX:	XV
FIGURE INDEX:	XIX
SCHEME INDEX:.....	XXI
TABLE INDEX:	XXIII
LIST OF ABBREVIATIONS AND SYMBOLS	XXV
OUTLINE OF THE DISSERTATION	XXVII
1. Introduction	1
1.1. The constant need for new drugs	3
1.2. Sources of new drugs	5
1.2.1. Marine environment as a drugs source	6
1.3. Drug discovery	7
1.4. Biophysicochemical properties	9
1.4.1. Lipophilicity	9
1.4.2. Solubility.....	10
1.4.3. pKa	10
1.4.4. Permeability	10
1.4.5. Plasma protein binding	11
1.5. Synthesis of xanthenes	12
1.5.1. <i>Via</i> one step synthesis.....	12
1.5.2. <i>Via</i> benzophenone	13
1.5.3. <i>Via</i> diaryl ether	15
1.5.4. <i>Via</i> chromen-4-ones.....	16
2. Aims	17
3. Experimental	21
3.1. General methods.	23
3.2. Synthesis of building block A.	25
3.2.1. Synthesis of (4-bromo-3,5-dimethoxyphenyl)methanol (2).....	25
3.2.2. Synthesis of ((4-bromo-3,5-dimethoxybenzyl)oxy)(tert-butyl)dimethylsilane (3).	26

3.3.	Synthesis of building block B.	27
3.3.1.	Synthesis of 1,3-bis(methoxymethoxy)-5-methylbenzene (5).	27
3.3.2.	Synthesis of 2,6-bis(methoxymethoxy)-4-methylbenzaldehyde (6). .	28
3.4.	Synthesis of building block C.	29
3.4.1.	Synthesis of methyl 2,6-bis(methoxymethoxy)-4-methylbenzoate (8).....	29
3.5.	Synthesis of building block D.....	30
3.5.1.	Synthesis of 1,3-bis(methoxymethoxy)benzene (10).	30
3.5.2.	Synthesis of 2,6-bis(methoxymethoxy)benzaldehyde (11).	31
3.6.	Synthesis of building block E.	32
3.6.1.	Synthesis of methyl 2,6-dihydroxybenzoate (13).	32
3.6.2.	Synthesis of methyl 2,6-bis(methoxymethoxy)benzoate (14).	33
3.7.	Synthesis of Yicathins C and B.	34
3.7.1.	Synthesis of (2,6-bis(methoxymethoxy)-4-methylphenyl)(4-(((tert-butyl)dimethylsilyl)oxy)methyl)-2,6-dimethoxyphenyl)methanol (15).	34
3.7.2.	Synthesis of (2,6-bis(methoxymethoxy)-4-methylphenyl)(4-(((tert-butyl)dimethylsilyl)oxy)methyl)-2,6-dimethoxyphenyl)methanone (16).	35
3.7.3.	Synthesis of (2,6-dihydroxy-4-methylphenyl)(4-(hydroxymethyl)-2,6-dimethoxyphenyl)methanone (17).	37
3.7.4.	Synthesis of 1-hydroxy-6-(hydroxymethyl)-8-methoxy-3-methyl-9H-xanthen-9-one (18).	38
3.7.5.	Synthesis of 8-hydroxy-1-methoxy-6-methyl-9-oxo-9H-xanthene-3-carboxylic acid - Yicathin C (19).	39
3.7.6.	Synthesis of methyl 8-hydroxy-1-methoxy-6-methyl-9-oxo-9H-xanthene-3-carboxylate - Yicathin B (20).	41
3.8.	Synthesis of Analogues C and B.	42
3.8.1.	Synthesis of (2,6-bis(methoxymethoxy)phenyl)(4-(((tert-butyl)dimethylsilyl)oxy)methyl)-2,6-dimethoxyphenyl)methanol (21).	42
3.8.2.	Synthesis of (2,6-bis(methoxymethoxy)phenyl)(4-(((tert-butyl)dimethylsilyl)oxy)methyl)-2,6-dimethoxyphenyl)methanone (22).	43
3.8.3.	Synthesis of (2,6-dihydroxyphenyl)(4-(hydroxymethyl)-2,6-dimethoxyphenyl)methanone (23).	45
3.8.4.	Synthesis of 8-hydroxy-3-(hydroxymethyl)-1-methoxy-9H-xanthen-9-one (24).	46
3.8.5.	Synthesis of 8-hydroxy-1-methoxy-9-oxo-9H-xanthene-3-carboxylic acid - Analogue C (25).	47

3.8.6. Synthesis of methyl 8-hydroxy-1-methoxy-9-oxo-9H-xanthene-3-carboxylate - Analogue B (26).....	48
4. Results and Discussion.....	49
4.1. Synthesis.....	51
4.1.1. Retrosynthesis and designing the synthetic process	51
4.1.2. Synthesis of Building Blocks.....	55
4.1.2.1. Synthesis of building block A.....	55
4.1.2.1.1. Synthesis of (4-bromo-3,5-dimethoxyphenyl)methanol (2)..	55
4.1.2.1.2. Synthesis of ((4-bromo-3,5-dimethoxybenzyl)oxy)(tert-butyl)dimethylsilane (3).....	56
4.1.2.2. Synthesis of building block B.	57
4.1.2.2.1. Synthesis of 1,3-bis(methoxymethoxy)-5-methylbenzene (5).....	57
4.1.2.2.2. Synthesis of 2,6-bis(methoxymethoxy)-4-methylbenzaldehyde (6).....	58
4.1.2.3. Synthesis of building block C.	59
4.1.2.3.1. Synthesis of methyl 2,6-bis(methoxymethoxy)-4-methylbenzoate (8).	59
4.1.2.4. Synthesis of building block D.....	60
4.1.2.4.1. Synthesis of 1,3-bis(methoxymethoxy)benzene (10).....	60
4.1.2.4.2. Synthesis of 2,6-bis(methoxymethoxy)benzaldehyde (11)....	61
4.1.2.5. Synthesis of building block E	61
4.1.2.5.1. Synthesis of methyl 2,6-dihydroxybenzoate (13).....	61
4.1.2.5.2. Synthesis of methyl 2,6-bis(methoxymethoxy)benzoate (14).....	63
4.1.3. Synthesis of Yicanthins B and C.....	64
4.1.3.1. Synthesis of (2,6-bis(methoxymethoxy)-4-methylphenyl)(4-(((tert-butyl)dimethylsilyl)oxy)methyl)-2,6-dimethoxyphenyl)methanol (15).....	64
4.1.3.2. Synthesis of (2,6-bis(methoxymethoxy)-4-methylphenyl)(4-(((tert-butyl)dimethylsilyl)oxy)methyl)-2,6-dimethoxyphenyl)methanone (16)....	67
4.1.3.2.1. <i>Via</i> oxidation of diarylmethanol (15).....	67
4.1.3.2.2. <i>Via</i> reaction of building block A with building block C.	69
4.1.3.3. Synthesis of (2,6-dihydroxy-4-methylphenyl)(4-(hydroxymethyl)-2,6-dimethoxyphenyl)methanone (17).....	69
4.1.3.4. Synthesis of 1-hydroxy-6-(hydroxymethyl)-8-methoxy-3-methyl-9H-xanthen-9-one (18).....	71

4.1.3.5. Synthesis of 8-hydroxy-1-methoxy-6-methyl-9-oxo-9H-xanthene-3-carboxylic acid - Yicathin C (19).....	72
4.1.3.6. Synthesis of methyl 8-hydroxy-1-methoxy-6-methyl-9-oxo-9H-xanthene-3-carboxylate - Yicathin B (20).....	74
4.1.4. Synthesis of Analogues B and C.....	76
4.1.4.1. Synthesis of (2,6-bis(methoxymethoxy)phenyl)(4-(((tert-butyl)dimethylsilyl)oxy)methyl)-2,6-dimethoxyphenyl)methanol (21).	76
4.1.4.2. Synthesis of 2,6-bis(methoxymethoxy)phenyl)(4-(((tert-butyl)dimethylsilyl)oxy)methyl)-2,6-dimethoxyphenyl)methanone (22).....	78
4.1.4.2.1. Via oxidation of diarylmethanol (21).....	78
4.1.4.2.2. Via reaction of building block A with building block E.	79
4.1.4.3. Synthesis of (2,6-dihydroxyphenyl)(4-(hydroxymethyl)-2,6-dimethoxyphenyl)methanone (23).....	80
4.1.4.4. Synthesis of 8-hydroxy-3-(hydroxymethyl)-1-methoxy-9H-xanthen-9-one (24).....	81
4.1.4.5. Synthesis of 8-hydroxy-1-methoxy-9-oxo-9H-xanthene-3-carboxylic acid - Analogue C (25).....	82
4.1.4.6. Synthesis of methyl 8-hydroxy-1-methoxy-9-oxo-9H-xanthene-3-carboxylate - Analogue B (26).	84
4.2. <i>In silico</i> biophysicochemical properties.....	87
4.2.1. Lipophilicity	87
4.2.2. pKa	90
4.2.3. Solubility	91
4.2.4. Permeability.....	93
4.2.5. Plasma protein binding.....	94
4.2.1. Guidelines for the prediction of general drug-likeness for oral bioavailability	94
5. Conclusions.....	97
6. References.....	101
7. Appendix.....	109
7.1. Appendix 1: NMR spectra for compounds 8 and 14 – 26.....	111
7.2. Appendix 2: General table with <i>in silico</i> acquired biophysicochemical properties of the eight compounds of interest.	125

FIGURE INDEX:

Figure 1: Comparison between the top 10 causes of death in 2000 and 2015.....	3
Figure 2: Comparison of sources of drugs in 1994 versus 2014.....	5
Figure 3: Structures of Yicathins B and C.....	6
Figure 4: Multidimensional optimization.....	8
Figure 5: General procedure for the determination of permeability.....	11
Figure 6: Main connectivities in HMBC spectrum for compound 8	59
Figure 7: Main connectivities in HMBC spectrum for compound 13	62
Figure 8: Main connectivities in HMBC spectrum for compound 14	63
Figure 9: Main connectivities in HMBC spectrum for compound 15	65
Figure 10: Principal fragments from EIMS.	68
Figure 11: Main connectivities in HMBC spectrum for compound 16	68
Figure 12: Main connectivities in HMBC spectrum for compound 17	70
Figure 13: Main connectivities in HMBC spectrum for compound 18	71
Figure 14: Main connectivities in HMBC spectrum for compound 19	73
Figure 15: Main connectivities in HMBC spectrum for compound 20	75
Figure 16: Principal fragments from EIMS.....	76
Figure 17: Main connectivities in HMBC spectrum for compound 21	77
Figure 18: Main connectivities in HMBC spectrum for compound 22	79
Figure 19: Main connectivities in HMBC spectrum for compound 23	80
Figure 20: Main connectivities in HMBC spectrum for compound 24	82
Figure 21: Main connectivities in HMBC spectrum for compound 25	83
Figure 22: Main connectivities in HMBC spectrum for compound 26	84
Figure 23: Synthetized compounds in study.	87
Figure 24: Representation of the variation of values for compound 19	89
Figure 25: ¹ H NMR of compound 8	111
Figure 26: ¹³ C NMR of compound 8	111
Figure 27: ¹ H NMR of compound 14	112
Figure 28: ¹³ C NMR of compound 14	112
Figure 29: ¹ H NMR of compound 15	113
Figure 30: ¹³ C NMR of compound 15	113
Figure 31: ¹ H NMR of compound 16	114
Figure 32: ¹³ C NMR of compound 16	114
Figure 33: ¹ H NMR of compound 17	115
Figure 34: ¹³ C NMR of compound 17	115
Figure 35: ¹ H NMR of compound 18	116

Figure 36: ^{13}C NMR of compound 18	116
Figure 37: ^1H NMR of compound 19	117
Figure 38: ^{13}C NMR of compound 19	117
Figure 39: ^1H NMR of compound 20	118
Figure 40: ^{13}C NMR of compound 20	118
Figure 41: ^1H NMR of compound 21	119
Figure 42: ^{13}C NMR of compound 21	119
Figure 43: ^1H NMR of compound 22	120
Figure 44: ^{13}C NMR of compound 22	120
Figure 45: ^1H NMR of compound 23	121
Figure 46: ^{13}C NMR of compound 23	121
Figure 47: ^1H NMR of compound 24	122
Figure 48: ^{13}C NMR of compound 24	122
Figure 49: ^1H NMR of compound 25	123
Figure 50: ^{13}C NMR of compound 25	123
Figure 51: ^1H NMR of compound 26	124
Figure 52: ^{13}C NMR of compound 26	124

SCHEME INDEX:

Scheme 1: Drug discovery pipeline .	7
Scheme 2: Commonly used pathways in the synthesis of xanthenes.....	12
Scheme 3: Main approaches for one step synthesis of xanthenes.	13
Scheme 4: Common approaches in the synthesis of benzophenones intermediates.....	14
Scheme 5: Common approaches in the cyclization of benzophenones.....	14
Scheme 6: Common approaches for the synthesis of diaryl ethers.....	15
Scheme 7: Common approaches for the cyclization of diaryl ethers.....	15
Scheme 8: Examples of xanthone synthesis vis chromen-4-one.....	16
Scheme 9: Retrosynthetic analysis from the previous work.	51
Scheme 10: Work developed by the fellow colleague.	52
Scheme 11: Retrosynthetic plan for the synthesis of Yicathins and respective analogues.	53
Scheme 12: Synthetic plan followed in this dissertation.	54
Scheme 13: Reduction of 4-Bromo-3,5-dimethoxybenzoic acid.	55
Scheme 14: Protection of (4-Bromo-3,5-dimethoxyphenyl)methanol.....	56
Scheme 15: Protection of orcinol.....	57
Scheme 16: Formylation of 1,3-bis(methoxymethoxy)-5-methylbenzene.	58
Scheme 17: Directed ortho-metalation mechanism.....	58
Scheme 18: Protection of methyl 2,6-dihydroxy-4-methylbenzoate.....	59
Scheme 19: Protection of resorcinol.....	60
Scheme 20: Formylation of 1,3-bis(methoxymethoxy)benzene.....	61
Scheme 21: O-Methylation of 2,6-dihydroxybenzoic acid.....	61
Scheme 22: Protection of methyl 2,6-dihydroxybenzoate.....	63
Scheme 23: Halogen/Lithium exchange of building block A and posterior S _E Ar with building block B.	64
Scheme 24: Oxidation of diarylmethanol to benzophenone.	67
Scheme 25: Halogen/lithium exchange of building block A and posterior S _E Ar with building block C.	69
Scheme 26: Deprotection of benzophenone 16	69
Scheme 27: Cyclization of compound 17	71
Scheme 28: Oxidation of compound 19	72
Scheme 29: Esterification of compound 19	74
Scheme 30: Halogen/Lithium exchange of building block A and posterior S _E Ar with building block D.	76

Scheme 31: Oxidation of diarylmethanol to benzophenone.....	78
Scheme 32: Halogen/lithium exchange of building block A and posterior S_EAr with building block E.....	79
Scheme 33: Deprotection of compound 22	80
Scheme 34: Cyclization of compound 23	81
Scheme 35: Oxidation of compound 24	82
Scheme 36: Esterification of compound 25	84

TABLE INDEX:

Table 1: Chemical shifts and assignments of compound 8	60
Table 2: Chemical shifts and assignments of compound 13	62
Table 3: Chemical shifts and assignments of compound 14	63
Table 4: Chemical shifts and assignments of compound 15	66
Table 5: Chemical shifts and assignments of compound 16	68
Table 6: Chemical shifts and assignments of compound 17	70
Table 7: Chemical shifts and assignments of compound 18	72
Table 8: Chemical shifts and assignments of compound 19	74
Table 9: Chemical shifts and assignments of compound 20	75
Table 10: Chemical shifts and assignments of compound 21	77
Table 11: Chemical shifts and assignments of compound 22	79
Table 12: Chemical shifts and assignments of compound 23	81
Table 13: Chemical shifts and assignments of compound 24	82
Table 14: Chemical shifts and assignments of compound 25	83
Table 15: Chemical shifts and assignments of compound 26	85
Table 16: Calculation of the partition coefficient of the 8 compounds in several softwares.	88
Table 17: Calculation of the distribution coefficient of the 8 compounds in three softwares.	90
Table 18: Results from the calculation of the pKa.	91
Table 19: Results from the calculation of the solubility in several softwares.	92
Table 20: Results from the calculation of intestinal permeability for the 8 compounds.	93
Table 21: Results from the prediction of plasma protein binding.....	94
Table 22: Calculated properties applied to three drug-like rules.....	95
Table 23: Data obtained with the study of in silico biophysicochemical properties of the compounds of interest.....	125

LIST OF ABBREVIATIONS AND SYMBOLS

δ_C	¹³ Carbon chemical shifts
δ_H	Proton chemical shifts
ν	Wavenumber
%PPB	Percentage of plasma protein binding
¹³ C NMR	¹³ Carbon Nuclear Magnetic Resonance
¹ H NMR	Proton Nuclear Magnetic Resonance
AB/Log P	Log P prediction provided by Pharma Algorithms
ACDLog P	Log P prediction provided by ACDLabs Percepta Predictors
ADME	Absorption, Distribution, Metabolism and Excretion
ADMET	Absorption, Distribution, Metabolism, Excretion and Toxicity
AIDS	Acquired immune deficiency syndrome
Caco-2	Human colon adenocarcinoma cell line
CLog P	Calculated Log P
<i>d</i>	Doublet
<i>dd</i>	Double doublet
DMF	Dimethylformamide
DMG	Directed Metalation Group
DMP	Dess-Martin Periodinane
DMSO	Dimethylsulfoxide
DMSO- <i>d</i> ₆	Deuterated dimethylsulfoxide
EIMS	Electron-Impact Mass Spectrometry
FTIR	Fourier transform infrared spectroscopy
GC	Gas chromatography
GC-MS	Gas chromatography – mass spectrometry
HIV	Human immunodeficiency virus
HMBC	Heteronuclear Multiple Bond Correlation
HPLC	High Performance Liquid Chromatography
HSQC	Heteronuclear Single Quantum Coherence
IBX	2-iodoxybenzoic acid
iLog P	Log P prediction provided by SwissADME
IR	Infrared Spectroscopy
IUPAC	International Union of Pure and Applied Chemistry
<i>J</i>	Coupling Constant
LC	Liquid Chromatography
Log K _A ^{HSA}	Logarithm of the Affinity constant to human serum albumin
Log D	Logarithm of the Distribution Coefficient between Octanol:buffer at a given pH
Log P	Partition Coefficient Octanol-Water
Log S	Logarithm of the intrinsic solubility in mol/L
<i>m</i>	Multiplet
MeCN	Acetonitrile

MeOH	Methanol
MLog P	Log P prediction provided by Moriguchi
MOM	Methoxymethyl
MOMCl	Methoxymethyl chloride
m.p.	Melting Point
MSTFA	<i>N</i> -Methyl- <i>N</i> -(trimethylsilyl)trifluoroacetamide
MW	Microwave heating
MW	Molecular weight
NMR	Nuclear Magnetic Resonance
P_{app}	Apparent permeability coefficient
P_e	Effective permeability
Perm.	Permeability
PK	Pharmacokinetics
PK/PD	Pharmacokinetics and Pharmacodynamics
PPB	Plasma Protein Binding
pKa	Acid dissociation constant
q	Quadruplet
RP-HPLC	Reverse phase high performance liquid chromatography
s	Singlet
t	Triplet
TBAHS	Tetrabutylammonium hydrogensulfate
TBDMS	<i>tert</i> -Butyldimethylsilyl
TBDMSCl	<i>tert</i> -butyldimethylsilyl chloride
THF	Tetrahydrofuran
TLC	Thin Layer Chromatography
TMEDA	<i>N,N,N',N'</i> -Tetramethylethylenediamine
TMS	Trimethylsilyl
tPSA	Topological Polar Surface Area
UV	Ultraviolet spectrometry
UV/Vis	Ultraviolet/Visible spectrometry
WHO	World Health Organization
WLog P	Log P prediction provided by Wildman and Crippen
XLog P₃	Log P prediction provided by Luhua Lai

OUTLINE OF THE DISSERTATION

The present dissertation is organized in seven chapters:

1. Introduction

This chapter begins showing why the discovery of new drugs are so important. The role of natural products, as sources of drugs, with particular emphasis on the recent progresses on marine natural products is discussed. The current drug discovery pipeline is described, showing the importance of organic synthesis and the concept of “multidimensional optimization”. The early assessment and continuous evaluation of biophysicochemical properties in drug discovery process is presented. Finally, the synthesis of xanthenes, involving the most usual methodologies, is exposed.

2. Aims

The aims for the work that leaded this dissertation are presented in this chapter.

3. Experimental

All the reagents, the experimental conditions and procedures for the synthesis, the purification steps and the structure elucidation of all synthesized compounds is described in this chapter.

4. Results and discussion

This chapter is divided into two main sections: i. synthesis of yicathins B and C and analogues; and ii. *in silico* acquiring of biophysicochemical properties of the synthesized substances, using different software.

The retrosynthetic analysis and the synthesis pathways to yicathins B and C is showed. All synthetic steps are discussed and structural elucidation of all buildings blocks, all intermediates and final products is presented and discussed. Lastly, the *in silico* determination of some biophysicochemical properties of the eight more interesting compounds is described and argued about.

5. Conclusions

In this section, general conclusions of this work are exposed and future work is appointed.

6. References

All the literature used as support in this dissertation is listed in this chapter. ACS system for bibliographic references was used.

7. Appendix

In this chapter, the NMR spectra of all new synthesized compounds are showed (Appendix 1). A table that gathers structural data and the calculated biophysicochemical properties is showed (appendix 2).

I
N
T
R
O
D
U
C
T
I
O
N

1.1. The constant need for new drugs

Drug discovery is a research field in continuous evolution, searching for new bioactive molecules that can be used in medicines.

Infectious diseases follow being an important cause of death and arise additional problems, such as the development of resistance mechanisms by the infectious agents. Antimicrobial resistance, including multidrug resistance, brings new challenges in the treatment of infectious diseases. The resistant microorganisms became insensitive to drugs that kill or stop the microorganisms of growing, resulting in the persistent and even growth of the infection. This problem is even worse in immunocompromised patients, which have a sensitive immunological system, increasing the risk of serious infections.^[1]

This reality is supported by the study made by the World Health Organization (WHO), which gathers data on causes of death worldwide in 2000 and 2015 and it is reported in figure 1^[2]. As it can be seen, the infectious diseases still are a very marked cause of death, corresponding to 3 of the 10 more common causes of death. Moreover, these diseases practically caused the same number of deaths between 2000 and 2015, even though 15 years have passed by.

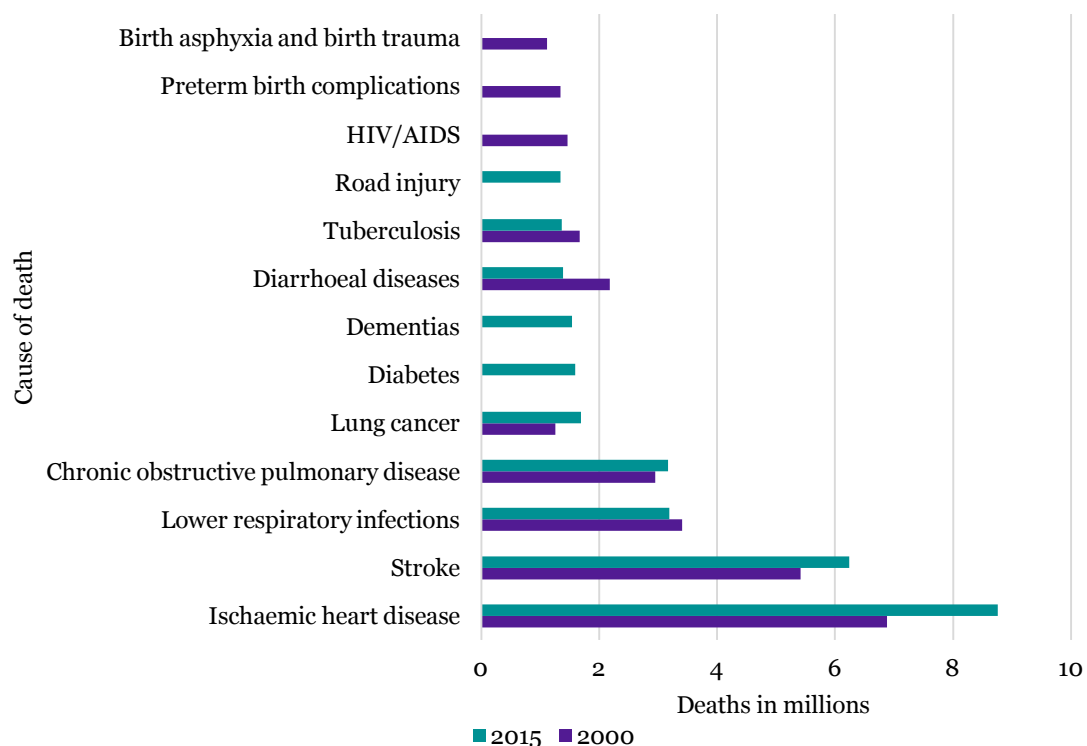


Figure 1: Comparison between the top 10 causes of death in 2000 and 2015 (adapted from ^[2]).

The same WHO study shows that in the low income countries the number of deaths caused by microorganisms increases, being half of the most common causes of death ^[2].

These facts prove that new and better drugs are required to treat infectious diseases and to deal with drug resistances.

Therefore, Medicinal Chemistry assumes here a relevant role, since one of its main objectives is the discovery of new and better drugs.

1.2. Sources of new drugs

Nature always provided inspiration for the treatment of diseases. The history of traditional medicine joins the history of mankind.

For centuries, fresh plants and their extracts have been used to cure diseases. With the advance of science and technology, the need to understand the composition of crude products and knowing the compounds responsible for the therapeutic activity led to fractionation of plants and their extracts, and to the identification of the compounds responsible for the therapeutic activity. Chemical synthesis brought the possibility of having active compounds at any time of the year, in the desired quantities. Structural elucidation and the understanding of structure-activity relationships inspired the design of new compounds allowing new and more effective drugs. In consequence, 20th century gave to humanity some drugs that changed the world and medicines became available globally.^[3]

In recent years, resulting from technology explosion, new approaches were explored in the quest for drug discovery, namely high-throughput screening, combinatorial chemistry, diversity oriented synthesis, fragment-based design, *in silico* techniques, among others ^[4-8]. However, nature still plays an important role in drug discovery, producing a highly structural diversity of active molecules, introducing new leads and drugs to be used in therapeutics ^[9]. Newman et al^[10, 11] showed that the percentage of drugs inspired by nature even had an increase in last years (figure 2).

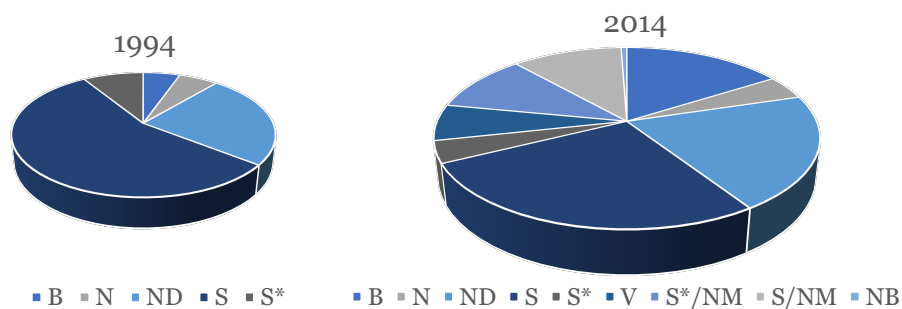


Figure 2: Comparison of sources of drugs in 1994 versus 2014 (adapted from ^[10, 11]).
B – biological macromolecule; N – unaltered natural product; ND – natural product derivative;
S – synthetic drug; S* – synthetic drug with natural product pharmacophore; V – vaccine;
/NM – mimic of natural product, either for S or S*; NB – botanical drug.

In the natural environment, sea represents the most part of the planet surface and is the least studied component of earth. The marine environment became one of the most desired areas of interest in drug discovery, in recent years.

1.2.1. Marine environment as a drugs source

The overexploration of secondary metabolites with terrestrial origin and the advance of sea exploration technologies led the marine environment as a source of drugs to be a wanted field to explore [12].

The sea occupies more than 70 % of earth^[13], with ecosystems not found in terrestrial environment. The undiscovered molecular diversity found under the sea provides us with a big spectrum of new compounds with potential biological activities, allowing a good perspective as new drug candidates.^[12]

Secondary metabolites from the marine environment have been extracted from sponges, algae and microorganisms, among others. Microorganisms have been the source of many compounds with several important utilizations, namely in medicine, agriculture and industry. The marine microorganisms live under stressful conditions with scarce sunlight, cold temperatures, high pressure, high salinity levels and specific nutrients, forcing them to develop different and original pathways in the biosynthesis of secondary metabolites. These aspects turn them into a valuable source of compounds, not available in terrestrial sources. This kind of metabolites provides potential biological activities, such as anticancer activity (56 % of total bioactive compounds), followed by the anti-infective activity - antimicrobial, antiviral and antifungal - (27 % of total bioactive compounds).^[12, 14]

Several molecules isolated from marine sources are currently being developed, others are in clinical trials, and some are already marketed drugs ^[15].

One of the classes of compounds found in nature, namely in the marine environment are xanthenes. Xanthenes are a class of natural products with dibenzo- γ -pyrone scaffold, that are produced by plants, fungi, lichens and other organisms ^[16]. They are considered as privileged structures since their structure is able to bind a spectrum of targets, producing a wide range of biological activities. In the marine world, xanthenes have been extracted from several fungi and bacteria and two new xanthenes have been described from a symbiotic connection between fungi and an algae ^[17]. Yicathins B and C (figure 3) were isolated from *Aspergillus wentii* founded in the tissue of an algae, *Gymnogongrus flabelliformis* ^[18]. These kinds of symbioses between micro- and macroorganisms are common in the marine environment, which constitutes a fascinating field of study, as they are extremely productive of secondary metabolites, offering a huge potential in drug discovery ^[19].

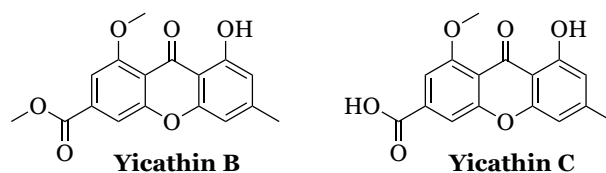
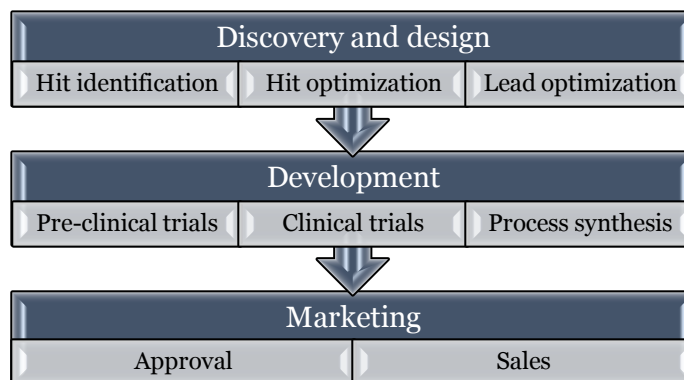


Figure 3: Structures of Yicathins B and C.

1.3. Drug discovery

The route to a new drug is a very rough and longstanding pathway, involving an enormous effort, both economical and in terms of personnel, with multiple teams working together to provide an effective and successful drug [20]. In scheme 1, it is represented the main steps in the 21st century drug discovery pipeline.



Scheme 1: Drug discovery pipeline (adapted from [20, 21]).

During this long process, most of the times more than ten years, chemists have an important role in all steps. It starts with a medicinal chemist, who is in charge of designing hit and lead compounds. At this stage, the main goal is to achieve the largest library of active compounds possible, in small amounts, allowing a big spectrum of possibilities of new drugs. After the hit is chosen, it has to be improved to achieve a lead. Several analogues have to be synthesized and tested. In this design process, drug-like concepts are always in mind. Using the same principles, lead compounds will give origin to a drug candidate. During clinical trials, development chemist takes action, designing the industrial synthesis of the drug candidate, doing the scale-up of the synthetic process, as well as the purification methods. [22, 23]

The road to a new drug candidate involves trial and error, i.e., involves structural modification to find the best candidates. This cannot be done blindly. Data from biological activity plays an important role in the molecular modifications, however, other factors need to be considered [24]. The multidimensional optimization relies on the relationship between data from the biological activity, determination of key biophysicochemical properties and the synthesis of new molecules (figure 4) [25].

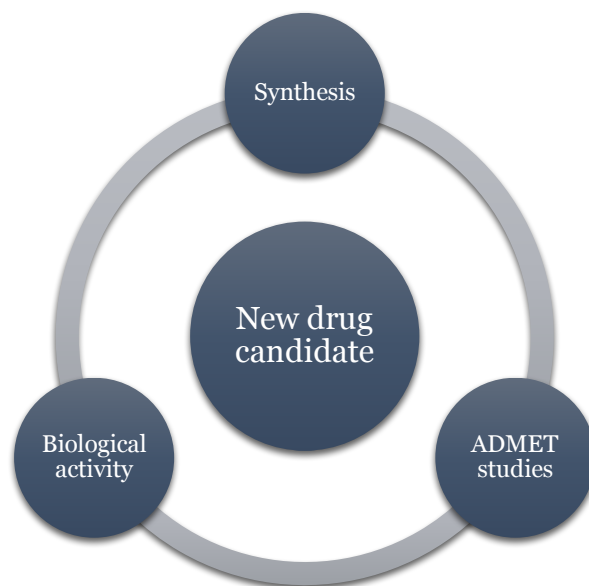


Figure 4: Multidimensional optimization.

The balance between the synthesis of new analogues, the evaluation of their biological activity and the determination of their biophysicochemical properties, it will provide the tools to synthesize a drug candidate capable of being potent, that reaches the desired target and becoming a marketed product.

1.4. Biophysicochemical properties

The biophysicochemical properties enters in the ADMET studies, since the determination of these factors helps to predict, in an early stage, the behavior of the molecule in the organism, regarding pharmacokinetics. Determinations such as the lipophilicity, solubility, acidity (pKa), permeability and plasma protein binding are crucial in the modification of hit/lead compounds.^[24]

1.4.1. Lipophilicity

Lipophilicity is the measure of affinity between a compound and a lipophilic environment. It is measured by the distribution of the compound between a biphasic system (equation 1), being described as logP, for nonionizable compounds, or by logD, for ionizable compounds.^[26]

LogP describes the partition coefficient (equation 2), usually, between *n*-octanol and water, even though recently new methods measure this coefficient with different systems ^[27].

LogD describe the distribution coefficient of an ionizable compound at a certain pH (equation 3 and 4), considering the distribution of the ionizable and nonionizable compound between the two phases ^[26].

$$\text{Lipophilicity} = \frac{[C]_{\text{organic}}}{[C]_{\text{aqueous}}} \quad (1)$$

$$\log P = \log \frac{[C]_{\text{n-octanol}}}{[C]_{\text{water}}} \quad (2)$$

$$\log D = \log \frac{[HA]_{\text{organic}}}{[HA]_{\text{aqueous}} + [A^-]_{\text{aqueous}}} \quad (3)$$

$$\log D = \log \frac{[B]_{\text{organic}}}{[B]_{\text{aqueous}} + [BH^+]_{\text{aqueous}}} \quad (4)$$

Lipophilicity has a big importance in the pharmacokinetics and pharmacodynamics of the drug candidate, as it affects the absorption, distribution, excretion and binding to plasma proteins, reason why its measurement is so important at early stages of drug discovery ^[28].

1.4.2. Solubility

Solubility is another measure of interest in drug discovery. It is described as the maximum amount of compound that can be soluble in a certain solvent, with an determined volume.^[29]

Solubility will influence the distribution and excretion of the compound from the organism and this reinforces the importance of taking this measure into account while lead optimization is being performed ^[30].

1.4.3. pKa

pKa represents the constant of ionization for acids and bases (equations 5 to 8) ^[31]. It tells the ionic state of the molecule at a determined pH ^[32].



$$\text{pK}_a = -\log \left(\frac{[\text{H}^+] \cdot [\text{A}^-]}{[\text{HA}]} \right) \quad (6)$$



$$\text{pK}_a = -\log \left(\frac{[\text{H}^+] \cdot [\text{B}]}{[\text{HB}^+]} \right) \quad (8)$$

pKa is an important measure in absorption, distribution and excretion, since the ionizable and nonionizable compound have different behaviors in each step of pharmacokinetics ^[31].

1.4.4. Permeability

Permeability is the study of the passage of a compound from one place to another, through a membrane. This study is made based on the permeation speed and performed *in vitro* in cell lines, according to a general procedure reported in figure 5.^[33]

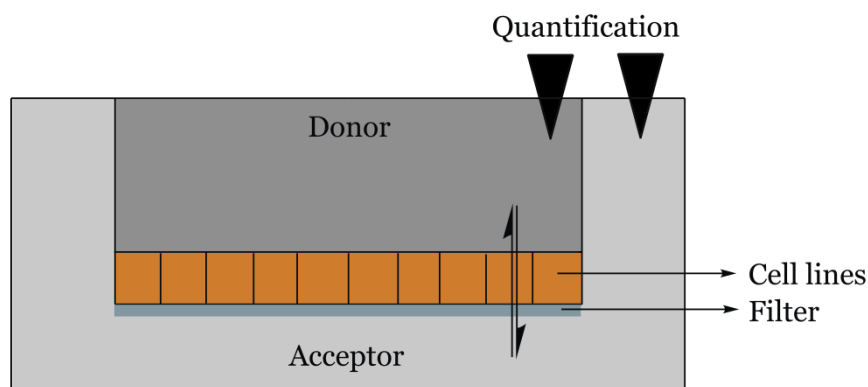


Figure 5: General procedure for the determination of permeability (adapted from [34]).

The study of the permeability of compounds is important because it influences the ADME process, more specifically, the absorption [33].

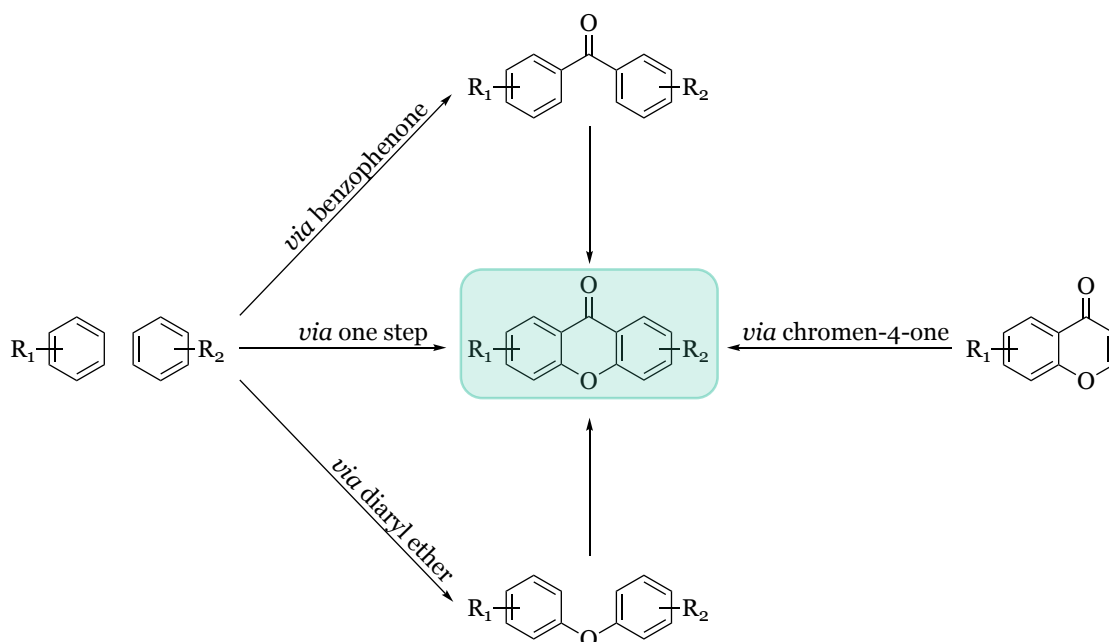
1.4.5. Plasma protein binding

The study of plasma protein binding reflects the affinity of the compound to the transporting proteins present in the bloodstream, which will transport the compound throughout the organism. However, if this interaction is too strong, the compound will not be able to be in the free form and to be absorbed by the membrane. So, this study is important in the prediction of the pharmacokinetic behavior of the compound.[34]

These measures can be made by *in vitro* assays and the biophysicochemical properties determined. However, these properties can be also predicted using computation models, i.e., *in silico* methodologies that predict the characteristics taking into account the features of the molecule and the property itself.[35]

1.5. Synthesis of xanthenes

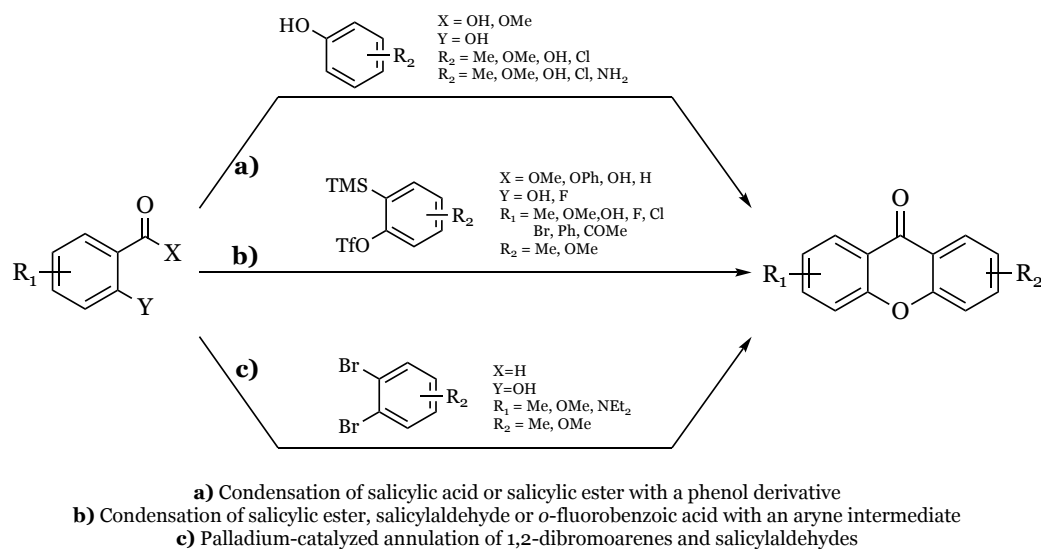
The synthesis of xanthenes until 2012 is well described in the literature [36, 37]. Herein, it will be presented a summary of the most common pathways to obtain xanthenes (scheme 2).



Scheme 2: Commonly used pathways in the synthesis of xanthenes (adapted from [36]).

1.5.1. Via one step synthesis

One step synthesis of xanthenes provides a fast way of producing xanthenes. However, this is not the most common methodology used since it uses harsh experimental conditions, not easily handled, and the building blocks needed to synthesize the desired substituted xanthone are hardly found commercially available. There are three main approaches for this methodology and they are presented in scheme 3.^[36]



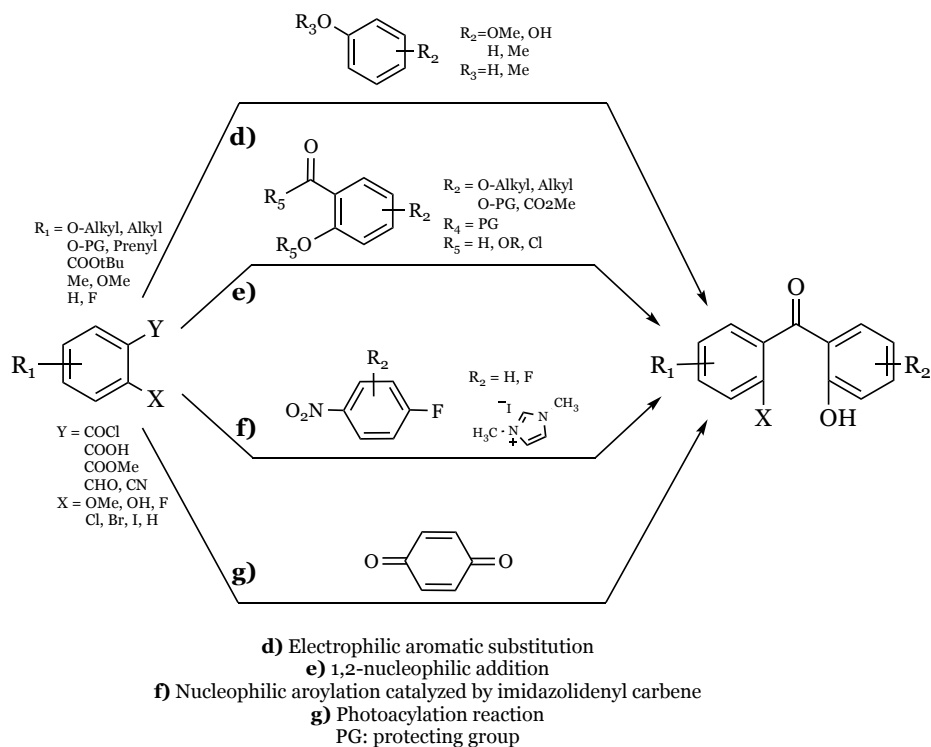
Scheme 3: Main approaches for one step synthesis of xanthenes (adapted from [36]).

As shown in the scheme, the synthesis of xanthenes can be performed by reaction of salicylic acid or esters with polyphenolic compounds and catalysed by strong Lewis or Brønsted acids (scheme 3, **a**) [38]. Another approach describes the formation *in situ* of an aryne, which will react with a salicylate derivative ortho-fluorobenzoate ester (scheme 3, **b**) [39, 40]. The third one describes the reaction of a salicylaldehyde with 1,2-dibromoarene derivatives, catalysed by palladium (scheme 3, **c**) [41].

1.5.2. Via benzophenone

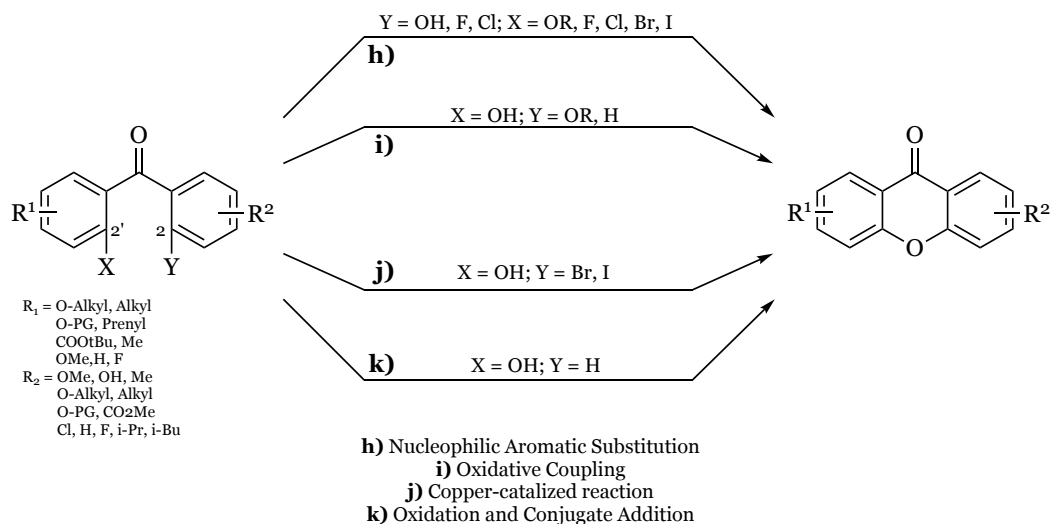
The synthesis of xanthenes *via* benzophenone is, beyond any doubt, the most common way to obtain the desired product with high yields [37]. It is built in a procedure that splits into two main reactions: the formation of the benzophenone and the benzophenone cyclization.

There are four main approaches for the synthesis of benzophenones, as intermediates in the synthesis of xanthenes: by Friedel-Crafts acylation (scheme 4, **d**) [42], 1,2-nucleophilic addition of an aryllithium intermediate to a carbonyl group (which may involve the oxidation of a diarylmethanol) (scheme 4, **e**) [43], the use of an organocatalist in the reaction of two electron-deficient building blocks (scheme 4, **f**) and photoacylation [44], *via* an acyl radical reaction (scheme 4, **g**) [45].



Scheme 4: Common approaches in the synthesis of benzophenone intermediates (adapted from [36]).

For the cyclization of the benzophenone and, consequently, the obtainment of the xanthone, there are 4 main approaches: the base-catalyzed nucleophilic aromatic substitution (scheme 5, **h**) [46], by oxidative coupling of polyoxygenated benzophenones (scheme 5, **i**) [47, 48], copper-catalyzed intramolecular *O*-arylation by Ullmann-coupling (scheme 5, **j**) [49] and by spontaneous cyclization of quinones obtained by oxidation of 2,5-dihydroxybenzophenones derivatives (scheme 5, **k**) [50, 51].

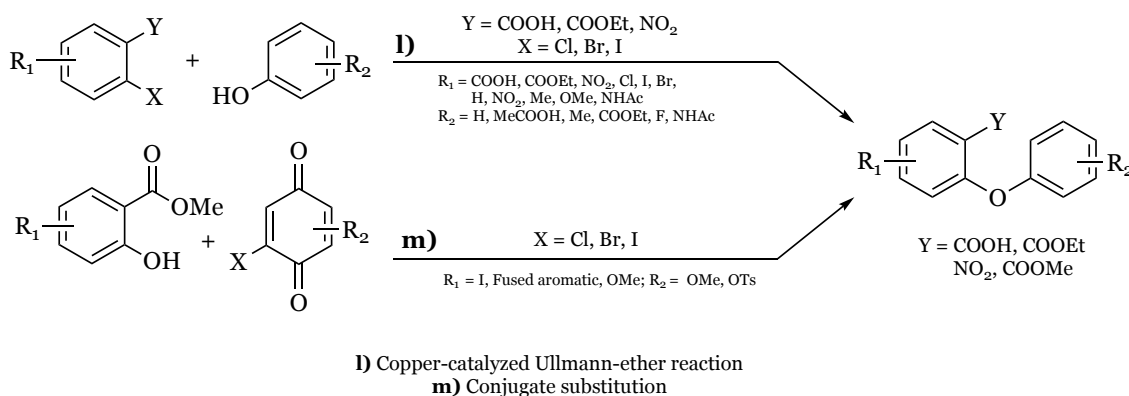


Scheme 5: Common approaches in the cyclization of benzophenones (adapted from [36]).

1.5.3. Via diaryl ether

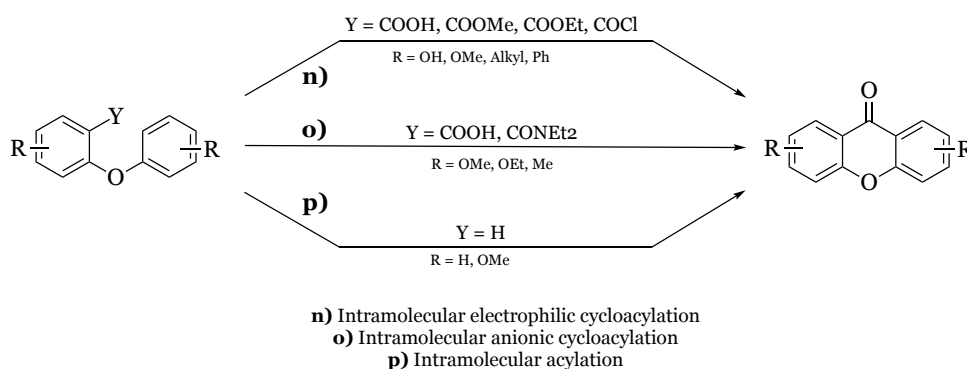
Just like in the benzophenone pathway, this one splits into two steps: the formation of the diaryl ether and then the formation of the xanthone, by cyclization.

For the synthesis of the diaryl ether there are two main approaches: the copper catalyzed coupling reaction between an aryl halide and a phenol derivative (scheme 6, **l**)^[52] and conjugate substitution of a phenol and a 1,4-halobenzoquinone (scheme 6, **m**)^[53, 54].



Scheme 6: Common approaches for the synthesis of diaryl ethers (adapted from ^[36]).

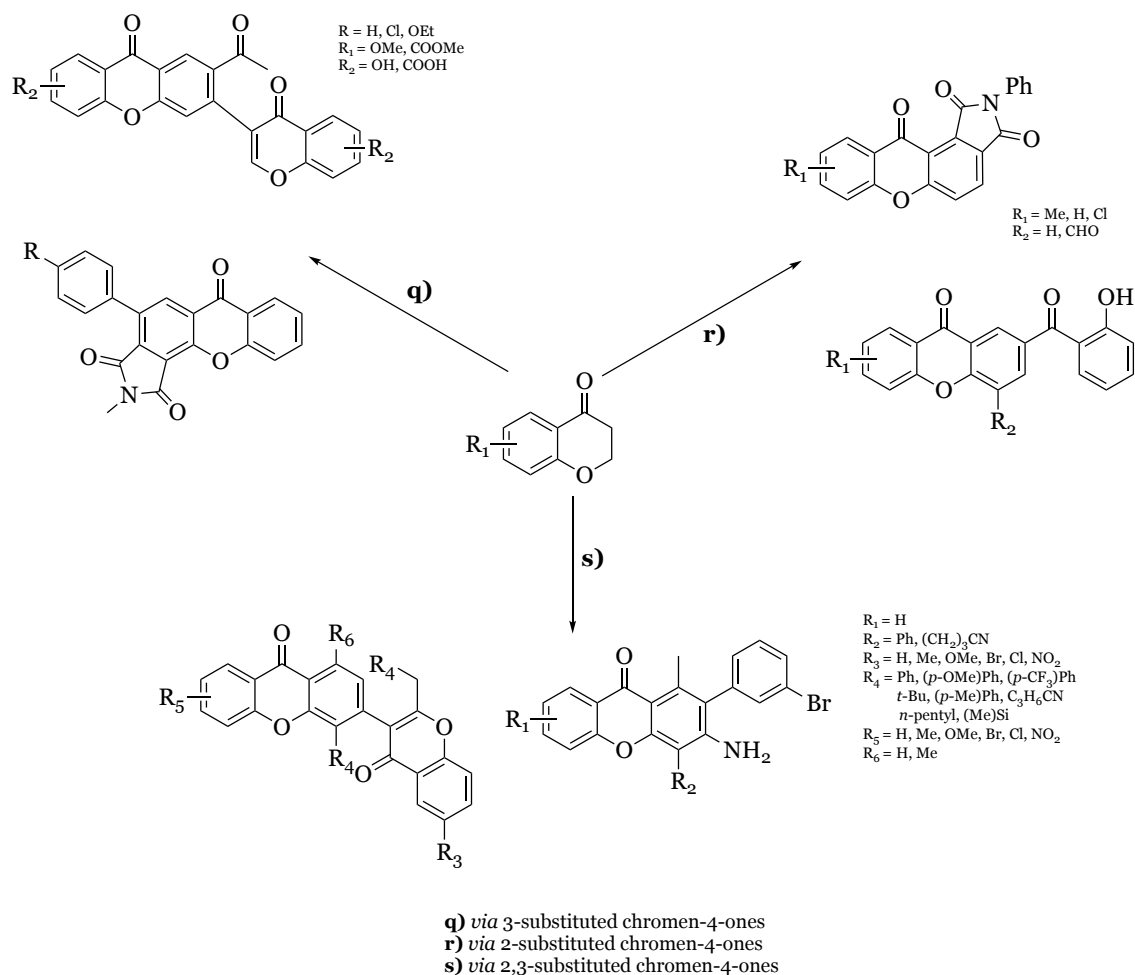
For the cyclization of the diaryl ether, there are three commonly used methodologies: acid-catalyzed intramolecular electrophilic cycloacylation (scheme 7, **n**)), base-catalyzed intramolecular anionic cycloacylation (scheme 7, **o**)) and intramolecular acylation (scheme 7, **p**)).^[55]



Scheme 7: Common approaches for the cyclization of diaryl ethers (adapted from ^[36]).

1.5.4. Via chromen-4-ones

Lastly, a recent approach in the synthesis of xanthenes was described in the literature. It uses a skeleton, which already has the ketone and the ether bridge, that reacts with other building blocks to provide highly substituted xanthenes (scheme 8).^[55]



Scheme 8: Examples of xanthone synthesis via chromen-4-one (adapted from ^[36]).

A
I
M
S

As said in the introduction chapter, yicathins were isolated from marine organisms but have never been synthesized in the laboratory. This work already started in our group and important advances were made^[56]. However small amounts of intermediates were obtained and the total synthesis was not achieved. Therefore, the total synthesis of the xanthones derivatives, yicathins B and C, as well as some analogues is the main aim of this dissertation.

Taking into account the previous work, new synthetic methodologies were thought in order to reduce the number of steps of the overall synthetic plan and to increase reactions yields.

Based on this main goal, the aims of the developed work were:

- i. Optimization of the overall plan for the total synthesis of yicathins B and C and respective analogues;
- ii. Synthesis of all building blocks needed;
- iii. Synthesis of yicathins B and C and some analogues, as well as their intermediates;
- iv. Optimize key reactions;
- v. Purify and elucidate the structure of the new compounds;
- vi. Predict biophysicochemical properties of the new compounds.

E
X
P
E
R
I
M
E
N
T
A
L

3.1. General methods.

All compounds were prepared in the Laboratory of Organic and Medicinal Chemistry of the Faculty of Pharmacy of the University of Porto.

All the reagents were purchased from Sigma Aldrich, Acros or TCI and all the solvents were PA used without further purification. Solvents were evaporated using rotary evaporator under reduced pressure (Buchi Waterchath B-480). Anhydrous solvents were either purchased from Sigma-Aldrich or dried according to the published procedures.^[57]

MW reactions were performed in a CEM Discovery SP from CEM Corporation. All experiments were performed in a closed vessel of 10 or 35 mL.

Reactions were monitored by TLC and/or GC-MS. The visualization of the chromatograms was made under UV light at 254 and 365 nm. Gas chromatography analyses (GC) were carried out on Trace GC 2000 Series (DB5 –capilar column, RTX® - 5MS (crossbond 5% diphenyl 95% dimethylpolysiloxane)) with electron-impact mass spectra recorded on GCQ plus and referred to m/e (fragments %). Injections were performed using compounds directly dissolved in ethyl acetate or previously derivatized with MSTFA at 80 °C for 30 minutes.

Purifications of compounds were performed by flash column chromatography by using Merck silica gel 60 (0.040-0.063 mm).

RP-HPLC analysis was performed on a Dionex Ultimate 3000 (Thermo Fisher Scientific, USA) equipped with a 3000 quaternary pump, a 3000 autosampler, and a 3000 Variable UV/Vis detector. Chromeleon software version 7.2 Ultimate (Thermo Fisher Scientific, USA) was used to manage chromatographic data. LC analysis was performed in a isocratic mode with using as mobile phase a mixture of methanol : water (1 % formic acid) (55:45, 75:25 or 92:8), and the eluent was monitored in UV/Vis at 254 nm. Preparative separation was carried out on a Interchrom UP5ODB.25M (Uptisphere 5µm WOD; 250 x 10 mm), with a flow rate set to 5 mL/min. and a volume of injection of 100 µL. All solvents used were HPLC grade, and prior to use, solvents were degassed in an ultrasonic bath for 15 minutes.

Melting points were obtained in a Köfler microscope and are uncorrected.

IR spectra were measured on a KBr microplate (cm⁻¹) in a FTIR spectrometer Nicolet iS10 from Thermo Scientific with Smart OMNI-Transmisson accessory (Software OMNIC 8.3).

¹H and ¹³C NMR spectra were performed in the Departamento de Química, Universidade de Aveiro, and were taken in DMSO-*d*₆ (Deutero GmbH) at room temperature, on Bruker Avance 300 (300.13 MHz for ¹H and 75.47 MHz for ¹³C) or Bruker DRX-500 (500.13 and/or 300.13 MHz for ¹H and 125.77 and/or 75.47 MHz for ¹³C)

spectrometers. Chemical shifts are expressed in δ (ppm) values relative to tetramethylsilane (TMS) as an internal reference and assignment abbreviations are the following: singlet (*s*), doublet (*d*), triplet (*t*), quartet (*q*), multiplet (*m*), doublet of doublets (*dd*). ^{13}C NMR assignments were made by 2D HSQC and HMBC experiments (long-range C, H coupling constants were optimized to 7 and 1 Hz) or by comparison with the assignments of similar molecules.

Compounds were identified according IUPAC nomenclature but the numbering used in NMR assignments was used for convenience.

3.2.Synthesis of building block A.

3.2.1. Synthesis of (4-bromo-3,5-dimethoxyphenyl)methanol (2).

Via borane complex with tetrahydrofuran.

4-bromo-3,5-dimethoxybenzoic acid (4g, 15 mmol) was dissolved with 30 mL of anhydrous THF in a two-necked round-bottom flask under nitrogen atmosphere. The solution was cooled until 0°C and then added borane-tetrahydrofuran complex (37 mL, 34 mmol) dropwise. The reaction was allowed to reach room temperature and stirred for 2 hours at room temperature. The reaction was quenched by the addition of a saturated solution of potassium carbonate and then extracted with ethyl acetate (3 x 30 mL). The organic phase was dried over Na₂SO₄ and the solvent evaporated under reduced pressure. The compound was used in the next step without further purification step was attained and the compound was obtained as a fine white powder (3.58 g, 95 %).

Via sodium borohydride and iodine.

In a round-bottom flask, it was placed the sodium borohydride (549 mg, 15 mmol) and anhydrous THF. To this solution, it was added, dropwise, a suspension of 4-bromo-3,5-dimethoxybenzoic acid (2.00 g, 8 mmol). The reaction mixture was cooled to 0 °C and then added a suspension of iodine (1.07 g, 4 mmol). After this addition, the system was slowly warmed to room temperature and then to 40 °C overnight. To the reaction mixture, it was added Na₂S₂O₃ and then acidified with HCl 5%. The mixture was extracted with ethyl acetate and the organic layer was dried under Na₂SO₄, filtered and the solvent evaporated. No further purification step was attained and the compound was obtained as a fine white powder (602 mg, 91 %).

m. p.: 97 – 99 °C

¹H NMR (300.13 MHz, DMSO-*d*₆) δ (ppm): 6,70 (2H, s), 5,35 (H, t, J = 5.6 Hz), 4.49 (2H, d, J = 5.6 Hz), 3.82 (6H, s).

IR ν_{max} (cm⁻¹) (KBr): 3223, 3003, 2929, 2840, 1346, 1076, 1055, 1035, 822, 633

EIMS m/z (%): 248 (79, [M+2]⁺), 246 (84, [M]⁺), 231 (17), 217 (21), 167 (18), 139 (100), 138 (72), 137 (17), 124 (92), 109 (28), 108 (40), 96 (17), 95 (19), 79 (27), 78 (26), 77 (38), 66 (18), 65 (30), 64 (27), 53 (38), 51 (40).

All spectroscopic values are in agreement with published data ^[58].

3.2.2. Synthesis of ((4-bromo-3,5-dimethoxybenzyl)oxy)(tert-butyl)dimethylsilane (3).

In a two-necked round-bottom flask of 100 mL was placed (4-bromo-3,5-dimethoxyphenyl)methanol (400 mg, 1.62 mmol), imidazole (275.5 mg, 4.05 mmol), and TBDMSCl (293 mg, 1.94 mmol). The mixture was placed under nitrogen atmosphere and 10 mL of DMF anhydrous was added. The solution was kept under stirring at room temperature for 5 hours. The reaction mixture was then poured into water (10 mL) and extracted with 3 x 15 mL of ethyl acetate. The organic phase was dried over Na₂SO₄, filtered and the solvent was removed by rotary evaporation. The crude product was purified by silica gel flash chromatography (*n*-hexane/ethyl acetate 8:2) and the compound was isolated as a colorless oil (515 mg, 88%).

¹H NMR (300.13 MHz, DMSO-*d*₆) δ (ppm): 6.66 (2H, s), 4.68 (2H, s), 3.79 (6H, s), 0.90 (9H, s), 0.07 (6H, s).

IR ν_{\max} (cm⁻¹) (KBr): 2955, 2929, 2856, 1590, 1462, 1417, 1258, 1232, 1126, 838, 815, 777.

EIMS *m/z* (%): 364 (2, [M+2]⁺), 362 (3, [M]⁺), 323 (12), 305 (28), 303 (36), 275 (52), 273 (48), 231 (100), 229 (84), 224 (61), 209 (17), 169 (13), 129 (26), 92 (33), 77 (21), 75 (17).

All spectroscopic values are in agreement with published data [58].

3.3.Synthesis of building block B.

3.3.1. Synthesis of 1,3-bis(methoxymethoxy)-5-methylbenzene (5).

In a two-necked round-bottom flask of 250 mL, it was placed orcinol (5.00 g, 8 mmol) and NaH (6.44 g of a 60% suspension in mineral oil, 161 mmol) under nitrogen atmosphere and then added 10 mL of DMF anhydrous. The system was cooled in an ice bath and after 15 minutes, it was added, dropwise, MOMCl (9.18 mL, 121 mmol). The mixture was kept stirring for 5 hours at room temperature. Water was added to the reaction mixture and it was then extracted with ethyl acetate (3 x 15 mL). The organic layer was dried under Na₂SO₄ and the solvent was evaporated under reduced pressure. The crude product was purified in a silica gel flash chromatography (*n*-hexane/ethyl acetate 8:2). The compound was obtained as a light yellowish oil (7.06 g, 83 %).

¹H NMR (300.13 MHz, DMSO-*d*₆) δ (ppm): 6.49 (2H, *dd*, *J* = 1.9 Hz, *J* = 0.5 Hz), 6.47 (H, *m*), 5.14 (4H, *s*), 3.36 (6H, *s*), 2.23 (3H, *s*).

IR ν_{\max} (cm⁻¹) (KBr): 2955, 2852, 2826, 2360, 2342, 1595, 1540, 1472, 1399, 1331, 1316, 1291, 1257, 1215, 1145, 1084, 1039, 996, 923, 839, 688, 669.

EIMS *m/z* (%): 213 ([M+1]⁺), 212 (100, [M]⁺), 181 (33), 151 (18).

All spectroscopic values are in agreement with published data ^[59].

3.3.2. Synthesis of 2,6-bis(methoxymethoxy)-4-methylbenzaldehyde (6).

In a two-necked round-bottom flask of 250 mL, it was placed 1,3-bis(methoxymethoxy)-5-methylbenzene (1.38 g, 6.50 mmol) under nitrogen atmosphere and then added anhydrous THF and anhydrous TMEDA (2.14 mL, 14.30 mmol). The mixture was cooled until -5 °C and then added *n*-BuLi (5.72 mL, 14.30 mmol) and kept at room temperature for 2 hours. After this period, DMF (1.50 mL, 19.51 mmol) was added and the mixture stayed at room temperature for 2 more hours. To the reaction mixture, it was added NH₄Cl, followed by extraction with ethyl acetate (3 x 30 mL). The organic layer was dried under Na₂SO₄ and the solvent was evaporated under reduced pressure. The crude product was purified in a silica gel flash chromatography (*n*-hexane/ethyl acetate 8:2), yielding the desired compound as a yellow oil (1.29 g, 83 %).

¹H NMR (300.13 MHz, DMSO-*d*₆) δ (ppm): 10.37 (H, s), 6.70 (2H, s), 5.25 (4H, s), 3.40 (6H, s), 2.31 (3H, s).

IR ν_{\max} (cm⁻¹) (KBr): 3525, 3359, 2956, 2829, 2780, 1683, 1607, 1455, 1392, 1309, 1241, 1195, 1154, 1049, 963, 921, 827, 801, 690.

EIMS *m/z* (%): 241 (12, [M+1]⁺), 240 (2, [M]⁺), 208 (10), 195 (10), 179 (28), 178 (100), 165 (16), 163 (15), 135 (11), 121 (14), 91 (13), 76 (11), 51 (13)

All spectroscopic values are in agreement with published data [59].

3.4.Synthesis of building block C.

3.4.1. Synthesis of methyl 2,6-bis(methoxymethoxy)-4-methylbenzoate (8).

In a two-necked round-bottom flask of 250 mL, it was placed methyl 2,6-dihydroxy-4-methylbenzoate (1.0 g, 5 mmol) and NaH (1.10 g of a 60% suspension in mineral oil, 27 mmol), under nitrogen atmosphere and then added 10 mL of anhydrous DMF. The system was cooled in an ice bath and, after 15 minutes, it was added, dropwise, MOMCl (1.67 mL, 22 mmol). The mixture was kept stirring for 5 hours at room temperature. Water was added to the reaction mixture and it was then extracted with ethyl acetate (3 x 15 mL). The organic layer was dried under Na₂SO₄ and the solvent was evaporated under reduced pressure. The crude product was purified in a silica gel flash chromatography (*n*-hexane/ethyl acetate 8:2). The compound was obtained as a slightly yellow oil (1.07 g, 72 %).

¹H NMR (300.13 MHz, DMSO-*d*₆) δ (ppm): 6.67 (2H, s), 5.17 (4H, s), 3.77 (3H, s), 3.34 (6H, s), 2.28 (3H, s).

¹³C NMR (75.47 MHz, DMSO-*d*₆) δ (ppm): 166.1, 153.9, 141.1, 112.8, 108.8, 94.0, 55.7, 52.1, 21.7.

IR ν_{max} (cm⁻¹) (KBr): 3001, 2966, 2920, 2856, 2829, 1732, 1610, 1459, 1393, 1316, 1300, 1276, 1243, 1207, 1159, 1046, 963, 949, 920, 906, 844, 822, 775.

EIMS m/z (%): 271 (32, [M+1]⁺), 270 (26, [M]⁺), 240 (12), 239 (83), 209 (18), 195 (34), 194 (100), 179 (22), 165 (82), 164 (14), 150 (25), 136 (18), 121 (13), 91 (10), 79 (10), 77 (15), 66 (13), 52 (14).

3.5.Synthesis of building block D.

3.5.1. Synthesis of 1,3-bis(methoxymethoxy)benzene (10).

In a two-necked round-bottom flask of 250 mL, it was placed resorcinol (1 g, 9 mmol) and NaH (1.1 g of a 60% suspension in mineral oil, 27 mmol), under nitrogen atmosphere, and then 30 mL of anhydrous DMF. The reaction mixture was kept at 0°C for 15 minutes and then it was added, dropwise, MOMCl (2.1 mL, 27 mmol). The mixture was warmed to room temperature gradually and kept for 6 hours in these conditions. The reaction mixture was then poured into water and extracted with ethyl acetate (3 x 20 mL). The organic phase was dried over Na₂SO₄, filtered and the solvent was removed by rotary evaporation. The crude product was purified by silica gel flash chromatography (*n*-hexane/ethyl acetate 8:2) and the compound was isolated as a colorless oil (1.45 g, 81 %).

¹H NMR (300.13 MHz, DMSO-*d*₆) δ (ppm): 7.20 (H, *m*), 6.66 (3H, *m*), 5.16 (4H, *s*), 3.37 (6H, *s*).

IR ν_{\max} (cm⁻¹) (KBr): 2954, 2923, 2854, 1458, 1377, 721.

EIMS *m/z* (%): 199 (28, [M+1]⁺), 198 (100, [M]⁺), 167 (300), 124 (100), 63 (26).

All spectroscopic values are in agreement with published data ^[60].

3.5.2. Synthesis of 2,6-bis(methoxymethoxy)benzaldehyde (11).

In a two-necked round-bottom flask of 100 mL, it was placed 1,3-bis(methoxymethoxy)benzene (1.4 g, 7 mmol), under nitrogen atmosphere, and then 15 mL of anhydrous DMF and TMEDA (2.3 mL, 16 mmol). The reaction mixture was cooled down until -5 °C and then added *n*-BuLi (10 mL, 16 mmol), dropwise. The reaction mixture was then heated to room temperature and stirred for 1.5 hours. Then, DMF was added dropwise and kept under stirring for 2 more hours. The reaction was quenched with NH₄Cl. The mixture was extracted with ethyl acetate (3 x 20mL). The organic layer was dried over Na₂SO₄, filtered and concentrated on a rotary evaporator. The crude product was purified by silica gel flash chromatography (*n*-hexane/ethyl acetate 7:3) and the compound was isolated as a yellow solid (710 mg, 44 %).

m. p.: 53 – 56 °C

¹H NMR (300.13 MHz, DMSO-*d*₆) δ (ppm): 10.42 (H, s) 7.50 (H, *t*, J = 8.5 Hz), 6.86 (2H, *d*, J = 8.5 Hz), 5.27 (4H, s), 3.4 (6H, s).

IR ν_{max} (cm⁻¹) (KBr): 2995, 2958, 2913, 2851, 2828, 2360, 2342, 1691, 1599, 1474, 1443, 1417, 1397, 1311, 1253, 1206, 1189, 1103, 919, 904, 820, 794, 729, 668, 658.

EIMS m/z (%): 227 (14, [M+1]⁺), 226 (5, [M]⁺), 225 (12), 195 (30), 166 (13), 165 (27), 164 (100), 151 (26), 149 (11), 77 (11), 65 (10), 64 (24), 63 (71), 62 (16), 53 (16), 52(13), 51 (32), 50 (12).

All spectroscopic values are in agreement with published data ^[60].

3.6.Synthesis of building block E.

3.6.1. Synthesis of methyl 2,6-dihydroxybenzoate (13).

In a two-necked round-bottom flask, it was placed 2,6-dihydroxybenzoic acid (1.00 g, 6.49 mmol) and potassium carbonate (897 mg, 6.49 mmol) in anhydrous acetone under nitrogen atmosphere. After 2 minutes, dimethyl sulfate (677 μ L, 7.14 mmol) was added to the mixture, staying stirring for 5 hours. The mixture was partially evaporated and HCl 5% and a saturated solution of NaHCO₃ were added and then extracted with ethyl acetate (3 x 15 mL). The organic layer was dried over Na₂SO₄, filtered and concentrated on a rotary evaporator. The crude product was purified by flash chromatography (*n*-hexane/ethyl acetate 9:1), yielding a white solid (76 %, 850 mg).

m. p.: 56 – 58 °C

¹H NMR (300.13 MHz, DMSO-*d*₆) δ (ppm): 9.99 (2H, s), 7.10 (H, *t*, J = 8.2 Hz), 6.35 (2H, *d*, J = 8.2 Hz), 3.99 (3H, s).

¹³C NMR (75.47 MHz, DMSO-*d*₆) δ (ppm): 168.4, 157.3, 132.4, 107.3, 106.8, 52.0.

IR ν_{\max} (cm⁻¹) (KBr): 3446, 2960, 2931, 2851, 2826, 2360, 2342, 1682, 1403, 1205, 1191, 955, 831, 758.

EIMS *m/z* (%): 169 (80, [M+1]⁺), 168 (100, [M]⁺), 137 (20), 108 (19), 53 (14), 52 (21), 51 (20).

All spectroscopic values are in agreement with published data [61].

3.6.2. Synthesis of methyl 2,6-bis(methoxymethoxy)benzoate (14).

In a two-necked round-bottom flask of 250 mL, it was placed methyl 2,6-dihydroxybenzoate (160 mg, 1 mmol) and NaH (152 mg of a 60% suspension in mineral oil, 4 mmol) and, under nitrogen atmosphere, 20 mL of anhydrous DMF. The reaction mixture was kept at 0°C for 15 minutes and then added dropwise MOMCl (0,3 mL, 4 mmol). The mixture was warmed to room temperature gradually and kept for 5 hours in these conditions. The reaction mixture was then poured into water and extracted with ethyl acetate (3 x 30 mL). The organic phase was dried over Na₂SO₄, filtered and the solvent was removed by rotary evaporation. The crude product was purified by silica gel flash chromatography (*n*-hexane/ethyl acetate 8:2) and the compound was isolated as a colorless oil (172 mg, 71%).

¹H NMR (300.13 MHz, DMSO-*d*₆) δ (ppm): 7.32 (H, *t*, *J* = 8.4 Hz), 6.84 (2H, *d*, *J* = 8.4 Hz), 5.20 (4H, *s*), 3.80 (3H, *s*), 3.35 (6H, *s*).

¹³C NMR (75.47 MHz, DMSO-*d*₆) δ (ppm): 165.8, 154.0, 130.9, 115.4, 108.1, 94.0, 55.7, 52.1.

IR ν_{\max} (cm⁻¹) (KBr): 3454, 2921, 2850, 1732, 1600, 1470, 1039.

EIMS *m/z* (%): 257 (23, [M+1]⁺), 256 (16, [M]⁺), 226 (10), 225 (100), 195 (10), 181 (34), 180 (95), 165 (18), 151 (50), 150 (15), 136 (25), 75 (12).

3.7. Synthesis of Yicathins C and B.

3.7.1. Synthesis of (2,6-bis(methoxymethoxy)-4-methylphenyl)(4-(((tert-butyldimethylsilyl)oxy)methyl)-2,6-dimethoxyphenyl)methanol (15).

In a two-necked round-bottomed flask of 250 mL, it was placed ((4-bromo-3,5-dimethoxybenzyl)oxy)(tert-butyl)dimethylsilane (1.60 g, 4.43 mmol) – building block A – and then added anhydrous THF, in argon atmosphere. The apparatus was cooled down to -78 °C and added, dropwise, *n*-BuLi (4.15 mL, 6.64 mmol), staying stirring for 7 minutes. After that time, 2,6-bis(methoxymethoxy)-4-methylbenzaldehyde (1.28 g, 5.31 mmol) – building block B – was added. The mixture stayed at -78 °C for 1.5 hours and then warmed to room temperature for 2 hours. To the reaction mixture, it was added a saturated solution of NH₄Cl and the solution was extracted with ethyl acetate (3 x 20 mL). The organic layer was dried under Na₂SO₄, filtered and the solvent evaporated. The crude product was purified by silica gel flash chromatography (*n*-hexane/ethyl acetate 8:2), allowing a colorless oil (921 mg, 41 %).

¹H NMR (300.13 MHz, DMSO-*d*₆) δ (ppm): 6.68 (2H, s), 6.64 (2H, s), 6.53 (OH, *d*, *J* = 10.3 Hz), 5.51 (H, *d*, *J* = 10.3 Hz), 5.22 (4H, s), 4.78 (2H, s), 3.84 (6H, s), 3.38 (6H, s), 2.34 (3H, s), 1.04 (9H, s), 0.20 (6H, s).

¹³C NMR (75.47 MHz, DMSO-*d*₆) δ (ppm): 157.7, 155.3, 141.3, 137.1, 118.9, 117.9, 108.5, 101.8, 94.1, 64.2, 63.4, 55.6, 55.4, 25.8, 21.4, 18.0, -5.3.

IR ν_{\max} (cm⁻¹) (KBr): 3565, 2956, 2859, 2827, 1613, 1586, 1456, 1396, 1294, 1223, 1112, 965, 923, 826, 781, 725, 684.

EIMS *m/z* (%): 523 (4, [M+1]⁺), 329 (30), 326 (25), 325 (54), 298 (25), 295 (100), 282 (59), 269 (78), 255 (44), 238 (27), 237 (88), 226 (60), 211 (58), 209 (67), 195 (72), 194 (87), 180 (38), 178 (32), 165 (42), 163 (37), 151 (66), 137 (30), 135 (42), 89 (56), 73 (83).

3.7.2. Synthesis of (2,6-bis(methoxymethoxy)-4-methylphenyl)(4-(((tert-butyl)dimethylsilyl)oxy)methyl)-2,6-dimethoxyphenyl)methanone (16).

Via oxidation of (2,6-bis(methoxymethoxy)-4-methylphenyl)(4-(((tert-butyl)dimethylsilyl)oxy)methyl)-2,6-dimethoxyphenyl)methanol (15).

To a solution of (2,6-bis(methoxymethoxy)-4-methylphenyl)(4-(((tert-butyl)dimethylsilyl)oxy)methyl)-2,6-dimethoxyphenyl)methanol (760 mg, 1.45 mmol) in dichloromethane (8 mL), it was added solid Dess-Martin periodinane (925 mg, 2.18 mmol), at room temperature, allowing a concentration of 0.3 M of DMP. The reaction mixture instantly turned bright pink and stayed stirring overnight. After that time, it was added a solution of NaOH 10% and a saturated solution of Na₂S₂O₃. The mixture was extracted with dichloromethane (3 x 10 mL). The organic layer was dried under Na₂SO₄, filtered and the solvent evaporated. The crude product was purified by silica gel flash chromatography (*n*-hexane/ethyl acetate 8:2), allowing a colorless oil (370 mg, 49 %).

To a solution of (2,6-bis(methoxymethoxy)-4-methylphenyl)(4-(((tert-butyl)dimethylsilyl)oxy)methyl)-2,6-dimethoxyphenyl)methanol (540 mg, 1.03 mmol) in DMSO, it was added IBX (707 mg, 1.14 mmol), at room temperature. The reaction mixture instantly turned bright pink and stayed stirring for 3 hours. After that time, the reaction mixture was treated with a solution of Na₂S₂O₃ 10% and a saturated solution of NaHCO₃ and then extracted with ethyl acetate (3 x 15 mL). The organic layer was dried under Na₂SO₄, filtered and the solvent evaporated. The crude product was used in the next step with no further purification (500 mg, 93 %).

Via reaction of building block A with C.

In a two-necked round-bottomed flask of 250 mL, it was placed ((4-bromo-3,5-dimethoxybenzyl)oxy)(tert-butyl)dimethylsilane (840 mg, 2.93 mmol) – building block A – and then added anhydrous THF, in argon atmosphere. The apparatus was cooled down to -78 °C and added, dropwise, *n*-BuLi (2.75 mL, 4.40 mmol), staying stirring for 7 minutes. After that time, methyl 2,6-bis(methoxymethoxy)-4-methylbenzoate (754 mg, 2.79 mmol) – building block C – was added. The mixture stayed at -78 °C for 1.5 hours and then warmed to room temperature for 2 hours. To the reaction mixture, it was added a saturated solution of NH₄Cl and the solution was extracted with ethyl acetate (3 x 15 mL). The organic layer was dried under Na₂SO₄, filtered and the solvent evaporated.

The crude product was purified by flash chromatography (*n*-hexane/ethyl acetate 8:2), allowing a colorless oil (250 mg, 21 %).

¹H NMR (500.16 MHz, DMSO-*d*₆) δ (ppm): 6.59 (2H, s), 6.54 (2H, s), 4.99 (4H, s), 4.68 (2H, s), 3.60 (6H, s), 3.17 (6H, s), 2.25 (3H, s), 0.91 (9H, s), 0.07 (6H, s).

¹³C NMR (75.47 MHz, DMSO-*d*₆) δ (ppm): 192.0, 157.9, 155.1, 145.2, 140.9, 120.4, 119.8, 108.6, 101.8, 93.9, 64.2, 55.9, 55.5, 25.9, 21.8, 18.1, -5.2.

IR ν_{\max} (cm⁻¹) (KBr): 2957, 2828, 1704, 1608, 1584, 1463, 1455, 1393, 1153, 1112, 1046.

EIMS m/z (%): 309 (22), 296 (17), 295 (100), 269 (17), 239 (18), 209 (16), 194 (22), 193 (24), 163 (23), 135 (38), 89 (32), 73 (50).

3.7.3. Synthesis of (2,6-dihydroxy-4-methylphenyl)(4-(hydroxymethyl)-2,6-dimethoxyphenyl)methanone (17).

In a round-bottom flask of 50 mL, it was placed (2,6-bis(methoxymethoxy)-4-methylphenyl) (4-(((tert-butyldimethylsilyl)oxy)methyl)-2,6-dimethoxyphenyl)methanone (100 mg, 100 μmol) in methanol. At once, it was added *p*-toluenesulfonic acid (91 mg, 480 μmol) and the mixture turned red. The apparatus was warmed until the boiling point of methanol, staying stirring for 5 hours. After that time, water was added to the mixture and the solution was extracted with ethyl acetate (3 x 10 mL). The organic layer was dried under Na_2SO_4 , filtered and the solvent evaporated. The product did not go for further purification, originating an orange solid. The crude product was used for the next reaction (88%, 54 mg).

Purification: The extract (35 mg) was washed with a solution of *n*-hexane/ethyl acetate/formic acid (7:3:0.1) and filtered. The solution was evaporated and the solid was then purified by preparative HPLC, yielding a yellow solid (1 mg).

m. p.: 83 – 86 °C.

^1H NMR (300.13 MHz, $\text{DMSO-}d_6$) δ (ppm): 11.62 (2OH, s), 6.67 (2H, s), 6.14 (2H, s), 5.10 (OH, s), 4.55 (2H, s), 3.70 (6H, s), 2.20 (3H, s).

^{13}C NMR (75.47 MHz, $\text{DMSO-}d_6$) δ (ppm): 198.8, 162.3, 155.7, 148.4, 144.8, 120.4, 109.1, 107.7, 101.9, 63.0, 55.7, 21.7.

IR ν_{max} (cm^{-1}) (KBr): 3447, 2922, 1717, 1641, 1611, 1583, 1465, 1418, 1385, 1373, 1294, 1265, 1237, 1214, 1127.

EIMS m/z (%): 535 (2, $[\text{M}+\text{TMS}]^+$), 520 (1), 519 (13), 416 (10), 415 (28), 283 (15), 282 (14), 281 (54), 267 (10), 209 (13), 191 (10), 163 (11), 149 (15), 147 (11), 89 (15), 75 (15), 73 (100).

3.7.4. Synthesis of 1-hydroxy-6-(hydroxymethyl)-8-methoxy-3-methyl-9H-xanthen-9-one (18).

In a reaction vessel of 35 mL, it was placed (2,6-dihydroxy-4-methylphenyl)(4-(hydroxymethyl)-2,6-dimethoxyphenyl)methanone (60 mg, 188 μmol) and then added water/methanol (9:1). To the solution was added NaOH (90 mg, 2.26 mmol) and the reaction vessel was placed in the microwave and heated until 130 °C for 10 minutes. After that time, HCl 5% and water were added to the vessel and mixture was filtered under pressure, allowing an orange solid and it was used for the next reaction (33 mg, 61 %).

Purification: The extract (70 mg) was firstly passed by flash chromatography and then purified by preparative HPLC, yielding a yellow solid (28 mg).

m. p.: 207 – 209 °C.

¹H NMR (300.13 MHz, DMSO-*d*₆) δ (ppm): 13.03 (OH, s), 7.02 (H, s), 6.92 (H, s), 6.78 (H, s), 6.57 (H, s), 5.61 (OH, *t*, J = 5.7 Hz), 4.62 (2H, *d*, J = 5.7 Hz), 3.90 (3H, s), 2.35 (3H, s).

¹³C NMR (75.47 MHz, DMSO-*d*₆) δ (ppm): 181.1, 161.0, 160.1, 157.4, 154.8, 152.9, 148.2, 111.0, 108.8, 106.8, 106.7, 106.2, 103.9, 62.4, 56.3, 21.9.

IR ν_{max} (cm⁻¹) (KBr): 3460, 2924, 2853, 1651, 1608, 1560, 1468, 1426, 1265, 1229, 1110, 1075, 1064, 1052, 1031, 819, 773.

EIMS *m/z* (%): 431 (1, [M+TMS]⁺), 416 (15), 415 (26), 311 (22), 310 (17), 283 (60), 253 (20), 237 (15), 89 (32), 73 (100), 59 (42).

3.7.5. Synthesis of 8-hydroxy-1-methoxy-6-methyl-9-oxo-9H-xanthene-3-carboxylic acid - Yicathin C (19).

In a Erlenmeyer of 50 mL, it was placed the sulfuric acid (2.81 mL, 53 mmol) and Chromium(VI) oxide (38 mg, 384 μmol) and then dissolved in water (4.39 mL). In a round-bottom flask, it was placed 1-hydroxy-6-(hydroxymethyl)-8-methoxy-3-methyl-9H-xanthen-9-one (22 mg, 77 μmol) and dissolved in acetone, posteriorly adding 84 μL of the $\text{H}_2\text{SO}_4/\text{CrO}_3$ solution. The reaction mixture stayed at room temperature, stirring for 30 minutes. After this time, 2-propanol was added and the solution was extracted with ethyl acetate (3 x 5 mL). The organic layer was dried under Na_2SO_4 , filtered and the solvent evaporated. The crude product has 4 products, being the desired product in only 30 %.

In a Erlenmeyer of 25 mL, it was placed the periodic acid (2,5 g, 11 mmol) and Chromium(VI) oxide (5 mg, 50 μmol) and then dissolved in wet acetonitrile (75 %). In a round-bottom flask was placed 1-hydroxy-6-(hydroxymethyl)-8-methoxy-3-methyl-9H-xanthen-9-one (246 mg, 859 μmol) and dissolved in wet acetonitrile (75 %), posteriorly adding 25 mL of the $\text{H}_5\text{IO}_6/\text{CrO}_3$ solution over 40 hours. The reaction mixture stayed at room temperature, stirring for 40 hours. After this time, NaHSO_3 was added and the solution was extracted with ethyl acetate (3 x 15 mL). The organic layer was dried under Na_2SO_4 , filtered and the solvent evaporated. The crude product was used for the next reaction (130 mg, 50 %).

In a round-bottom flask, it was placed 1-hydroxy-6-(hydroxymethyl)-8-methoxy-3-methyl-9H-xanthen-9-one (170 mg, 598 μmol) in dioxane. To the flask, it was added a solution of KOH (50 mg, 897 μmol) and then KMnO_4 (164 mg, 1.49 mmol). The reaction mixture stayed stirring for 4 days. The solution was filtered through Celite and extracted with ether (2 x 10 mL). The aqueous phase was acidified with HCl 5% and then extracted with ether (3 x 15 mL). The organic layer was dried over Na_2SO_4 , filtered and the solvent evaporated. The reaction allows a yellow solid, which contain a mixture of the starting material and the desired product in 99:1 proportion.

In a reaction vessel of 10 mL, it was placed 1-hydroxy-6-(hydroxymethyl)-8-methoxy-3-methyl-9H-xanthen-9-one (66 mg, 207 μmol), $\text{Na}_2\text{WO}_4 \cdot 2\text{H}_2\text{O}$ (3 mg, 9.22 μmol) and TBAHS (3 mg, 9.22 μmol). To the mixture, it was added a solution of H_2O_2 30 % (119 μL , 1.15 mmol), which was stirred in a vortex. The reaction vessel, it was placed in the microwave, heated until 90 °C for 30 minutes. To the reaction vessel was added a solution of Na_2CO_3 20% and then extracted with ethyl acetate (2 x 10 mL). The aqueous phase was acidified and extracted with ethyl acetate (3 x 15 mL). The reaction barely occurred, with a percentage of about 1 % of the desired product.

Purification: The extract (40 mg) was washed with a solution of *n*-hexane/ethyl acetate/formic acid (7:3:0.1) and filtered. The solution was evaporated and the solid was then purified by preparative HPLC, yielding a yellow solid (7 mg).

m. p.: 203 – 206 °C.

¹H NMR (500.16 MHz, DMSO-*d*₆) δ (ppm): 13.85 (OH, *s*), 12.74 (OH, *s*), 7.54 (1H, *d*, *J* = 1.4 Hz), 7.36 (1H, *d*, *J* = 1.4 Hz), 6.83 (1H, *q*, *J* = 1.3 Hz), 6.63 (1H, *q*, *J* = 1.3 Hz), 3.93 (3H, *s*), 2.39 (3H, *s*).

¹³C NMR (125.77 MHz, DMSO-*d*₆) δ (ppm): 180.8, 164.8, 160.9, 160.4, 157.0, 154.7, 148.9, 135.9, 112.9, 111.4, 110.2, 107.1, 107.0, 105.8, 53.0, 21.9.

IR ν_{\max} (cm⁻¹) (KBr): 3446, 2924, 2853, 1718, 1652, 1615, 1559, 1478, 1419, 1386, 1329, 1301, 1250, 1203, 1141, 1115, 1087, 1006, 895, 824, 770.

EIMS *m/z* (%): 445 (0.5, [M+TMS]⁺), 429 (10), 369 (10), 313 (22), 312 (100), 297 (21), 283 (33), 241 (15), 217 (15).

All spectroscopic values are in agreement with published data ^[18].

3.7.6. Synthesis of methyl 8-hydroxy-1-methoxy-6-methyl-9-oxo-9H-xanthene-3-carboxylate - Yicathin B (20).

In a round-bottom flask, it was placed 8-hydroxy-1-methoxy-6-methyl-9-oxo-9H-xanthene-3-carboxylic acid (45 mg, 150 μmol) in methanol and then added sulfuric acid (24 μL , 450 μmol). The reaction mixture was heated until the boiling point of methanol and stayed stirring over the weekend. Water and sodium bicarbonate was added to the flask and the solution extracted with ethyl acetate (3 x 5 mL). The organic layer was dried under Na_2SO_4 , filtered and the solvent evaporated. The crude product was purified by flash chromatography (*n*-hexane/ethyl acetate 8:2), allowing a yellow solid (23 mg, 55 %).

m. p.: 155 -157 $^{\circ}\text{C}$.

^1H NMR (500.16 MHz, $\text{DMSO-}d_6$) δ (ppm): 12.72 (OH, s), 7.51 (H, *d*, $J = 1.4$ Hz), 7.34 (H, *d*, $J = 1.4$ Hz), 6.81 (H, *q*, $J = 1.3$ Hz), 6.62 (H, *q*, $J = 1.3$ Hz), 5.76 (3H, s), 3.93 (3H, s), 2.83 (3H, s).

^{13}C NMR (125.77 MHz, $\text{DMSO-}d_6$) δ (ppm): 180.8, 164.8, 160.8, 160.4, 157.0, 154.7, 148.9, 135.8, 112.9, 111.4, 110.2, 107.0, 106.9, 105.7, 54.9, 53.0, 21.9.

IR ν_{max} (cm^{-1}) (KBr): 3004, 2955, 2920, 2850, 1735, 1659, 1564, 1508, 1474, 1428, 1360, 1333, 1305, 1272, 1242, 1209, 1189, 1155, 1139, 1114, 1090, 989, 880, 835, 823, 807.

EIMS m/z (%): 387 (1, $[\text{M}+\text{TMS}]^+$), 371 (18), 356 (14), 312 (10), 299 (16), 298 (83), 297 (10), 271 (22), 270 (100), 269 (18), 242 (17), 241 (51), 227 (10), 143 (18), 134 (11).

All spectroscopic values are in agreement with published data ^[18].

3.8.Synthesis of Analogues C and B.

3.8.1. Synthesis of (2,6-bis(methoxymethoxy)phenyl)(4-(((tert-butyl)dimethylsilyl)oxy)methyl)-2,6-dimethoxyphenyl)methanol (21).

In a two-necked round-bottomed flask of 250 mL, it was placed ((4-bromo-3,5-dimethoxybenzyl)oxy)(tert-butyl)dimethylsilane (1.00 g, 2.77 mmol) – building block A – and then added anhydrous THF, in argon atmosphere. The apparatus was cooled down to -78 °C and added, dropwise, *n*-BuLi (2.59 mL, 4.15 mmol), staying stirring for 7 minutes. After that time, 2,6-bis(methoxymethoxy)benzaldehyde (751 mg, 3.32 mmol) – building block D – was added. The mixture stayed at -78 °C for 1.5 hours and then warmed to room temperature for 2 hours. To the reaction mixture, it was added a saturated solution of NH₄Cl and the solution was extracted with ethyl acetate (3 x 20 mL). The organic layer was dried under Na₂SO₄, filtered and the solvent evaporated. The crude product was purified by silica gel flash chromatography (*n*-hexane/ethyl acetate 8:2), yielding a colorless oil (1.22 g, 87 %).

m. p.: 62- 65 °C.

¹H NMR (300.13 MHz, DMSO-*d*₆) δ (ppm): 7.07 (2H, *d*, *J* = 8.3 Hz), 6.68 (2H, *d*, *J* = 8.3 Hz), 6.56 (2H, *s*), 6.45 (OH, *d*, *J* = 10.2 Hz), 5.42 (H, *d*, *J* = 10.2 Hz), 5.11 (4H, *s*), 4.65 (2H, *s*), 3.71 (6H, *s*), 3.25 (6H, *s*), 0.91 (9H, *s*), 0.07 (6H, *s*).

¹³C NMR (75.47 MHz, DMSO-*d*₆) δ (ppm): 157.7, 155.5, 141.4, 127.7, 121.8, 117.8, 107.8, 101.8, 94.1, 64.2, 63.5, 55.7, 55.5, 25.8, 18.0, -5.3.

IR ν_{\max} (cm⁻¹) (KBr): 3511, 2956, 2893, 2857, 1608, 1584, 1472, 1418, 1361, 1256, 1242, 1226, 1150, 1105, 1080, 1051, 1021, 965, 923, 907, 840, 816, 778.

EIMS *m/z* (%): 309 (28), 296 (19), 295 (100), 239 (15), 227 (19), 181 (24), 151 (26), 91 (18), 89 (25), 73 (68).

3.8.2. Synthesis of (2,6-bis(methoxymethoxy)phenyl)(4-(((tert-butyl)dimethylsilyl)oxy)methyl)-2,6-dimethoxyphenyl)methanone (22).

Via oxidation of (2,6-bis(methoxymethoxy)phenyl)(4-(((tert-butyl)dimethylsilyl)oxy)methyl)-2,6-dimethoxyphenyl)methanol (21).

To a solution of (2,6-bis(methoxymethoxy)phenyl)(4-(((tert-butyl)dimethylsilyl)oxy)methyl)-2,6-dimethoxyphenyl)methanol (1.50 g, 2.95 mmol) in dichloromethane (15 mL), it was added solid Dess-Martin periodinane (1.88 g, 4.42 mmol), at room temperature, allowing a concentration of 0.3 M of DMP. The reaction mixture instantly turned bright pink and stayed stirring overnight. After that time, it was added a solution of NaOH 10% and a saturated solution of Na₂S₂O₃. The mixture was extracted with dichloromethane (3 x 10 mL). The organic layer was dried under Na₂SO₄, filtered and the solvent evaporated. The crude product was used in the next step (1.30 g, 87 %).

To a solution of (2,6-bis(methoxymethoxy)phenyl)(4-(((tert-butyl)dimethylsilyl)oxy)methyl)-2,6-dimethoxyphenyl)methanol (50 mg, 98 μmol) in DMSO, it was added IBX (67 mg, 108 μmol), at room temperature. The reaction mixture instantly turned bright pink and stayed stirring for 3 hours. After that time, the reaction mixture was treated with a solution of Na₂S₂O₃ 10% and a saturated solution of NaHCO₃ and then extracted with ethyl acetate (3 x 15 mL). The organic layer was dried under Na₂SO₄, filtered and the solvent evaporated. The crude product was purified by preparative TLC (*n*-hexane/ethyl acetate 1:1 with 1% of formic acid), yielding a colorless oil (36 mg, 80 %).

Via reaction of building block A with E.

In a two-necked round-bottomed flask of 250 mL, it was placed ((4-bromo-3,5-dimethoxybenzyl)oxy)(tert-butyl)dimethylsilane (1.00 g, 2.77 mmol) – building block A – and then added anhydrous THF, in argon atmosphere. The apparatus was cooled down to -78 °C and added, dropwise, *n*-BuLi (2.59 mL, 4.15 mmol), staying stirring for 7 minutes. After that time, methyl 2,6-bis(methoxymethoxy)benzoate (851 mg, 3.32 mmol) – building block E – was added. The mixture stayed at -78 °C for 1.5 hours and the warmed to room temperature for 2 hours. To the reaction mixture, it was added a saturated solution of NH₄Cl and the solution was extracted with ethyl acetate (3 x 15 mL). The organic layer was dried under Na₂SO₄, filtered and the solvent evaporated. The crude product was purified by flash chromatography (*n*-hexane/ethyl acetate 8:2), allowing a colorless oil (260 mg, 19 %).

¹H NMR (300.13 MHz, DMSO-*d*₆) δ (ppm): 7.27 (H, *t*, *J* = 8.4 Hz), 6.75 (2H, *d*, *J* = 8.4 Hz), 6.64 (2H, *s*), 5.06 (4H, *s*), 4.73 (2H, *s*), 3.63 (6H, *s*), 3.21 (6H, *s*), 0.95 (9H, *s*), 0.11 (6H, *s*).

¹³C NMR (75.47 MHz, DMSO-*d*₆) δ (ppm): 191.7, 158.1, 154.9, 145.5, 130.6, 123.0, 119.3, 107.8, 101.8, 93.9, 64.1, 55.8, 55.4, 25.8, 18.0, -5.3.

IR ν_{\max} (cm⁻¹) (KBr): 2958, 2931, 2901, 2856, 1682, 1593, 1474, 1412, 1363, 1308, 1253, 1228, 1153, 1125, 1095, 1049, 964, 917, 899, 848, 837, 815, 797.

EIMS *m/z* (%): 297 (10), 296 (18), 295 (100), 269 (20), 237 (15), 225 (27), 209 (10), 193 (23), 163 (12), 135 (14), 89 (13), 73 (18).

3.8.3. Synthesis of (2,6-dihydroxyphenyl)(4-(hydroxymethyl)-2,6-dimethoxyphenyl)methanone (23).

In a round-bottom flask of 50 mL, it was placed (2,6-bis(methoxymethoxy)phenyl)(4-((tert-butyldimethylsilyl)oxy)-2,6-dimethoxyphenyl)methanone (1.25 g, 2.47 mmol) in methanol. At once, it was added the *p*-toluenesulfonic acid (1.03 g, 5.43 mmol) and the mixture turned red. The apparatus was warmed until the boiling point of methanol, staying stirring overnight. After that time, water was added to the mixture and the solution was extracted with ethyl acetate (3 x 10 mL). The organic layer was dried under Na₂SO₄, filtered and the solvent evaporated. The crude product was used in the next step (550 mg, 73 %).

Purification: The crude product (40 mg) was purified by flash chromatography (*n*-hexane/ethyl acetate 6:4 with 1% of formic acid), allowing a yellow solid (21 mg).

m. p.: 111 - 113 °C.

¹H NMR (300.13 MHz, DMSO-*d*₆) δ (ppm): 11.59 (2OH, s), 7.26 (H, *t*, *J* = 8.2 Hz), 6.65 (2H, s), 6.27 (2H, *d*, *J* = 8.2 Hz), 5.32 (OH, s), 4.52 (2H, s), 3.67 (6H, s).

¹³C NMR (75.47 MHz, DMSO-*d*₆) δ (ppm): 199.6, 162.4, 155.8, 145.0, 137.2, 120.4, 111.2, 107.0, 101.9, 63.1, 55.7.

IR ν_{\max} (cm⁻¹) (KBr): 3545, 3385, 2940, 2360, 2342, 1589, 1456, 1418, 1351 1275, 1255, 1239, 1121, 827, 766, 752, 710.

EIMS *m/z* (%): 505 (4), 402 (12), 401 (28), 312 (13), 311 (10), 270 (12), 269 (28), 268 (26), 267 (100), 265 (14), 244 (12), 195 (10), 177 (17), 149 (16), 147 (11), 90 (12), 75 (11), 73 (83).

3.8.4. Synthesis of 8-hydroxy-3-(hydroxymethyl)-1-methoxy-9H-xanthen-9-one (24).

In a reaction vessel of 35 mL, it was placed (2,6-dihydroxyphenyl)(4-(hydroxymethyl)-2,6-dimethoxyphenyl)methanone (550 mg, 1.52 mmol) and then added water/methanol (9:1). To the solution was added NaOH (868 mg, 21.69 mmol) and the reaction vessel was placed in the microwave, heated until 130°C for 10 minutes. After that time, HCl 5 % and water were added to the vessel and mixture was filtered under pressure, yielding an orange solid and it was used for the next reaction (311 mg, 63 %).

Purification: The crude product (15 mg) was purified by preparative TLC (*n*-hexane/ethyl acetate 7:3 with 1% of formic acid), allowing a yellow solid (8 mg).

m. p.: 236 – 238 °C.

¹H NMR (500.16 MHz, DMSO-*d*₆) δ (ppm): 13.12 (OH, s), 7.65 (H, t, J = 8.2 Hz), 7.08 (H, s), 6.98 (H, d, J = 8.2 Hz), 6.97 (H, s), 6.75 (H, d, J = 8.2 Hz), 5.64 (OH, t, J = 5.0 Hz), 4.64 (2H, d, J = 5.0 Hz), 3.92 (3H, s).

¹³C NMR (125.77 MHz, DMSO-*d*₆) δ (ppm): 181.6, 161.3, 160.2, 157.5, 155.0, 153.2, 136.8, 110.4, 108.8, 108.8, 106.6, 106.2, 104.0, 62.4, 56.4.

IR ν_{\max} (cm⁻¹) (KBr): 3471, 2920, 2851, 1655, 1607, 1558, 1504, 1476, 1464, 1428, 1361, 1327, 1264, 1224, 1209, 1133, 1111, 1091, 1068, 826, 790.

EIMS m/z (%): 416 (0.5, [M+TMS]⁺), 401 (52), 341 (21), 315 (21), 314 (18), 312 (20), 311 (18), 299 (30), 298 (16), 297 (36), 296 (16), 287 (16), 286 (18), 285 (27), 272 (18), 270 (28), 269 (72), 253 (15), 252 (25), 239 (27), 237 (16), 223 (19), 89 (31), 73 (100), 59 (31).

3.8.5. Synthesis of 8-hydroxy-1-methoxy-9-oxo-9H-xanthene-3-carboxylic acid - Analogue C (25).

In Erlenmeyer of 25 mL, it was placed the periodic acid (2.99 g, 13.1 mmol) and Chromium(VI) oxide (6 mg, 63 μmol) and then dissolved in wet acetonitrile (75 %). In a round-bottom flask, it was placed 1-hydroxy-6-(hydroxymethyl)-8-methoxy-3-methyl-9H-xanthen-9-one (150 mg, 845 μmol) and dissolved in wet acetonitrile (75 %), posteriorly adding 6.6 mL of the $\text{H}_5\text{IO}_6/\text{CrO}_3$ solution over 3 hours. The reaction mixture stayed at room temperature, stirring for 3 hours. After this time, NaHSO_3 was added and the solution was extracted with ethyl acetate (3 x 15 mL). The organic layer was dried under Na_2SO_4 , filtered and the solvent evaporated. The crude product was used for the next reaction (50 mg, 37 %).

Purification: The crude product (50 mg) was purified by preparative TLC (*n*-hexane/ethyl acetate 7:3 with 1% of formic acid), allowing a yellow solid (7 mg).

m. p.: 239 – 241 °C.

^1H NMR (500.16 MHz, $\text{DMSO-}d_6$) δ (ppm): 13.19 (OH, s), 7.65 (H, t, $J = 8.2$ Hz), 7.46 (H, s), 7.43 (H, s), 6.99 (H, d, $J = 8.2$ Hz), 6.74 (H, d, $J = 8.2$ Hz), 3.93 (3H, s).

^{13}C NMR (125.77 MHz, $\text{DMSO-}d_6$) δ (ppm): 181.8, 165.8, 161.3, 159.6, 157.0, 155.2, 136.5, 129.4, 110.0, 109.9, 108.8, 107.2, 106.6, 106.5, 56.0.

IR ν_{max} (cm^{-1}) (KBr): 3447, 2922, 1708, 1654, 1594, 1473, 1384, 1352, 1261, 1100.

EIMS m/z (%): 416 (19), 415 (22), 372 (13), 371 (13), 343 (14), 299 (14), 297 (60), 295 (11), 269 (11), 253 (12), 245 (16), 241 (13), 74 (14), 73 (100).

3.8.6. Synthesis of methyl 8-hydroxy-1-methoxy-9-oxo-9H-xanthene-3-carboxylate - Analogue B (26).

In a round-bottom flask, it was placed 8-hydroxy-1-methoxy-9-oxo-9H-xanthene-3-carboxylic acid (40 mg, 133 μmol) in methanol and then added sulfuric acid (21 μL , 400 μmol). The reaction mixture was heated until the boiling point of methanol and stayed stirring over the weekend. To the flask, it was added water and sodium bicarbonate and the solution extracted with ethyl acetate (3 x 10 mL). The organic layer was dried under Na_2SO_4 , filtered and the solvent evaporated. The crude product was purified by preparative TLC (*n*-hexane/ethyl acetate 7:3 with 1% of formic acid), allowing a yellow solid (5 mg, 12 %).

m. p.: 177 – 179 $^{\circ}\text{C}$.

^1H NMR (500.16 MHz, $\text{DMSO-}d_6$) δ (ppm): 12.82 (H, s), 7.71 (H, t, $J = 8.3$ Hz), 7.62 (H, s), 7.42 (H, s), 7.03 (H, d, $J = 8.3$ Hz), 6.81 (H, d, $J = 8.3$ Hz), 4.02 (H, s), 3.95 (H, s).

^{13}C NMR (125.77 MHz, $\text{DMSO-}d_6$) δ (ppm): 181.5, 164.8, 161.1, 160.5, 157.1, 154.9, 137.2, 136.1, 113.0, 110.7, 110.2, 109.4, 106.0, 102.8, 56.7, 53.1.

IR ν_{max} (cm^{-1}) (KBr): 3446, 2921, 2851, 1728, 1647, 1636, 1617, 1592, 1559, 1472, 1458, 1435, 1419, 1325, 1307, 1231, 1209, 1114, 1098, 762.

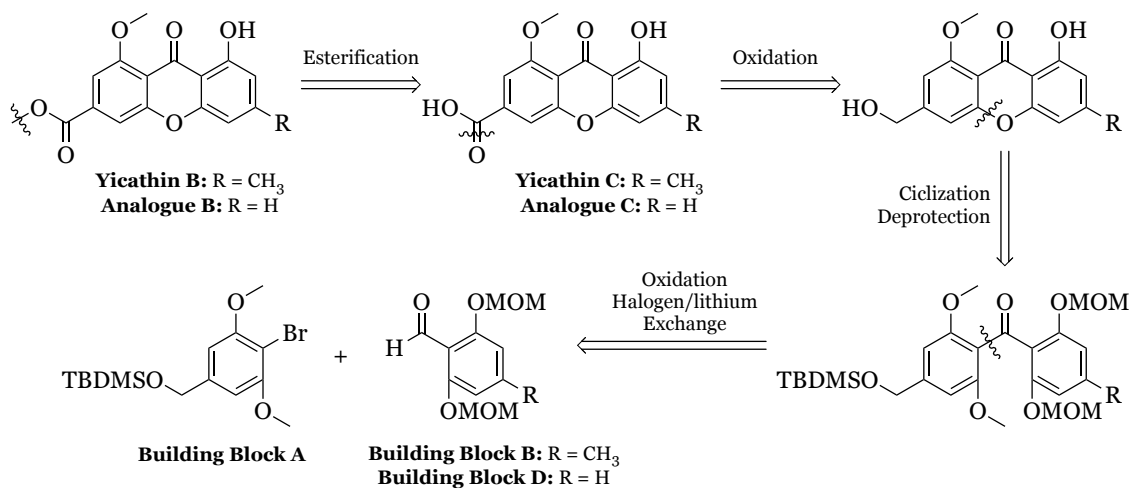
EIMS m/z (%): 372 (2, $[\text{M}+\text{TMS}]^+$), 358 (12), 357 (48), 322 (21), 285 (24), 284 (100), 283 (12), 257 (22), 256 (99), 255 (18), 202 (12), 198 (11), 185 (13), 165 (11), 73 (10).

R D
E I
S S
U C
L U
T U
S S
S
A I
N O
D N

4.1. Synthesis

4.1.1. Retrosynthesis and designing the synthetic process

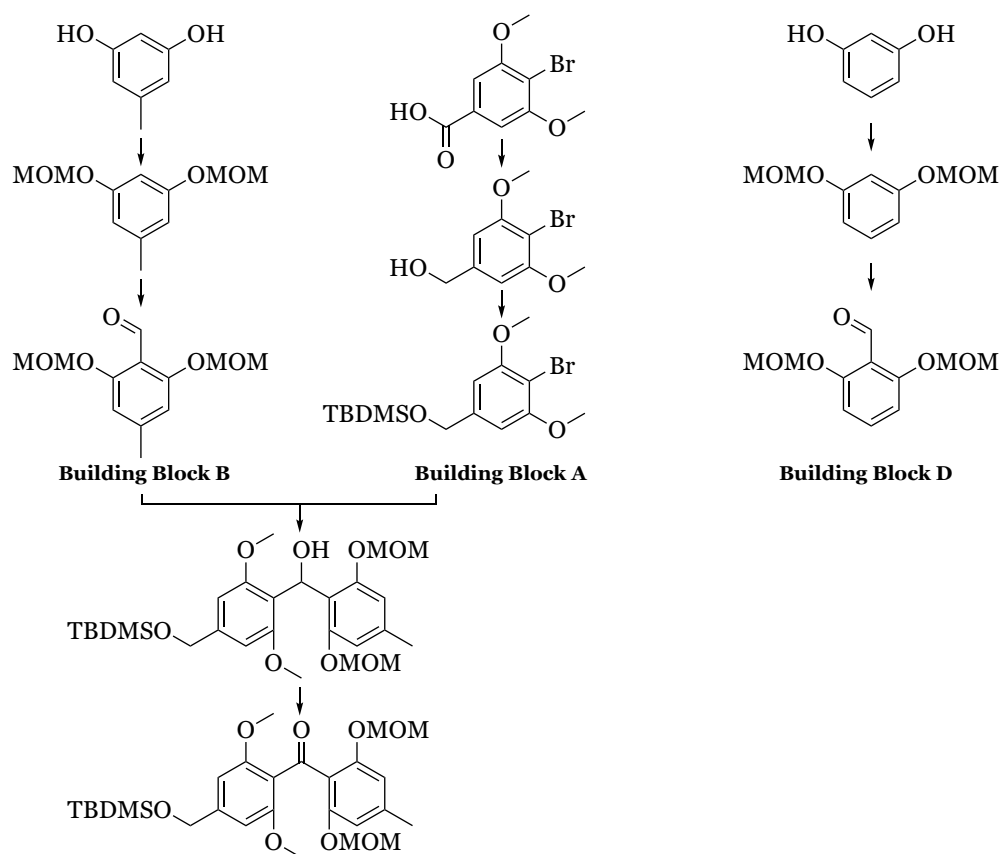
The first step towards the total synthesis of Yicathins B and C is the retrosynthetic analysis, materialized in the retrosynthetic plan show in scheme 9.



Scheme 9: Retrosynthetic analysis from the previous work.

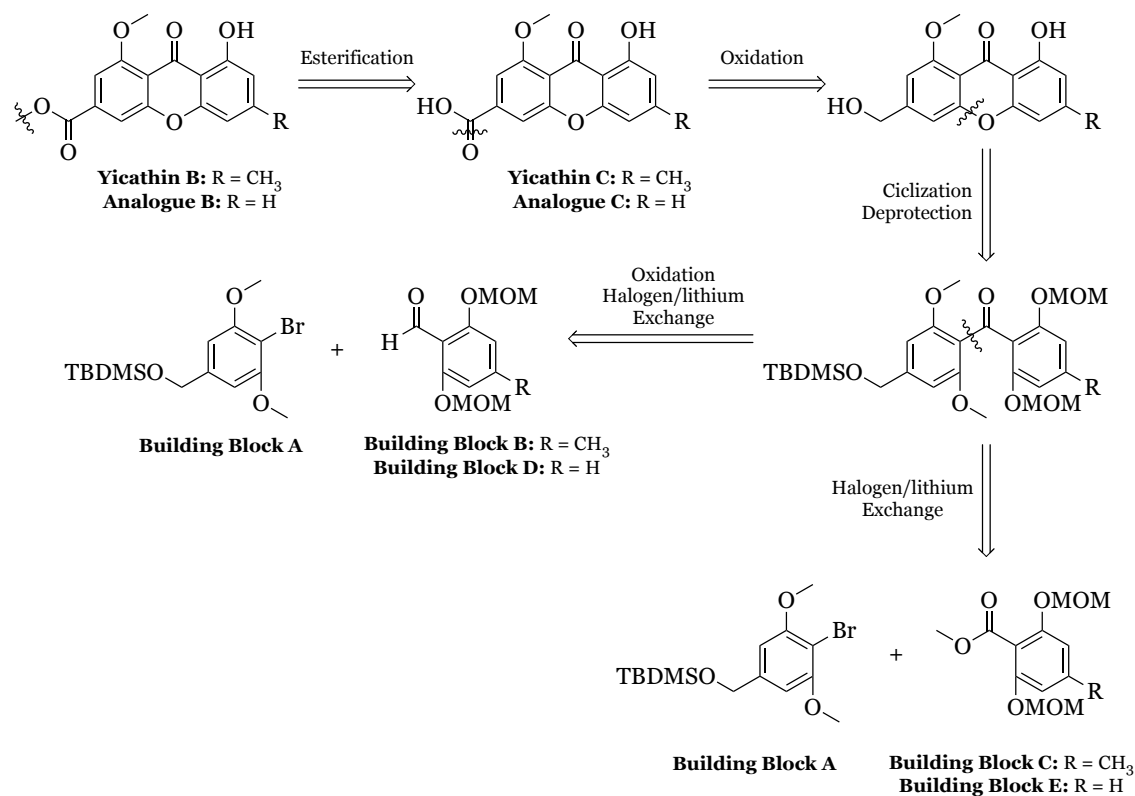
Taking into account the designed pathway, Yicathin C can be synthesized in 7 steps and Yicathin B can be synthesized from Yicathin C with an extra step. This pathway started with the synthesis of the building blocks, which will allow the synthesis of a key benzophenone by halogen/lithium exchange and posterior oxidation. The xanthone moiety is achieved by deprotection of the key benzophenone and posterior cyclization by aromatic nucleophilic substitution. Yicathin C is achieved by oxidation of the benzylic alcohol and the following esterification will yield Yicathin B.

Total synthesis of Yicathins B and C was initiated in a previous work, leading up to the key benzophenone intermediate (scheme 10).



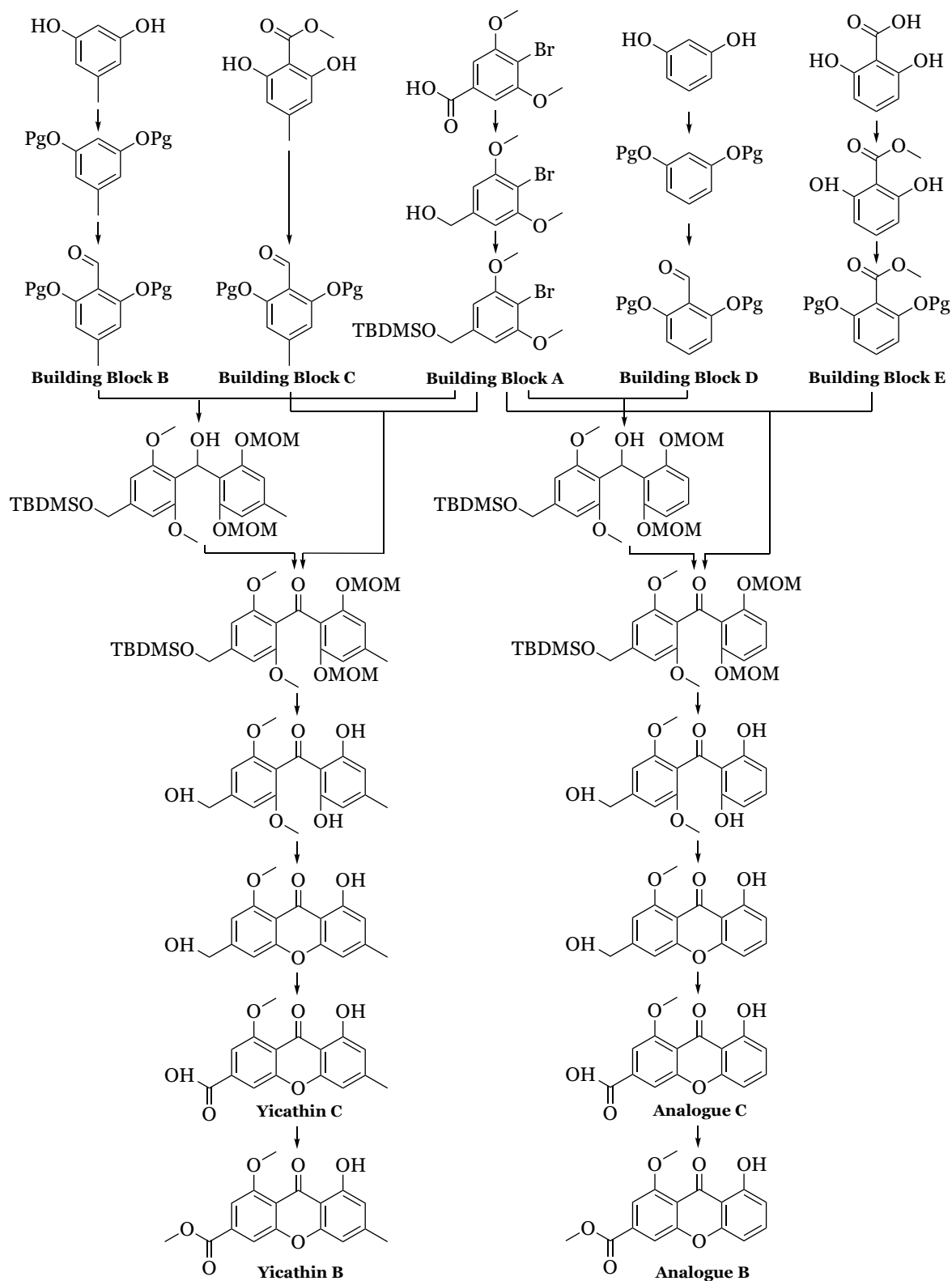
Scheme 10: Work developed by the fellow colleague.

As mentioned before, this work aimed for the improvement of the already followed synthetic pathway and for exploration of the synthesis pathway from the key benzophenone towards the desired yicathins and analogues. Therefore, a new retrosynthetic plan was thought and it is represented in scheme 11.



Scheme 11: Retrosynthetic plan for the synthesis of Yicathins and respective analogues.

The new retrosynthesis plan would decrease the number of steps in the synthesis of Yicathins, allowing a faster way to achieve the desired products. Exploiting two new building blocks, the key benzophenone can be obtained directly by a halogen/lithium exchange. The synthetic plan designed for this dissertation is summarized in scheme 12.



Scheme 12: Synthetic plan followed in this dissertation.

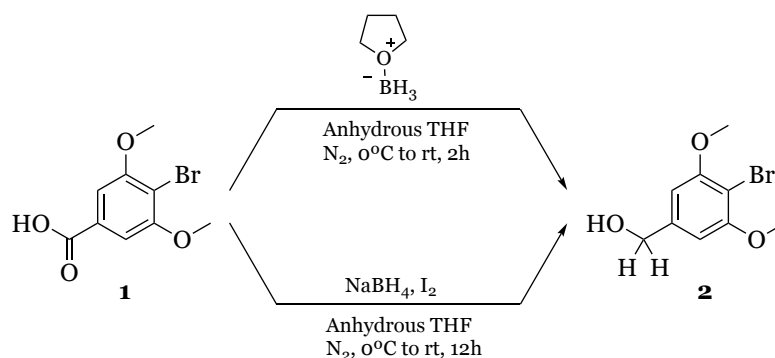
For a better understanding, this chapter is divided into three main sections, wherein the first describing the synthesis of all building blocks and the final two are dedicated to the synthesis of Yicathin B and C and Analogues B and C.

4.1.2. Synthesis of Building Blocks.

4.1.2.1. Synthesis of building block A.

4.1.2.1.1. Synthesis of (4-bromo-3,5-dimethoxyphenyl)methanol (**2**).

Scheme 13 shows the two pathways used to synthesize (4-bromo-3,5-dimethoxyphenyl)methanol (**2**).



Scheme 13: Reduction of 4-Bromo-3,5-dimethoxybenzoic acid.

The first step requires the reduction of the carboxylic acid of 4-bromo-3,5-dimethoxybenzoic acid to the corresponding benzylic alcohol.

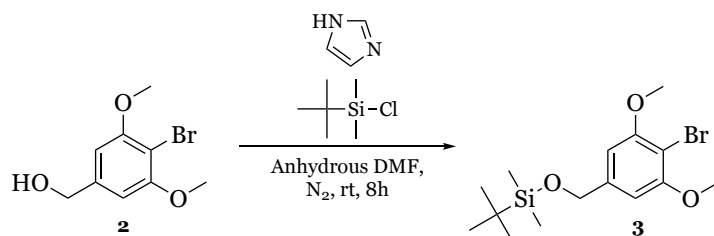
The most commonly used reducing agents are LiAlH_4 and BH_3 . LiAlH_4 is a promiscuous reagent, reducing various functional groups, however it is a slowly reducing agent when it comes to carboxylic acids [62]. Borane is a very strong Lewis acid allowing the selective and a rapid reduction of carboxylic acids [63, 64]. Borane is commercially available as a complex with tetrahydrofuran or can be formed *in situ* through the reaction between sodium borohydride and iodine [65]. Therefore, the reduction of 4-bromo-3,5-dimethoxybenzoic acid was performed with borane, either by a complex with tetrahydrofuran or by *in situ* formation by reaction of sodium borohydride with iodine.

To 4-bromo-3,5-dimethoxybenzoic acid in tetrahydrofuran, it was added borane:tetrahydrofuran complex. The reaction mixture was allowed to stir at room temperature for 2 hours, giving the desired product after work-up. Alternatively, to a suspension of sodium borohydride, it was added a suspension of the starting material, followed by addition of a suspension of iodine. The reaction mixture was allowed to stir at 40°C for 12 hours, giving the desired product after work-up. Compound **2** was obtained following the two procedures with similar yields but with a difference in terms of time of reaction.

Compound **2** was identified based on FTIR, EIMS and ^1H NMR. The FTIR spectrum showed a large stretching attributed to O-H at 3223 cm^{-1} and the absence of the characteristic band to the stretching of C=O. The EIMS show the typical bromine isotopic pattern with m/z 248 ($[\text{M}+2]^+$, 79 %) and m/z 246 ($[\text{M}]^+$, 84 %). The ^1H NMR spectrum showed the two protons of the methylene group δ_{H} 4.49 (2H, d), the signal for the hydroxyl group δ_{H} 5.35 (H, t), the signals of the two methoxy groups δ_{H} 3.82 (6H, s) and the aromatic protons δ_{H} 6.70 (2H, s).

4.1.2.1.2. Synthesis of ((4-bromo-3,5-dimethoxybenzyl)oxy)(tert-butyl)dimethylsilane (**3**).

Scheme 14 shows the synthesis of ((4-bromo-3,5-dimethoxybenzyl)oxy)(tert-butyl)dimethylsilane (**3**).



Scheme 14: Protection of (4-Bromo-3,5-dimethoxyphenyl)methanol.

In order to obtain the desired building block A, the protection of the hydroxyl with *tert*-butyldimethylsilyl group was performed. Among the several protection groups of primary alcohol, the silyl ether is one of the most popular one ^[66]. The hydroxyl group protection is needed since it would interfere with further reactions, namely the halogen/lithium exchange, and the TBDMS ether is stable under this basic conditions ^[67].

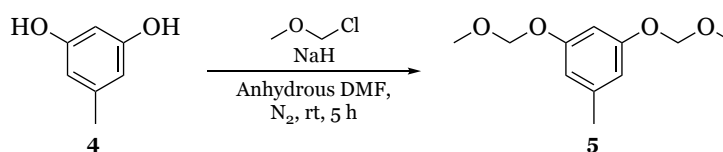
So, TBDMSCl was added to the (4-Bromo-3,5-dimethoxyphenyl)methanol in anhydrous DMF, in the presence of imidazole, and the reaction was stirred at room temperature for 5 hours ^[68]. The desired product was achieved with 88 % yield.

Compound **3** was identified based on FTIR, EIMS and ^1H NMR. The FTIR spectrum showed the absence of the stretching band attributed to O-H bond. The EIMS show the typical bromine isotopic pattern with m/z 364 ($[\text{M}+2]^+$, 2 %) and m/z 362 ($[\text{M}]^+$, 3 %). The ^1H NMR spectrum showed the signals for the methyl groups directly attached to the silyl group δ_{H} 0.07 (6H, s), the *tert*-butyl protons δ_{H} 0.90 (9H, s), two methoxy groups δ_{H} 3.79 (6H, s), the two protons of the methylene group δ_{H} 4.68 (2H, d) and the aromatic protons δ_{H} 6.66 (2H, s).

4.1.2.2. Synthesis of building block B.

4.1.2.2.1. Synthesis of 1,3-bis(methoxymethoxy)-5-methylbenzene (**5**).

Scheme 15 shows the synthesis of 1,3-bis(methoxymethoxy)-5-methylbenzene (**5**).



Scheme 15: Protection of orcinol.

The first step in the synthesis of building block B is the protection of the hydroxyl groups of orcinol with a methoxymethyl (MOM) group.

In a similar way to the building block A, protection of the hydroxyl groups is a required step before the treatment with a strong base, such as *n*-BuLi.

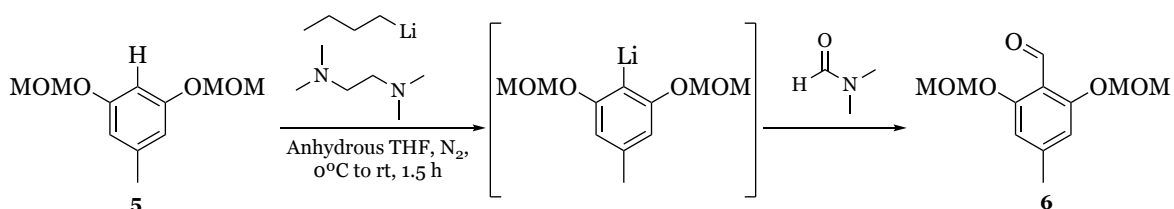
Keeping this in mind, the protect group should be resistant to basic conditions and later easily cleaved at mild conditions, so the MOM protection was used [67].

So, orcinol was treated with MOMCl in anhydrous DMF, in the presence of NaH.[69] The desired 1,3-bis(methoxymethoxy)-5-methylbenzene (**5**) was isolated, after purification, in 83 % yield.

Compound **5** was identified based on FTIR, EIMS and ¹H NMR. The FTIR spectrum showed the absence of phenol groups, as expected, and EIMS showed a structure congruent molecular peak with *m/z* 212 ([M]⁺). The ¹H NMR spectrum showed the expected signals for the methyl group δ_{H} 2.23 (3H, s), the aromatic protons δ_{H} 6.47 (H, m) and δ_{H} 6.49 (2H, dd) and the protons characteristic from the introduction of the protecting group δ_{H} 3.36 (6H, s) and δ_{H} 5.14 (4H, s).

4.1.2.2.2. Synthesis of 2,6-bis(methoxymethoxy)-4-methylbenzaldehyde (**6**).

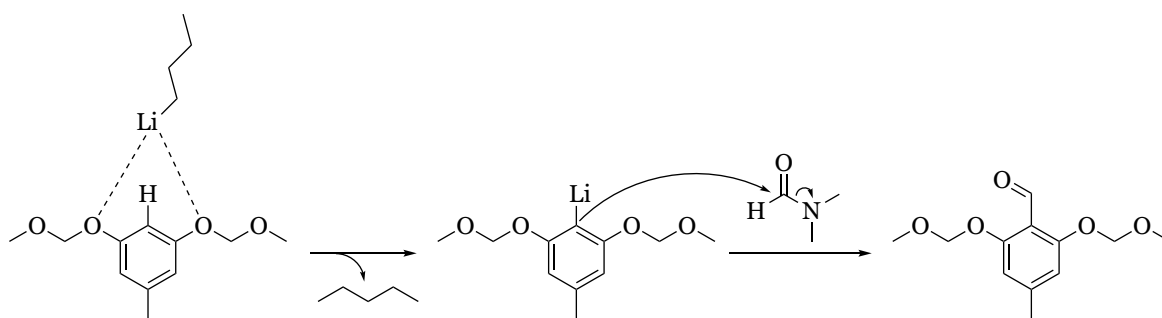
Scheme 16 shows the synthesis of 2,6-bis(methoxymethoxy)-4-methylbenzaldehyde (**6**).



Scheme 16: Formylation of 1,3-bis(methoxymethoxy)-5-methylbenzene.

The formylation at the desired position needed to obtain the desired building block **B**, was achieved by directed *ortho*-metalation followed by an aromatic electrophilic substitution.

The directed *ortho*-metalation consists in the deprotonation of the carbon *ortho* to a direct metalation group (DMG). In a first step, the alkyl lithium base coordinates with the heteroatom present in the DMG, in this case, the two MOM groups. After the coordination, the deprotonation takes place, yielding a nucleophilic lithiated intermediate. The lithiated intermediate is then treated with DMF, yielding a hemiaminal which is easily hydrolyzed during the work up into the desired aldehyde (scheme 17) [70, 71].



Scheme 17: Directed ortho-metalation mechanism.

So, *n*-BuLi was added at 0°C to 1,3-bis(methoxymethoxy)-5-methylbenzene in anhydrous THF, in the presence of TMEDA. After 1.5 hours stirring at room temperature, anhydrous DMF was added and the reaction was stirred at room temperature for 2 hours.^[69] The desired building block **B** was obtained, after purification, in 83 % yield.

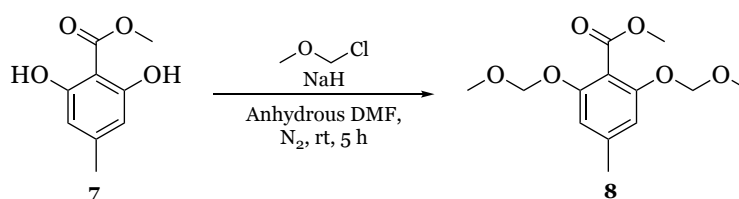
Compound **6** was identified based on FTIR, EIMS and ¹H NMR. The FTIR spectrum showed the typical carbonyl band at 1683, and EIMS showed an peak with *m/z* 241 ([*M*+1]⁺). The ¹H NMR spectrum showed the signal of the aldehyde proton δ_{H} 10.37 (H, s).

Additionally, the ^1H NMR spectrum also showed the expected signals for the methyl group δ_{H} 2.31 (3H, s), the aromatic protons δ_{H} 6.70 (2H, s) and the protons characteristic of the protecting group δ_{H} 3.40 (6H, s) and δ_{H} 5.25 (4H, s).

4.1.2.3. Synthesis of building block C.

4.1.2.3.1. Synthesis of methyl 2,6-bis(methoxymethoxy)-4-methylbenzoate (**8**).

Scheme 18 show the synthesis of methyl 2,6-bis(methoxymethoxy)-4-methylbenzoate (**8**).



Scheme 18: Protection of methyl 2,6-dihydroxy-4-methylbenzoate.

As previously discussed in section **4.1.2.2.1.**, the protection of the phenol group is mandatory and it was also achieved by reaction with chloro methyl methylether.

So, methyl 2,6-dihydroxy-4-methylbenzoate was treated with MOMCl in anhydrous DMF, in the presence of NaH ^[69], giving the compound **8** in 72 % yield.

Compound **8** was identified based on FTIR, EIMS, ^1H NMR, ^{13}C NMR, HSQC and HMBC. The FTIR spectrum showed the absence of the band attributed to the phenol group and EIMS showed a compatible molecular peak of m/z 270 ($[\text{M}]^+$). The ^1H NMR spectrum showed the expected signals for the methyl group δ_{H} 2.28 (3H, s), the protons from the ester group δ_{H} 3.77 (3H, s), the aromatic protons δ_{H} 6.67 (2H, s) and the protons characteristic of the MOM group δ_{H} 3.34 (6H, s) and δ_{H} 5.17 (4H, s). The ^{13}C NMR presented 9 signals. The main connectivities of HMBC are presented in figure 6 and all the assignments are summarized in table 1.

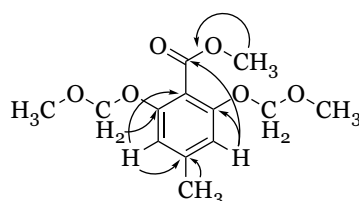
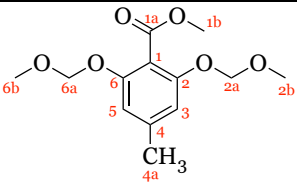


Figure 6: Main connectivities in HMBC spectrum for compound 8.

Table 1: Chemical shifts and assignments of compound **8**.

¹ H NMR chemical shifts ^a		¹³ C NMR chemical shifts ^b	
1b-H	3.77 (s)	1	112.8
2a-H and 6a-H	5.17 (s)	1b	52.1
2b-H and 6b-H	3.34 (s)	1a	166.1
3-H and 5-H	6.67 (s)	2 and 6	153.9
4a-H	2.28 (s)	3 and 5	108.8
		2a and 6a	94.0
		2b and 6b	55.7
		4	141.1
		4a	21.7

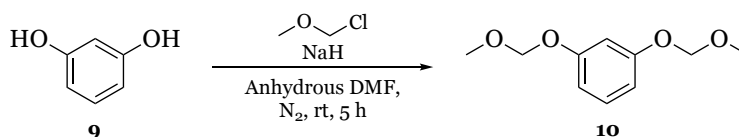
^aValues in ppm (δ_H) measured at 300.13 MHz, multiplicity and *J* values (Hz) are shown in parentheses;

^bValues in ppm (δ_C) measured at 75.47 MHz.

4.1.2.4. Synthesis of building block D.

4.1.2.4.1. Synthesis of 1,3-bis(methoxymethoxy)benzene (**10**).

Scheme 19 shows the synthesis of 1,3-bis(methoxymethoxy)benzene (**10**).



Scheme 19: Protection of resorcinol.

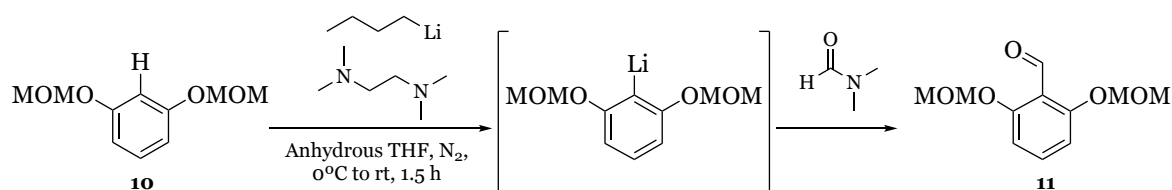
The first step in the synthesis of building block D is the MOM protection of resorcinol phenol groups.

In a similar way to **4.1.2.2.1.**, resorcinol was treated with MOMCl in anhydrous DMF, in the presence of NaH^[69], giving the desired 1,3-bis(methoxymethoxy)benzene (**10**) in 81 % yield.

Compound **10** was identified based on FTIR, EIMS and ¹H NMR. The FTIR spectrum showed the absence of the band attributed to the phenol groups, and EIMS showed the peak with *m/z* 199 ($[M+1]^+$) and with *m/z* 198 ($[M]^+$). The ¹H NMR spectrum showed the expected signals for the aromatic protons δ_H 7.20 (H, m) and δ_H 6.66 (3H, m) and the signals ascribed to the protecting group δ_H 3.37 (6H, s) and δ_H 5.16 (4H, s).

4.1.2.4.2. Synthesis of 2,6-bis(methoxymethoxy)benzaldehyde (**11**).

Scheme 20 shows the synthesis of 2,6-bis(methoxymethoxy)benzaldehyde (**11**).



Scheme 20: Formylation of 1,3-bis(methoxymethoxy)benzene.

To obtain the desired building block D, an aldehyde, it is needed the formylation of the protected resorcinol by directed *ortho*-metalation.

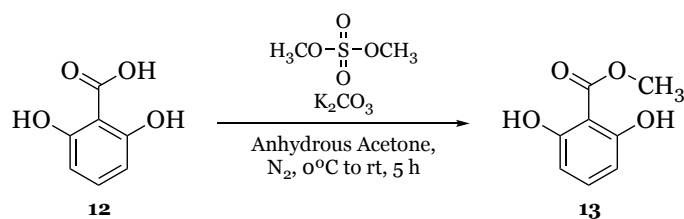
As established before in **4.1.2.2.2.**, to 1,3-bis(methoxymethoxy)benzene and TMEDA in anhydrous THF, it was added *n*-BuLi, at 0°C. After 1.5 hours stirring at room temperature, it was added anhydrous DMF, staying at room temperature for 2 hours.^[69] The desired building block D was obtained, after purification, in 44 % yield.

Compound **11** was identified based on FTIR, EIMS and ¹H NMR. The FTIR spectrum showed the appearance of carbonyl group and EIMS showed *m/z* 227 ([*M*+1]⁺) and *m/z* 226 ([*M*]⁺). The ¹H NMR spectrum showed the expected signals for the aromatic protons δ_H 7.50 (H, t) and δ_H 6.86 (2H, d), the protons characteristic of the protecting group δ_H 3.40 (6H, s) and δ_H 5.27 (4H, s) and the proton from the aldehyde δ_H 10.42 (H, s).

4.1.2.5. Synthesis of building block E

4.1.2.5.1. Synthesis of methyl 2,6-dihydroxybenzoate (**13**).

Scheme 21 shows the synthesis of methyl 2,6-dihydroxybenzoate (**13**).



Scheme 21: O-Methylation of 2,6-dihydroxybenzoic acid.

The first step in the synthesis of building block E is the esterification of 2,6-dihydroxybenzoic acid, which was achieved by an *O*-methylation with dimethyl sulphate.

Dimethyl sulphate have been used as an alkylating agent for alcohols, carboxylic acids, phenols, lactams and other nucleophilic groups [72]. In 1964, Stodola *et al.*[73] described a methodology using dimethyl sulfate to produce methyl esters from carboxylic acids. Later, in 2005, Henry and Townsend[74] used dimethyl sulphate and potassium carbonate for the selective esterification of trihydroxybenzoic acid.

So, to 2,6-dihydroxibenzoic acid and potassium carbonate in anhydrous acetone, dimethyl sulfate was added and the reaction was stirred at room temperature for 5 hours [74]. After purification, the desired product was achieved in 76 %.

Compound **13** was identified based on FTIR, EIMS, ¹H NMR, ¹³C NMR, HSQC and HMBC. The FTIR spectrum showed the typical band absorption of esters at 1205 and EIMS showed the peak with *m/z* 169 ([M+1]⁺) and with *m/z* 168 ([M]⁺). The ¹H NMR spectrum showed the expected signals of the aromatic protons δ_H 6.35 (2H, d) and δ_H 7.10 (H, t), the hydroxyl groups δ_H 9.99 (2OH, s) and the protons from the ester moiety δ_H 3.99 (3H, s). The ¹³C NMR presented 6 signals. The main connectivities of HMBC are presented in figure 7 and all the assignments are presented in table 2.

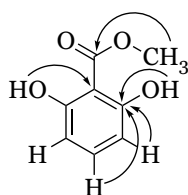


Figure 7: Main connectivities in HMBC spectrum for compound **13**.

Table 2: Chemical shifts and assignments of compound **13**.

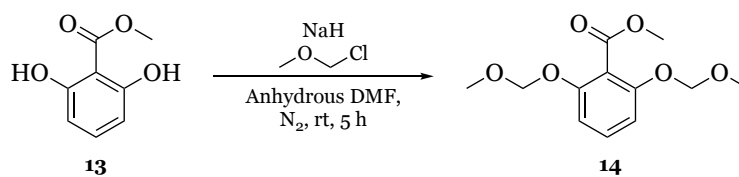
¹ H NMR chemical shifts ^a		¹³ C NMR chemical shifts ^b	
1b-H	3.99 (s)	1	107.3
2-OH and 6-OH	9.99 (s)	1a	168.4
3-H and 5-H	6.65 (<i>d</i> , <i>J</i> = 8.2)	1b	52.0
4-H	7.10 (<i>t</i> , <i>J</i> = 8.2)	2 and 6	157.3
		3 and 5	106.8
		4	132.4

^aValues in ppm (δ_H) measured at 300.13 MHz, multiplicity and *J* values (Hz) are shown in parentheses;

^bValues in ppm (δ_C) measured at 75.47 MHz.

4.1.2.5.2. Synthesis of methyl 2,6-bis(methoxymethoxy)benzoate (**14**).

Scheme 22 shows the synthesis of methyl 2,6-bis(methoxymethoxy)benzoate (**14**).



Scheme 22: Protection of methyl 2,6-dihydroxybenzoate.

The following step towards the building block E is the MOM protection of the phenol groups.

In a similar way to **4.1.2.2.1.**, methyl 2,6-dihydroxybenzoate was treated with MOMCl in anhydrous DMF, in the presence of NaH [69]. The desired product was obtained, after purification, in 71 % yield.

Compound **14** was identified based on FTIR, EIMS, ¹H NMR, ¹³C NMR, HSQC and HMBC. The FTIR spectrum showed the absence of the band ascribed to the phenol group and EIMS showed a structure congruent molecular peak with *m/z* 256 ([M]⁺). The ¹H NMR spectrum showed the protons of MOM group δ_H 3.35 (6H, s) and δ_H 5.20 (4H, s). The ¹³C NMR presented 9 signals. The main connectivities of HMBC are presented in figure 8 and all the assignments are presented in table 3.

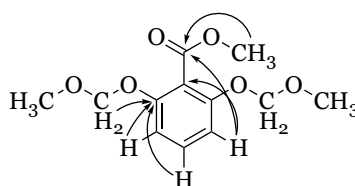
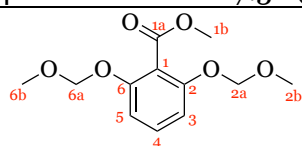


Figure 8: Main connectivities in HMBC spectrum for compound 14.

Table 3: Chemical shifts and assignments of compound 14.

¹ H NMR chemical shifts ^a		¹³ C NMR chemical shifts ^b	
1b-H	3.80 (s)	1	115.4
2a-H and 6a-H	5.20 (s)	1a	165.8
2b-H and 6b-H	3.35 (s)	1b	52.1
3-H and 5-H	6.84 (d, <i>J</i> = 8.4)	2 and 6	154.0
4-H	7.32 (t, <i>J</i> = 8.4)	2a and 6a	94.0
		2b and 6b	55.7
		3 and 5	108.1
		4	130.9



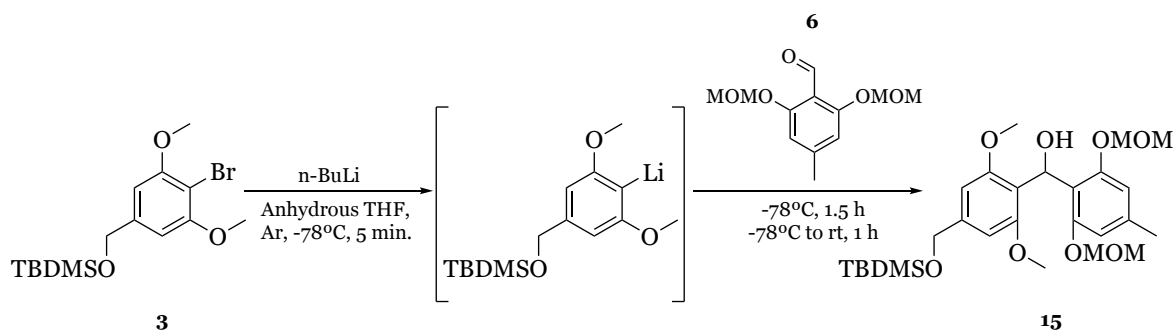
^aValues in ppm (δ_H) measured at 300.13 MHz, multiplicity and *J* values (Hz) are shown in parentheses;

^bValues in ppm (δ_C) measured at 75.47 MHz.

4.1.3. Synthesis of Yicanthins B and C.

4.1.3.1. Synthesis of (2,6-bis(methoxymethoxy)-4-methylphenyl)(4-(((tert-butyldimethylsilyl)oxy)methyl)-2,6-dimethoxyphenyl)methanol (**15**).

Scheme 23 shows the synthesis of (2,6-bis(methoxymethoxy)-4-methylphenyl)(4-(((tert-butyldimethylsilyl)oxy)methyl)-2,6-dimethoxyphenyl)methanol (**15**).



Scheme 23: Halogen/Lithium exchange of building block A and posterior S_EAr with building block B.

As discussed in the introduction chapter, the most common route to xanthenes involves the synthesis of a benzophenone as a key intermediate [37, 55]. Among the several methodologies described for the synthesis of benzophenones, halogen/lithium exchange is one of the most successful, allowing the synthesis of structural diverse benzophenones with good yields [55].

The halogen/lithium exchange was first described by Wittig in 1938 but it was only in 1939 that was reported in the introduction of new groups in halogenated compounds [43]. The exact mechanism has not been fully elucidated, however two possible mechanisms have been proposed: the first one involves radical intermediates and the second one is through to be a nucleophilic substitution.

In this case, the halogen/lithium exchange of building block A leads to formation of a lithiated intermediate, which is added to the aldehyde in building block B, yielding a diarylmethanol, by an aromatic electrophilic substitution

So, *n*-BuLi was added, at -78°C, to building block A in freshly dried THF. After 5 minutes, building block B was added, staying at -78°C for 1.5 h. After this time, the mixture was allowed to warm up until room temperature and is stirred for 1.5 h. The desired diarylmethanol was obtained in 41 % yield.

From a practical point of view, this reaction is very sensitive to the experimental conditions, namely in the anhydrous state of solvents/reaction. Therefore, two variations of the abovementioned procedure were tested. The use of nitrogen flow and THF distilled

under sodium^[57] and kept in 3Å sieves^[75] resulted in the synthesis of compound **15** in low yield (5 %) . The major product corresponded to the dehalogenated product of building block A. It was hypothesized that the quantity of water present in this apparatus promoted the protonation of lithiated intermediate, avoiding the reaction with building block B. The use of argon atmosphere and the use of THF directly from the distillation apparatus resulted in the synthesis of compound **15** in higher yield (41% vs. 5%).

Compound **15** was identified based on FTIR, EIMS, ¹H NMR, ¹³C NMR, HSQC and HMBC. The FTIR spectrum showed the typical alcohol OH stretching band at 3565 cm⁻¹ and EIMS spectrum showed a peak with *m/z* 523 ([M+1]⁺). ¹H NMR showed the signals similar to the ones attributed in building block A and B. From building block A, it was attributed the signals corresponding to the methyl groups directly attached to the silyl group δ_H 0.20 (6H, s), the *tert*-butyl protons δ_H 1.04 (9H, s), two methoxyl groups δ_H 3.84 (6H, s), the two protons of the methylene group δ_H 4.78 (2H, d), and the aromatic protons δ_H 6.68 (2H, s). From building block B, it was attributed the signals corresponding to the proton from the methyl group δ_H 2.34 (3H, s), the MOM protons δ_H 3.34 (6H, s) and δ_H 5.22 (4H, s) and the aromatic protons δ_H 6.64 (2H, s). The diarylmethanol moiety was confirmed by the presence of the hydroxyl proton δ_H 6.53 (OH, d) and the proton of the attached carbon δ_H 5.51 (H, d), with equal coupling constants (*J* = 10.3 Hz). The ¹³C NMR presented 17 signals. The main connectivities of HMBC are presented in figure 9 and all the assignments are presented in table 4.

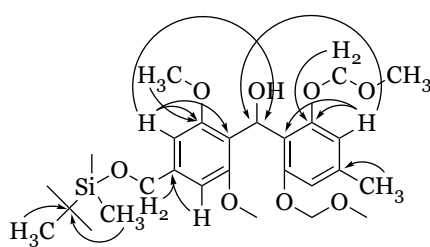
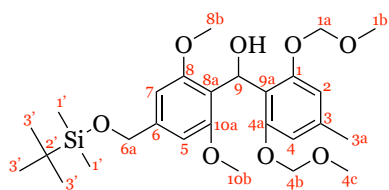


Figure 9: Main connectivities in HMBC spectrum for compound **15**.

Table 4: Chemical shifts and assignments of compound **15**.

¹ H NMR chemical shifts ^a		¹³ C NMR chemical shifts ^b	
1a-H and 4b-H	5.22 (s)	1 and 4a	155.3
1b-H and 4c-H	3.34 (s)	1a and 4b	94.1
2-H and 4-H	6.64 (s)	1b and 4c	55.5
3a-H	2.34 (s)	2 and 4	108.5
5-H and 7-H	6.68 (s)	3	137.1
6a-H	4.78 (s)	3a	21.4
8b-H and 10b-H	3.84 (s)	5 and 7	101.8
9-H	5.51 (d, <i>J</i> = 10.3)	6	141.3
9-OH	6.53 (d, <i>J</i> = 10.3)	6a	64.2
1'-H	0.20 (s)	8 and 10a	157.7
3'-H	1.04 (s)	8a	117.9
		8b and 10b	55.6
		9	63.4
		9a	118.9
		1'	-5.3
		2'	18.0
		3'	25.8



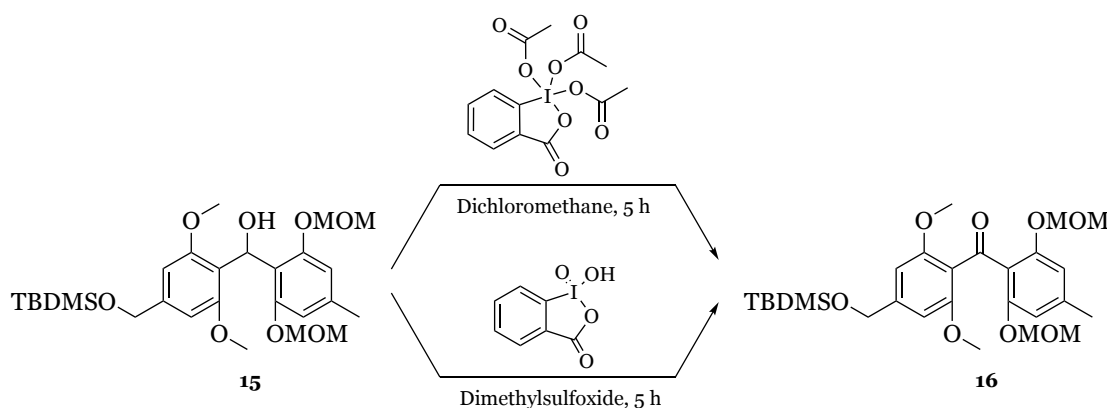
^aValues in ppm (δ_H) measured at 300.13 MHz, multiplicity and *J* values (Hz) are shown in parentheses;

^bValues in ppm (δ_C) measured at 75.47 MHz.

4.1.3.2. Synthesis of (2,6-bis(methoxymethoxy)-4-methylphenyl)(4-(((tert-butyldimethylsilyl)oxy)methyl)-2,6-dimethoxyphenyl)methanone (16).

4.1.3.2.1. Via oxidation of diarylmethanol (15).

Scheme 24 shows the synthesis of (2,6-bis(methoxymethoxy)-4-methylphenyl)(4-(((tert-butyldimethylsilyl)oxy)methyl)-2,6-dimethoxyphenyl)methanone (**16**).



Scheme 24: Oxidation of diarylmethanol to benzophenone.

The treatment of the lithiated intermediate, formed by halogen/lithium exchange, with an aldehyde, such as building block B, yields a diarylmethanol, which need to be further oxidized to benzophenone.

The oxidation of this secondary alcohol to ketone will allow the formation of the key intermediate, the benzophenone. This can be done by various oxidating agents, such as manganese dioxide, Dess-Martin periodinane (DMP) and 2-iodoxybenzoic acid (IBX).^[76, 77] In our previous work, manganese dioxide does not produced the desired compound.^[56]

So, DMP was added to the diarylmethanol in dichloromethane and the reaction was stirred at room temperature for 5 hours. The desired benzophenone was obtained, after purification, in 49 % yield. Additionality, IBX was added to the diarylmethanol in DMSO and the reaction was stirred at room temperature for 15 hours. The desired benzophenone was obtained in 90 % yield.

Compound **16** was identified based on FTIR, EIMS, ¹H NMR, ¹³C NMR, HSQC and HMBC. The FTIR spectrum showed the presence of the band ascribed to the carbonyl group at 1704 cm⁻¹. The EIMS spectrum did not show a peak with *m/z* value compatible with the molecular mass of the desired compound. Nevertheless, several peaks were identified as fragments compatible with the fragmentation of the desired compound (figure 10).

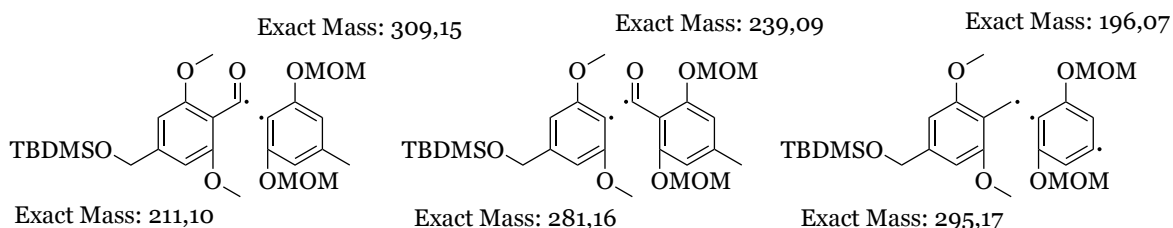


Figure 10: Principal fragments from EIMS.

The ^1H NMR and ^{13}C NMR showed a similar profile to compound **15**, with the expected exception of the hydroxyl signal absence in the ^1H NMR spectrum and the presence of the carbonyl signal in the ^{13}C NMR spectrum. The main connectivities of HMBC are presented in figure 11 and all the assignments are presented in table 5.

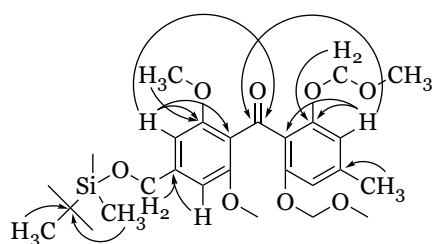


Figure 11: Main connectivities in HMBC spectrum for compound **16**.

Table 5: Chemical shifts and assignments of compound **16**.

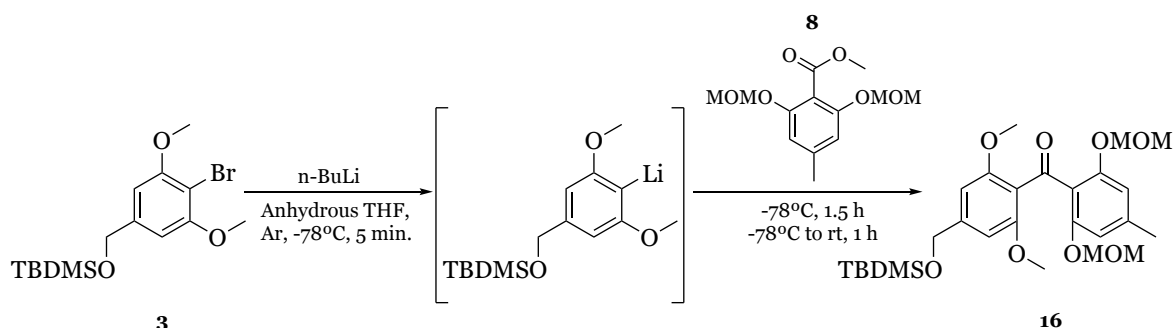
^1H NMR chemical shifts ^a		^{13}C NMR chemical shifts ^b	
1a-H and 4b-H	4.99 (s)	1 and 4a	155.1
1b-H and 4c-H	3.17 (s)	1a and 4b	93.9
2-H and 4-H	6.54 (s)	1b and 4c	55.5
3a-H	2.25 (s)	2 and 4	108.6
5-H and 7-H	6.59 (s)	3	140.9
6a-H	4.68 (s)	3a	21.8
8b-H and 10b-H	3.60 (s)	5 and 7	101.8
1'-H	0.07 (s)	6	145.2
3'-H	0.91 (s)	6a	64.2
		8 and 10a	157.9
		8a	119.8
		8b and 10b	55.9
		9	192.0
		9a	120.4
		1'	-5.2
		2'	18.1
		3'	25.9

^aValues in ppm (δ_{H}) measured at 500.16 MHz, multiplicity and J values (Hz) are shown in parentheses;

^bValues in ppm (δ_{C}) measured at 75.47 MHz.

4.1.3.2.2. Via reaction of building block A with building block C.

Scheme 25 shows the synthesis of (2,6-bis(methoxymethoxy)-4-methylphenyl)(4-(((tert-butyldimethylsilyl)oxy)methyl)-2,6-dimethoxyphenyl)methanone (**16**).



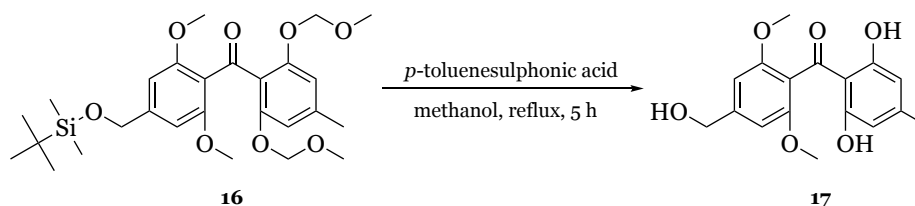
Scheme 25: Halogen/lithium exchange of building block A and posterior S_EAr with building block C.

A similar approach to the diarylmethanol synthesis, a halogen/lithium exchange and posterior S_EAr was used. However, in this case, an ester was used as the electrophile, which allows the synthesis of the key intermediate in just one step.

So, *n*-BuLi was added to building block A in freshly dried THF at -78°C . After 5 minutes, building block C was added and the reaction was stirred for 1.5 h. After this time, the reaction mixture was allowed to warm up until room temperature for another 1 h. The desired benzophenone was obtained, after purification, in relatively low yield (21 %).

4.1.3.3. Synthesis of (2,6-dihydroxy-4-methylphenyl)(4-(hydroxymethyl)-2,6-dimethoxyphenyl)methanone (**17**).

Scheme 26 shows the synthesis of (2,6-dihydroxy-4-methylphenyl)(4-(hydroxymethyl)-2,6-dimethoxyphenyl)methanone (**17**).



Scheme 26: Deprotection of benzophenone 16.

The next step for the synthesis of the xanthone scaffold is the deprotection of the phenolic function. There are several methodologies for deprotection of phenols protected with MOM groups [78]. Under acid conditions promoted by *p*-toluenesulphonic acid, it is

expected that besides the MOM deprotection, the cleavage of the TBMSDS protecting group can also occur [79]. This methodology was followed since the non-selective deprotection do not influence the course of the following reactions.

So, *p*-toluenesulphonic acid was added to (2,6-bis(methoxymethoxy)-4-methylphenyl)(4-(((tert-butyldimethylsilyl)oxy)methyl)-2,6-dimethoxyphenyl)methanone in methanol and the mixture was kept at 50 °C for 5 hours. The desired compound was achieved in 88% yield.

Compound **17** was identified based on FTIR, EIMS, ¹H NMR, ¹³C NMR, HSQC and HMBC. The FTIR spectrum showed the typical OH stretching band at 3447 cm⁻¹ and EIMS spectrum showed a structure compatible molecular peak with *m/z* 534 ([M+TMS]⁺). The ¹H NMR shows the signals attributed to the protons resulting from the deprotection: the phenol groups δ_H 11.62 (2OH, s) and the primary alcohol δ_H 5.10 (OH, s). The ¹³C NMR shows 12 signals. The main connectivities of HMBC are presented in figure 12 and all the assignments are in table 6.

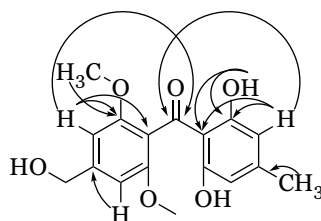
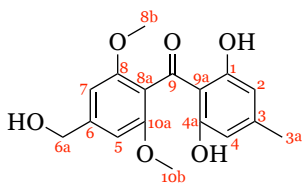


Figure 12: Main connectivities in HMBC spectrum for compound **17**.

Table 6: Chemical shifts and assignments of compound **17**.

¹ H NMR chemical shifts ^a		¹³ C NMR chemical shifts ^b	
1-OH and 4a-OH	11.62 (s)	1 and 4a	162.3
2-H and 4-H	6.14 (s)	2 and 4	107.7
3a-H	2.20 (s)	3	148.4
5-H and 7-H	6.67 (s)	3a	21.7
6a-H	4.55 (s)	5 and 7	101.9
6a-OH	5.10 (s)	6	144.8
8a-H and 10b-H	3.70 (s)	6a	63.0
		8 and 10a	155.7
		8a	120.4
		8b and 10b	55.7
		9	198.8
		9a	109.1

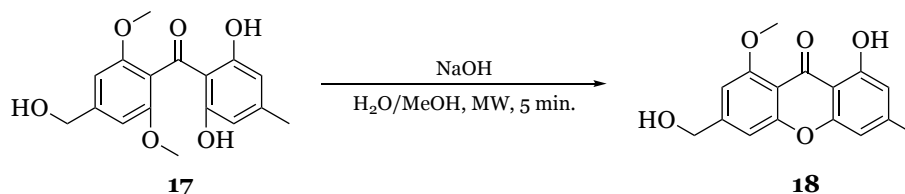


^aValues in ppm (δ_H) measured at 300.13 MHz, multiplicity and *J* values (Hz) are shown in parentheses;

^bValues in ppm (δ_C) measured at 75.47 MHz.

4.1.3.4. Synthesis of 1-hydroxy-6-(hydroxymethyl)-8-methoxy-3-methyl-9H-xanthen-9-one (18).

Scheme 27 shows the synthesis of 1-hydroxy-6-(hydroxymethyl)-8-methoxy-3-methyl-9H-xanthen-9-one (**18**).



Scheme 27: Cyclization of compound 17.

Once deprotected, the benzophenone can be easily cyclized to the xanthone skeleton by a nucleophilic aromatic substitution. It has been described in the literature several methods to promote this cyclization [55]. Our group of investigation have reported a green methodology assisted by microwave heating and using water as a solvent [80].

So, compound **17** dissolved in a mixture of water/methanol (9:1), in the presence of NaOH was heated under microwave for 5 minutes and the desired product was obtained by precipitation and filtration.

Compound **18** was identified based on FTIR, EIMS, ¹H NMR, ¹³C NMR, HSQC and HMBC. The FTIR spectrum showed the presence of a band ascribed to the carbonyl group at 1651 cm⁻¹ and the EIMS spectrum showed a structure compatible molecular peak with *m/z* 431 ([M+TMS]⁺). The ¹H NMR shows the disappearance of protons from one methoxy and one phenol group. The ¹³C NMR shows 16 signals. The main connectivities of HMBC are presented in figure 13 and all the assignments are presented in table 7.

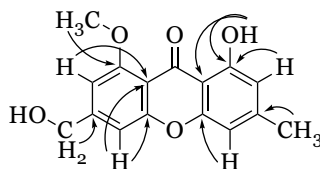
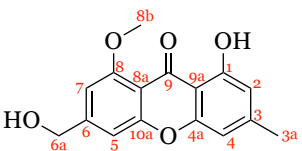


Figure 13: Main connectivities in HMBC spectrum for compound 18.

Table 7: Chemical shifts and assignments of compound **18**.

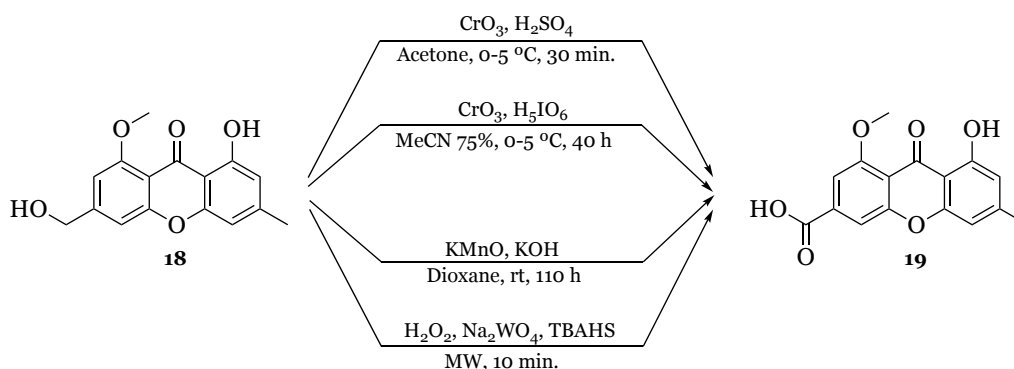
¹ H NMR chemical shifts ^a		¹³ C NMR chemical shifts ^b	
1-OH	13.03 (s)	1	161.0
2-H	6.57 (s)	2	111.0
3a-H	2.35 (s)	3	148.2
4-H	6.78 (s)	3a	21.9
5-H	7.02 (s)	4	106.8
6a-H	4.62 (d, <i>J</i> = 5.7)	4a	154.8
6a-OH	5.61 (t, <i>J</i> = 5.7)	5	106.2
7-H	6.92 (s)	6	152.9
8b-H	3.90 (s)	6a	62.4
		7	103.9
		8	160.1
		8a	108.8
		8b	56.3
		9	181.1
		9a	106.7
		10a	157.4

^aValues in ppm (δ_H) measured at 300.13 MHz, multiplicity and *J* values (Hz) are shown in parentheses;

^bValues in ppm (δ_C) measured at 75.47 MHz.

4.1.3.5. Synthesis of 8-hydroxy-1-methoxy-6-methyl-9-oxo-9H-xanthene-3-carboxylic acid - Yicathin C (**19**).

Scheme 28 shows the synthesis of Yicathin C (**19**).



Scheme 28: Oxidation of compound **19**.

The final step for the synthesis of Yicathin C is the oxidation of the primary alcohol attached to the carbon 6. There are several ways to oxidize a primary alcohol to a carboxylic acid, which can be grouped in chromium-based, permanganate-based and oxygen-based methods [81].

In this work, several methods were employed. The first method tested was the classical Jones oxidation, a mixture of chromic trioxide in diluted sulfuric acid, which forms

chromic acid *in situ* [82]. So, solution with sulfuric acid and chromium (VI) oxide was added to compound **18** dissolved in acetone. By monitoring the reaction by TLC, it was possible to observe the full disappearance of the starting material within only 30 minutes. However, the crude product was composed by 4 products, in similar concentrations. Compound **19** was obtained in 20 % yield.

A modified version of the Jones oxidation, where periodic acid is used instead of sulfuric acid, was also used, since it has been described in the literatures with greater yields [83]. So, a solution of periodic acid and chromium (VI) oxide was added to compound **18** dissolved in wet acetonitrile at 0°C. The reaction was followed by TLC and only after 40h the complete disappearance of the starting material was observed. Compound **19** was obtained in 50% yield.

An classical potassium permanganate oxidation[84] and a greener MW-assisted hydrogen peroxide-based oxidation[85] were also tested. However, the desired compound was not achieved, being the major product the starting material, compound **18**.

Compound **19** was identified based on FTIR, EIMS, ¹H NMR, ¹³C NMR, HSQC and HMBC. The FTIR spectrum showed the bands at 3446 cm⁻¹ and 1718 cm⁻¹ ascribed to the hydroxyl and carbonyl stretching of the carboxylic acid. The EIMS spectrum showed the structure compatible molecular peak with m/z 445 ([M+TMS]⁺). The ¹H NMR spectrum showed the disappearance of the two methylene protons. The ¹³C NMR showed 16 signals. The main connectivities of HMBC are presented in figure 14 and all the assignments are presented in table 8.

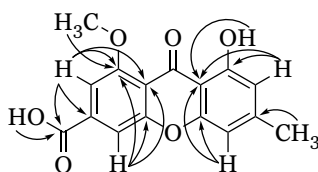
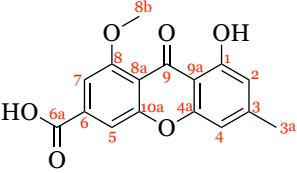


Figure 14: Main connectivities in HMBC spectrum for compound **19**.

Table 8: Chemical shifts and assignments of compound **19**.

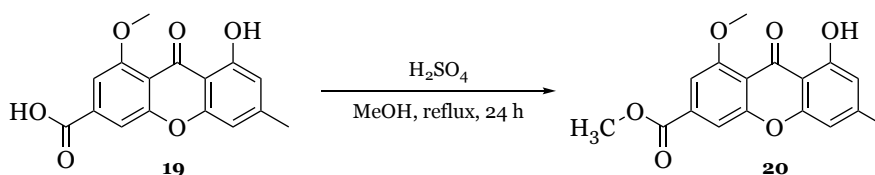
¹ H NMR chemical shifts ^a		¹³ C NMR chemical shifts ^b	
1-OH	12.74 (s)	1	160.9
2-H	6.63 (q, <i>J</i> = 1.3)	2	111.4
3a-H	2.39 (s)	3	148.9
4-H	6.83 (q, <i>J</i> = 1.3)	3a	21.9
5-H	7.54 (d, <i>J</i> = 1.4)	4	107.0
6a-OH	13.85 (s)	4a	154.7
7-H	7.36 (d, <i>J</i> = 1.4)	5	110.2
8b-H	3.93 (s)	6	135.9
		6a	160.4
		7	105.8
		8	164.8
		8a	112.9
		8b	53.0
		9	180.8
		9a	107.1
		10a	154.7

^aValues in ppm (δ_H) measured at 500.16 MHz, multiplicity and *J* values (Hz) are shown in parentheses;

^bValues in ppm (δ_C) measured at 125.77 MHz.

4.1.3.6. Synthesis of methyl 8-hydroxy-1-methoxy-6-methyl-9-oxo-9H-xanthene-3-carboxylate - Yicathin B (**20**).

Scheme 29 shows the synthesis of Yicathin B (**20**).



Scheme 29: Esterification of compound **19**.

Accordingly to the retrosynthetic plan, Yicathin B can be obtained by esterification of Yicathin C, by a simple Fischer esterification [86]. So, compound **19** dissolved in methanol, in the presence of sulfuric acid, was refluxed overnight. The desired product was achieved after purification in 55 % yield.

Compound **20** was identified based on FTIR, EIMS, ¹H NMR, ¹³C NMR, HSQC and HMBC. The FTIR spectrum showed absence of the band ascribed to the hydroxyl of the carboxylic acid and the EIMS spectrum showed the structure compatible molecular peak with *m/z* 387 ([*M*+TMS]⁺). The ¹H NMR is similar to the previous compound, except in the absence of the hydroxyl signal from the carboxylic acid and the presence of the methyl group

from the ester at δ_{H} 5.76 (3H, s). The ^{13}C NMR showed 17 signals. The main connectivities of HMBC are presented in figure 15 and all the assignments are presented in table 9.

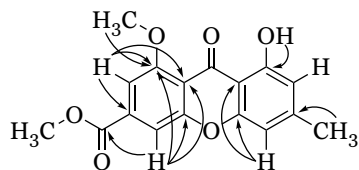
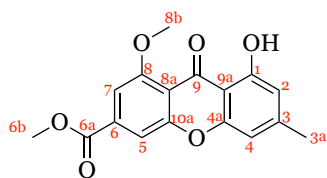


Figure 15: Main connectivities in HMBC spectrum for compound **20**.

Table 9: Chemical shifts and assignments of compound **20**.

^1H NMR chemical shifts ^a		^{13}C NMR chemical shifts ^b	
1-OH	12.72 (s)	1	160.8
2-H	6.62 (q, $J = 1.3$)	2	111.4
3a-H	2.83 (s)	3	148.9
4-H	6.81 (q, $J = 1.3$)	3a	21.9
5-H	7.51 (d, $J = 1.4$)	4	107.0
6b-H	3.98 (s)	4a	154.7
7-H	7.34 (d, $J = 1.4$)	5	110.2
8b-H	3.93 (s)	6	135.8
		6a	160.4
		6b	56.6
		7	105.7
		8	164.8
		8a	112.9
		8b	53.0
		9	180.8
		9a	106.9
		10a	157.0



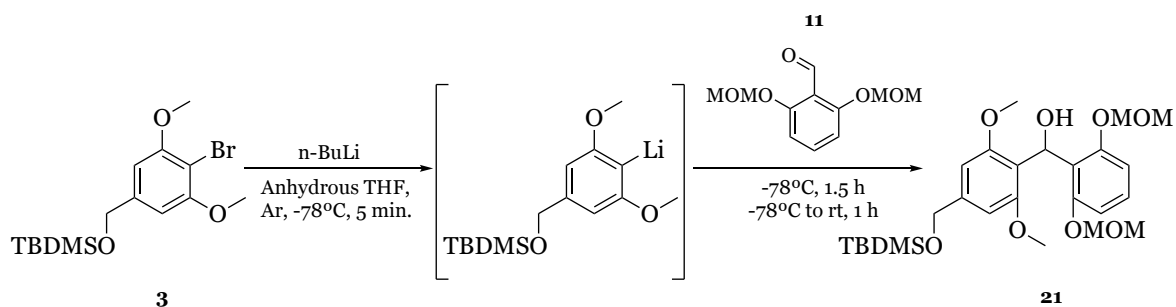
^aValues in ppm (δ_{H}) measured at 500.16 MHz, multiplicity and J values (Hz) are shown in parentheses;

^bValues in ppm (δ_{C}) measured at 125.77 MHz.

4.1.4. Synthesis of Analogues B and C.

4.1.4.1. Synthesis of (2,6-bis(methoxymethoxy)phenyl)(4-(((tert-butyl)dimethylsilyl)oxy)methyl)-2,6-dimethoxyphenyl)methanol (**21**).

Scheme 30 shows the synthesis of ((2,6-bis(methoxymethoxy)phenyl)(4-(((tert-butyl)dimethylsilyl)oxy)methyl)-2,6-dimethoxyphenyl)methanol (**21**).



Scheme 30: Halogen/Lithium exchange of building block A and posterior S_EAr with building block D.

In a similar way to **4.1.3.1.**, the halogen/lithium exchange and posterior S_EAr with an aldehyde will produce the precursor diarylmethanol intermediate.

So, *n*-BuLi was added at -78°C to building block A in freshly dried THF. After 5 minutes, building block D was added and the reaction was stirred for 1.5 h at -78°C . After this time, the mixture was allowed to warm up until room temperature for 1 h. The desired diarylmethanol was obtained, after purification, in 87 % yield.

Compound **21** was identified based on FTIR, EIMS, ^1H NMR, ^{13}C NMR, HSQC and HMBC. The FTIR spectrum showed the presence of the alcohol band ascribed at 3511 cm^{-1} . The EIMS spectrum did not show a peak with m/z value compatible with the molecular mass of the desired compound. Nevertheless, several peaks were identified as fragments compatible with the fragmentation of the desired compound (figure 16).

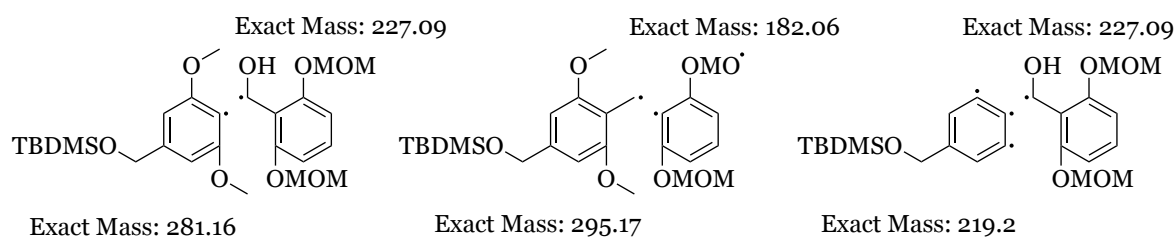


Figure 16: Principal fragments from EIMS.

^1H NMR shows the signals for corresponding to the part of the structure derived from building block A and D. From building block A, it was identified the signals from the

methyl groups directly attached to the silyl group δ_{H} 0.07 (6H, s), the *tert*-butyl protons δ_{H} 0.91 (9H, s), two methoxyl groups δ_{H} 3.71 (6H, s), the two protons of the methylene group δ_{H} 4.65 (2H, d) and the aromatic protons δ_{H} 6.56 (2H, s). From building block D, it was identified the signals from the MOM protons δ_{H} 3.25 (6H, s) and δ_{H} 5.11 (4H, s) and the aromatic protons δ_{H} 6.68 (2H, d, $J = 8.3$ Hz) and δ_{H} 7.07 (H, t, $J = 8.3$ Hz). The diarylmethanol moiety is confirmed by the presence of the hydroxyl proton δ_{H} 6.45 (OH, d, $J = 10.2$ Hz) and the proton of the attached carbon δ_{H} 5.42 (H, d, $J = 10.2$ Hz). The ^{13}C NMR presented 16 signals. The main connectivities of HMBC are presented in figure 17 and all the assignments are presented in table 10.

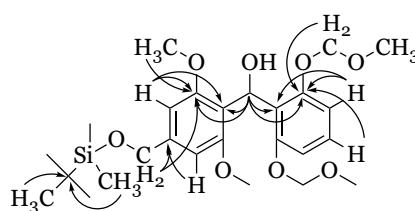


Figure 17: Main connectivities in HMBC spectrum for compound **21**.

Table 10: Chemical shifts and assignments of compound **21**.

^1H NMR chemical shifts ^a		^{13}C NMR chemical shifts ^b	
1a-H and 4b-H	5.11 (s)	1 and 4a	155.5
1b-H and 4c-H	3.25 (s)	1a and 4b	94.1
2-H and 4-H	6.68 (d, $J = 8.3$)	1b and 4c	55.5
3-H	7.07 (t, $J = 8.3$)	2 and 4	107.8
5-H and 7-H	6.56 (s)	3	127.7
6a-H	4.65 (s)	5 and 7	101.8
8b-H and 10b-H	3.71 (s)	6	141.4
9-H	5.42 (d, $J = 10.2$)	6a	64.2
9-OH	6.45 (d, $J = 10.2$)	8 and 10a	157.7
1'-H	0.07 (s)	8a	117.8
3'-H	0.91 (s)	8b and 10b	55.7
		9	63.5
		9a	121.8
		1'	-5.2
		2'	18.0
		3'	25.8

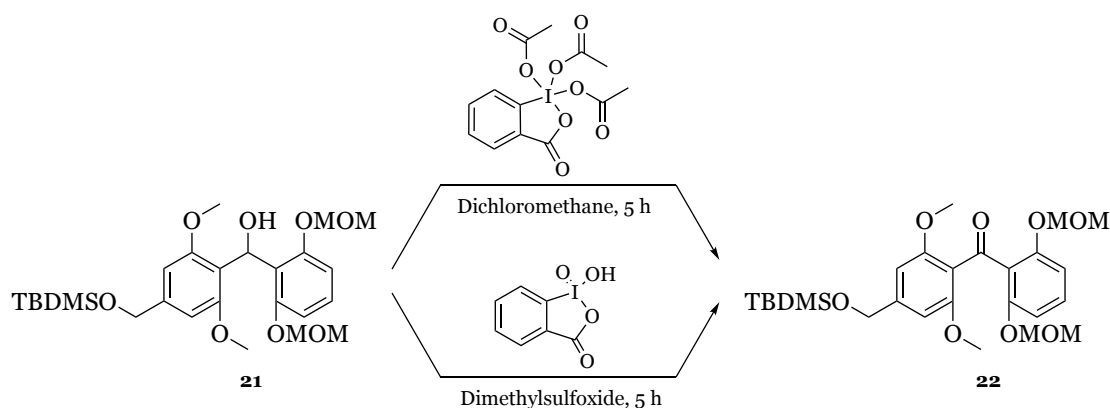
^aValues in ppm (δ_{H}) measured at 300.13 MHz, multiplicity and J values (Hz) are shown in parentheses;

^bValues in ppm (δ_{C}) measured at 75.47 MHz.

4.1.4.2. Synthesis of 2,6-bis(methoxymethoxy)phenyl(4-(((tert-butyl)dimethylsilyl)oxy)methyl)-2,6-dimethoxyphenyl)methanone (**22**).

4.1.4.2.1. Via oxidation of diarylmethanol (**21**).

Scheme 31 shows the synthesis of 2,6-bis(methoxymethoxy)phenyl(4-(((tert-butyl)dimethylsilyl)oxy)methyl)-2,6-dimethoxyphenyl)methanone (**22**).



Scheme 31: Oxidation of diarylmethanol to benzophenone.

In a similar way to **4.1.3.2.1.**, two oxidating agents were used to produce the benzophenone from the diarylmethanol intermediate.

So, DMP was added to the diarylmethanol, in dichloromethane, and the reaction was stirred at room temperature for 5 hours. The desired benzophenone was obtained in 87 % yield. Additionally, IBX was added to diarylmethanol, in DMSO, and the reaction was stirred at room temperature for 5 hours. The desired benzophenone was achieved, after purification, with 80 % yield.

Compound **22** was identified based on FTIR, EIMS, ^1H NMR, ^{13}C NMR, HSQC and HMBC. The FTIR spectrum showed the absence of the band ascribed to the hydroxyl group, and the presence of the carbonyl band at 1682 cm^{-1} . The EIMS spectrum showed the fragments with m/z 295, 237 and 193 compatible with fragmentation of the desired compound.

The ^1H NMR and ^{13}C NMR spectra are similar to the compound **21** spectra. The differences were the absence in ^1H NMR spectrum of the signal attributed to the hydroxyl group and the presence in the ^{13}C NMR spectrum of a carbonyl signal at 191.7 ppm. The main connectivities of HMBC are presented in figure 18 and all the assignments are presented in table 11.

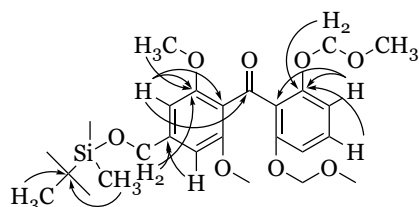


Figure 18: Main connectivities in HMBC spectrum for compound **22**.

Table 11: Chemical shifts and assignments of compound **22**.

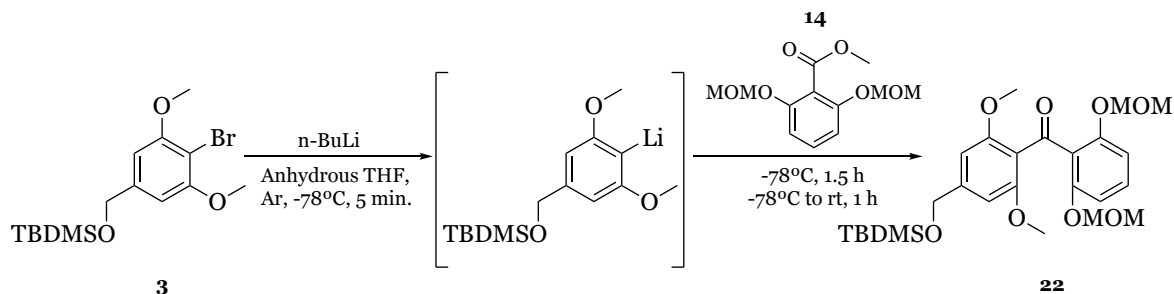
¹ H NMR chemical shifts ^a		¹³ C NMR chemical shifts ^b	
1a-H and 4b-H	5.06 (s)	1 and 4a	154.9
1b-H and 4c-H	3.21 (s)	1a and 4b	93.9
2-H and 4-H	6.75 (d, <i>J</i> = 8.4)	1b and 4c	55.8
3-H	7.27 (t, <i>J</i> = 8.4)	2 and 4	107.8
5-H and 7-H	6.64 (s)	3	130.6
6a-H	4.73 (s)	5 and 7	101.8
8b-H and 10b-H	3.63 (s)	6	145.5
1'-H	0.11 (s)	6a	64.1
3'-H	0.95 (s)	8 and 10a	158.1
		8a	119.3
		8b and 10b	55.4
		9	191.7
		9a	123.0
		1'	-5.3
		2'	18.0
		3'	25.8

^aValues in ppm (δ_H) measured at 500.16 MHz, multiplicity and *J* values (Hz) are shown in parentheses;

^bValues in ppm (δ_C) measured at 75.47 MHz.

4.1.4.2.2. Via reaction of building block A with building block E.

Scheme 32 shows the synthesis of 2,6-bis(methoxymethoxy)phenyl(4-(((tert-butyl)dimethylsilyl)oxy)methyl)-2,6-dimethoxyphenyl)methanone (**22**).



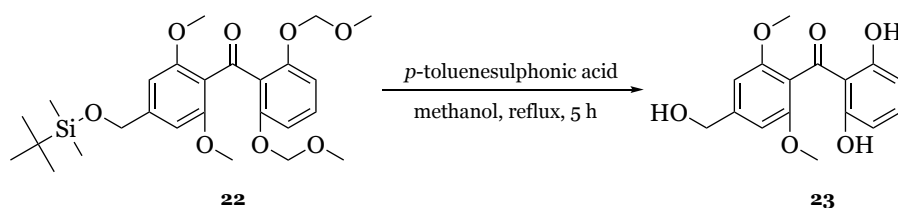
Scheme 32: Halogen/lithium exchange of building block A and posterior *S_EAr* with building block E.

The one step synthesis of the benzophenone was also performed using an ester, building block E, as electrophile.

So, *n*-BuLi was added to building block A in freshly dried THF at -78°C. After 5 minutes, building block E was added and the reaction was stirred at -78 °C for 1.5 h. After this time, the reaction mixture was allowed to warm up until room temperature for another 1 h. The desired benzophenone was obtained, after purification, in relatively low yield (19 %).

4.1.4.3. Synthesis of (2,6-dihydroxyphenyl)(4-(hydroxymethyl)-2,6-dimethoxyphenyl)methanone (**23**).

Scheme 33 shows the synthesis of (2,6-dihydroxyphenyl)(4-(hydroxymethyl)-2,6-dimethoxyphenyl)methanone (**23**).



Scheme 33: Deprotection of compound 22.

In a similar way to **4.1.3.3.**, the deprotection of the benzophenone was conducted under acidic conditions. So, *p*-toluenesulphonic acid was added to compound **22** dissolved in methanol and the reaction was kept at 50 °C for 5 hours.

Compound **23** was identified based on FTIR, EIMS, ¹H NMR, ¹³C NMR, HSQC and HMBC. The FTIR showed the appearance of O-H stretching bands at 3385 cm⁻¹ and the EIMS spectrum did not show a structural compatible peak, however several peaks were identified as fragments compatible with the fragmentation of the desired compound. The ¹H NMR showed the alcohol hydroxyl proton at δ_H 5.32 (OH, s) and the phenolic protons δ_H 11.59 (2OH, s). The ¹³C NMR showed 11 signals. The main connectivities of HMBC are presented in figure 19 and all the assignments are presented in table 12.

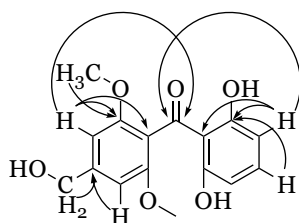
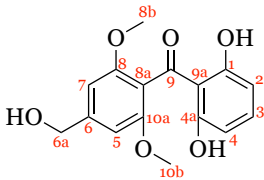


Figure 19: Main connectivities in HMBC spectrum for compound 23.

Table 12: Chemical shifts and assignments of compound **23**.

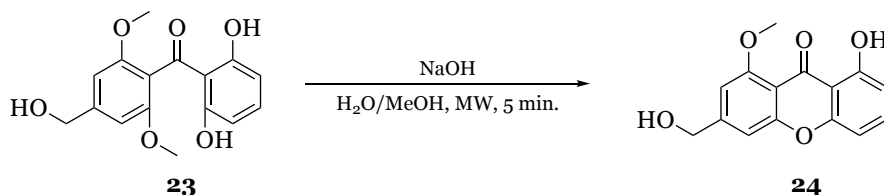
¹ H NMR chemical shifts ^a		¹³ C NMR chemical shifts ^b	
1-OH and 4a-OH	11.59 (s)	1 and 4a	162.4
2-H and 4-H	6.27 (d, <i>J</i> = 8.2)	2 and 4	107.0
3-H	7.26 (t, <i>J</i> = 8.2)	3	137.2
5-H and 7-H	6.65 (s)	5 and 7	101.9
6a-H	4.52 (s)	6	145.0
6a-OH	5.32 (s)	6a	63.1
8a-H and 10b-H	3.67 (s)	8 and 10a	155.8
		8a	120.4
		8b and 10b	55.7
		9	199.6
		9a	111.2

^aValues in ppm (δ_H) measured at 300.13 MHz, multiplicity and *J* values (Hz) are shown in parentheses;

^bValues in ppm (δ_C) measured at 75.47 MHz.

4.1.4.4. Synthesis of 8-hydroxy-3-(hydroxymethyl)-1-methoxy-9H-xanthen-9-one (**24**).

Scheme 34 shows the synthesis of 8-hydroxy-3-(hydroxymethyl)-1-methoxy-9H-xanthen-9-one (**24**).



Scheme 34: Cyclization of compound **23**.

In a similar way to **4.1.3.4.**, the cyclization towards xanthone was performed under MW irradiation. So, compound **23** dissolved in a mixture of water/methanol (9:1), in the presence of NaOH was heated under microwave for 5 minutes and the desired product was obtained by precipitation and filtration.

Compound **24** was identified based on FTIR, EIMS, ¹H NMR, ¹³C NMR, HSQC and HMBC. The FTIR spectrum showed the presence of the band ascribed to the hydroxyl group at 3471 cm⁻¹. The EIMS showed a structure compatible molecular peak with *m/z* 416 ([M+TMS]⁺). The ¹H NMR spectrum showed the disappearance of the protons from one methoxy and one phenol group. The ¹³C NMR showed 15 signals. The main connectivities of HMBC are presented in figure 20 and all the assignments are presented in table 13.

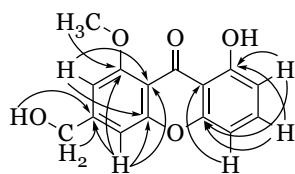


Figure 20: Main connectivities in HMBC spectrum for compound **24**.

Table 13: Chemical shifts and assignments of compound **24**.

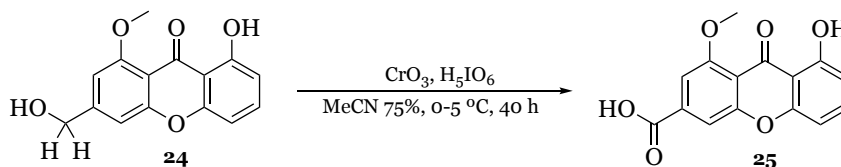
¹ H NMR chemical shifts ^a		¹³ C NMR chemical shifts ^b	
1-OH	13.12 (s)	1	161.3
2-H	6.98 (d, <i>J</i> = 8.2)	2	106.6
3-H	7.65 (t, <i>J</i> = 8.2)	3	136.8
4-H	6.75 (d, <i>J</i> = 8.2)	4	110.4
5-H	6.97 (s)	4a	155.0
6a-H	4.64 (d, <i>J</i> = 5.0)	5	106.2
6a-OH	5.64 (t, <i>J</i> = 5.0)	6	153.2
7-H	7.08 (s)	6a	62.4
8b-H	3.92 (s)	7	104.0
		8	160.2
		8a	108.8
		8b	56.4
		9	181.6
		9a	108.8
		10a	157.5

^aValues in ppm (δ_H) measured at 500.16 MHz, multiplicity and *J* values (Hz) are shown in parentheses;

^bValues in ppm (δ_C) measured at 125.77 MHz.

4.1.4.5. Synthesis of 8-hydroxy-1-methoxy-9-oxo-9H-xanthene-3-carboxylic acid - Analogue C (**25**).

Scheme 35 shows the synthesis of Analogue C (**25**).



Scheme 35: Oxidation of compound **24**.

Taking into account the topic discussed in section 4.1.3.5., Analogue C was synthesized by a modified Jones oxidation. So, a solution of periodic acid and chromium (VI) oxide was added to compound **24** dissolved in wet acetonitrile, at 0°C, and the reaction was stirred for 4 hours. The desired product was obtained in 37 % yield.

Compound **25** was identified based on FTIR, EIMS, ¹H NMR, ¹³C NMR, HSQC and HMBC. The FTIR spectrum showed the bands at 3447 cm⁻¹ and 1708 cm⁻¹ ascribed to the

hydroxyl and carbonyl stretching of the carboxylic acid. The EIMS spectrum showed the structure compatible molecular peak with m/z 430 ($[M+TMS]^+$). The 1H NMR spectrum did not show the hydroxyl from the carboxylic acid, however, it also did not show the protons from the methylene group. The main connectivities of HMBC are presented in figure 21 and all the assignments are presented in table 14.

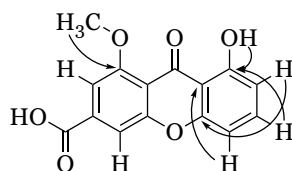
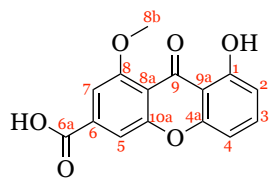


Figure 21: Main connectivities in HMBC spectrum for compound **25**.

Table 14: Chemical shifts and assignments of compound **25**.

1H NMR chemical shifts ^a		^{13}C NMR chemical shifts ^b	
1-OH	13.19 (s)	1	161.3
2-H	6.99 (d, J = 8.2)	2	106.5
3-H	7.65 (t, J = 8.2)	3	136.6
4-H	6.74 (d, J = 8.2)	4	110.0
5-H	7.43 (s)	4a	155.2
7-H	7.46 (s)	5	106.6
8b-H	3.93 (s)	6	129.4
6a-OH	-	6a	165.8
		7	109.9
		8	159.6
		8a	108.8
		8b	56.0
		9	181.8
		9a	107.2
		10a	157.0

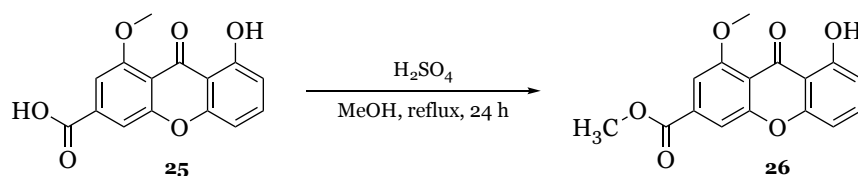


^aValues in ppm (δ_H) measured at 500.16 MHz, multiplicity and J values (Hz) are shown in parentheses;

^bValues in ppm (δ_C) measured at 125.77 MHz.

4.1.4.6. Synthesis of methyl 8-hydroxy-1-methoxy-9-oxo-9H-xanthene-3-carboxylate - Analogue B (26).

Scheme 36 shows the synthesis of Analogue B (**26**).



Scheme 36: Esterification of compound 25.

In a similar way to **4.1.3.6.**, a Fischer esterification was used to produce analogue B from analogue C. So, compound **25** dissolved in methanol, in the presence of sulfuric acid, was refluxed overnight. The desired product was achieved after purification in 12 % yield.

Compound **26** was identified based on FTIR, EIMS, ¹H NMR, ¹³C NMR, HSQC and HMBC. The FTIR spectrum showed absence of the band ascribed to the hydroxyl of the carboxylic acid and the EIMS spectrum showed the structure compatible molecular peak with *m/z* 372 ([M+TMS]⁺). The main connectivities of HMBC are presented in figure 22 and all the assignments are presented in table 15.

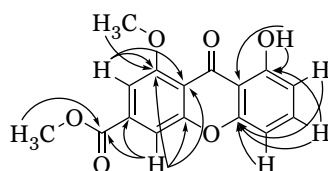
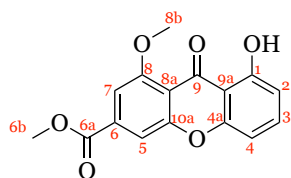


Figure 22: Main connectivities in HMBC spectrum for compound 26.

Table 15: Chemical shifts and assignments of compound **26**.

¹ H NMR chemical shifts ^a		¹³ C NMR chemical shifts ^b	
1-OH	12.82 (s)	1	161.1
2-H	7.03 (d, <i>J</i> = 8.3)	2	102.8
3-H	7.71 (t, <i>J</i> = 8.3)	3	137.2
4-H	6.81 (d, <i>J</i> = 8.3)	4	110.7
5-H	7.42 (s)	4a	154.9
6b-H	4.02 (s)	5	106.0
7-H	7.62 (s)	6	136.1
8b-H	3.95 (s)	6a	160.5
		6b	56.7
		7	110.2
		8	164.8
		8a	113.0
		8b	53.1
		9	181.5
		9a	109.4
		10a	157.1



^aValues in ppm (δ_{H}) measured at 500.16 MHz, multiplicity and *J* values (Hz) are shown in parentheses;

^bValues in ppm (δ_{C}) measured at 125.77 MHz.

4.2. *In silico* biophysicochemical properties

To become a successful drug candidate, a hit compound should have suitable pharmacodynamics and pharmacokinetics behaviors. Whereas pharmacodynamics is mainly associated with the interactions with a putative receptor, pharmacokinetics is mainly dictated by the biophysicochemical properties [87]. Both PK/PD should be optimized since an early stage of development [88]. For this purpose, four biophysicochemical properties and a pharmacokinetic parameter were predicted using *in silico* methods.

Eight of the synthesized compounds (**17 – 20** and **23 -26**) were studied (figure 23). These compounds were selected since they hold a scaffold, xanthone or benzophenone, for which antifungal and/or antibacterial activity have been reported [89]. Nine different software (EPI Suite™, ChemDraw Professional®, ChemAxon® MarvinSketch, Molinspiration Cheminformatics® MiLogP, Swiss Institute of Bioinformatics® SwissADME, Institute for Genomics and Bioinformatics® AquaSol, pkCSM, BMDRC® PreADMET and ACD/Labs® ACD Percepta Predictors) were used and the methodologies applied in each one will be discussed within this chapter.

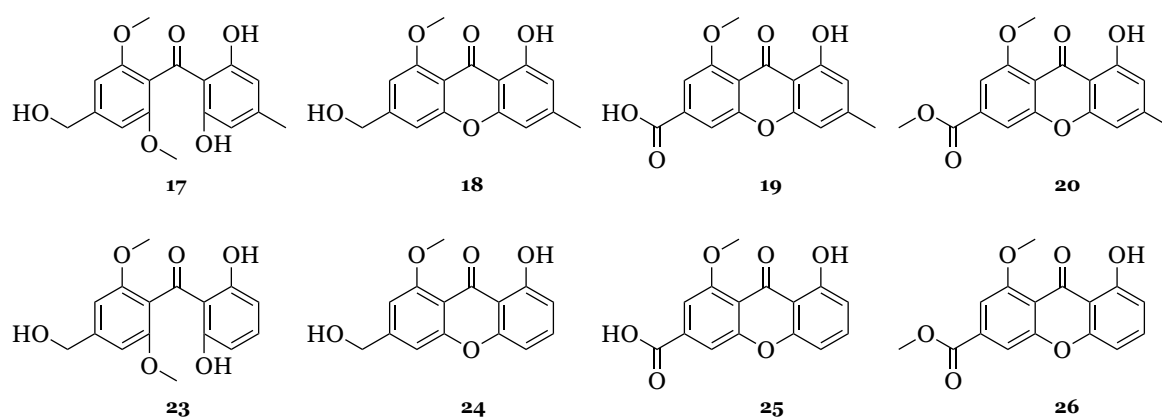


Figure 23: Synthesized compounds in study.

4.2.1. Lipophilicity

As said detailed in the introduction, lipophilicity is one of the most important physicochemical properties in drug discovery. Lipophilicity is usually expressed by the partition coefficient of a drug between octanol and water [26]. This partition coefficient, known as log P, can be calculated by *in silico* methods [35].

To access lipophilicity by *in silico*, three main methodologies can be used: atom based, fragment based and property based methodologies. The atom based methodology considers the individual contribution to lipophilicity of each atom present in the

molecule [35]. The fragment based methodology considers the contribution of fragments obtained from cutting the molecule and uses correction factor to compensate the intramolecular interaction between fragments [35]. Whereas atom and fragment-based methods considered structural contributions to lipophilicity, property based methodologies considers properties shown by the entire molecule, either by using the 3D-structure representation or by using topological descriptors [35].

The predicted partition coefficient for each of the studied compounds are presented in table 16. Table 16 is organized according to the methodology used for the prediction, mentioning the software provider and the term encoded by each software.

Table 16: Calculation of the partition coefficient of the 8 compounds in several softwares.

	Provider	Term	17	18	19	20	23	24	25	26	
Atom	MarvinSketch	LogP	3.13	2.40	2.75	3.38	2.66	1.93	2.28	2.91	
	PreADMET	LogP	2.54	2.54	2.96	2.99	1.97	1.98	2.40	2.43	
	SwissADME	WLogP	1.99	2.31	2.67	2.76	1.69	2.00	2.36	2.45	
		XLogP3	2.53	2.61	3.02	3.35	2.16	2.24	2.66	2.98	
	ChemDraw	Broto's	1.76	2.23	2.33	2.80	1.35	1.81	1.92	2.39	
				2.39	2.42	2.75	3.06	1.97	1.99	2.32	2.63
		Average		±	±	±	±	±	±	±	±
			1.01	0.63	0.74	0.77	0.96	0.63	0.74	0.76	
Fragment	EPI Suite	LogKow	3.53	3.85	4.65	4.60	2.98	3.30	4.10	4.06	
	Molinspiration	LogP	2.98	3.00	3.58	3.83	2.58	2.60	3.17	3.43	
	ChemDraw	Crippen's	2.12	2.14	2.27	2.54	1.64	1.66	1.79	2.05	
		Viswanadhan's	2.13	2.05	2.28	2.31	1.66	1.58	1.81	1.84	
		CLogP	2.42	2.59	3.92	4.29	1.92	2.56	3.42	3.79	
	SwissADME	Silicos-IT LogP	2.90	3.35	2.90	3.43	2.38	2.85	2.39	2.92	
	ACDLabs	A/BLogP	3.08	3.15	3.48	3.69	2.59	2.65	2.89	3.26	
		ACDLogP	2.88	1.85	3.17	3.23	2.42	1.39	2.71	2.77	
				2.76	2.75	3.28	3.49	2.27	2.32	2.79	3.02
		Average		±	±	±	±	±	±	±	±
			1.06	1.28	1.38	1.36	1.05	1.26	1.36	1.35	
Property	SwissADME	MLogP	0.78	0.81	1.00	1.24	0.54	0.56	0.75	1.00	
		iLogP	2.25	2.55	2.28	2.41	2.03	2.46	1.42	2.78	

The predicted partition coefficient values varied greatly using different approaches, which is reflected on the high standard deviation values. Figure 24 shows the log P values predicted for compound **19** using different approaches. Comparing atom and fragment-based methods, similar average values were found. However, the standard deviation found on atom-based methods is smaller. For instance, compound **19** have 2.75 ± 0.74 and

3.28 ± 1.38 with atom and fragment-based methods, respectively. The results provided by property based methodology MLogP were far off the results given by the other methodologies, which suggest the lack of accuracy of this type of methodology.

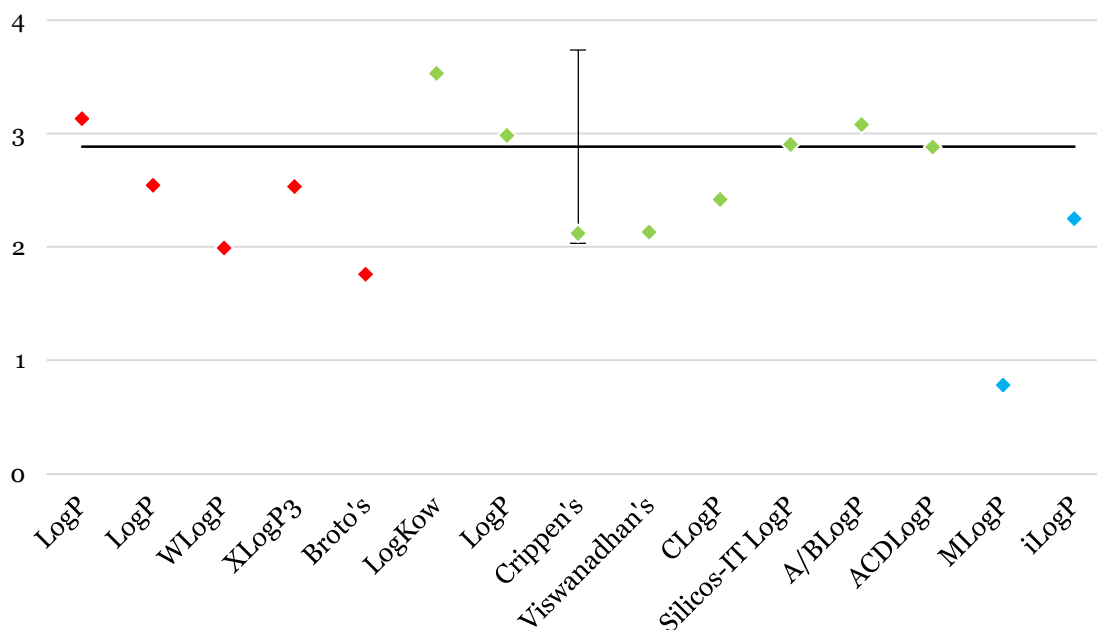


Figure 24: Representation of the variation of values for compound 19. Red – atom-based method, Green – fragment-based method; Blue_ property-based method.

The distribution constant, known as log D, is another important way to evaluate lipophilicity. Similar to log P, log D takes into account the ionization of the molecule by considering the drug partition coefficient between octanol and buffered solution at a certain pH value. The distribution constant at four different pH values, representing the pH found on different compartments (1.5 – stomach, 5.0 – saliva, 6.5 – urine, 7.4 – physiological)^[90], are summarized in table 17.

Table 17: Calculation of the distribution coefficient of the 8 compounds in three softwares.

Provider	pH	17	18	19	20	23	24	25	26	
Atom	MarvinSketch	Log D _{1.5}	3.13	2.40	2.74	3.38	2.66	1.93	2.27	2.91
		Log D _{5.0}	3.12	2.40	1.07	3.38	2.65	1.93	0.6	2.91
		Log D _{6.5}	3.01	2.39	-0.32	3.37	2.52	1.92	-0.78	2.91
		Log D _{7.4}	2.57	2.39	-0.82	3.34	2.02	1.88	-1.30	2.87
	PreADMET	Log D _{7.4}	2.54	2.54	1.71	2.99	1.97	1.98	1.15	2.43
		Log D _{1.5}	3.08	3.14	3.45	3.68	2.59	2.64	2.86	3.25
	ACDLabs	Log D _{5.0}	3.08	3.15	1.83	3.69	2.59	2.65	1.24	3.26
		Log D _{6.5}	3.08	3.15	0.38	3.69	2.59	2.65	-0.20	3.26
		Log D _{7.4}	3.08	3.15	-0.29	3.69	2.58	2.65	-0.88	3.26
	Average		3.11	2.77	3.10	3.53	2.63	2.29	2.57	3.08
		Log D _{1.5}	±	±	±	±	±	±	±	±
		0.04	0.52	0.50	0.21	0.05	0.50	0.42	0.24	
		3.10	2.78	1.45	3.54	2.62	2.29	0.92	3.09	
Log D _{5.0}		±	±	±	±	±	±	±	±	
		0.03	0.53	0.54	0.22	0.04	0.51	0.45	0.25	
		3.05	2.77	0.03	3.53	2.56	2.29	-0.49	3.09	
Log D _{6.5}		±	±	±	±	±	±	±	±	
		0.05	0.54	0.49	0.23	0.05	0.52	0.41	0.25	
		2.73	2.69	0.20	3.34	2.19	2.17	-0.34	2.85	
Log D _{7.4}		±	±	±	±	±	±	±	±	
		0.30	0.40	1.33	0.35	0.34	0.42	1.31	0.42	

The log D values of compounds **17** – **18**, **20** – **24** and **26** were similar between the different pH values. However, compound **19** and **25** shown a decreased in its log D_{6.5} and log D_{7.4} values. In common, these compounds have a carboxylic acid, which is deprotonated at these pH values. Therefore, the affinity to an octanol hydrophobic phase deeply decreases when the compound is at an ionized state. Taking into account the parallelism between affinity to octanol and the ability to permeate biological membranes, it is reasonable to assume that compound **19** and **25** will be mainly absorbed in stomach (log D_{1.5} vs. Log D_{7.4}).

4.2.2. pKa

The conclusions previously discussed are linked to the pKa value of each compound.

The pKa values were obtained by two different programs, MarvinSketch and ACDLabs Percepta, which are based on the partial charge of atoms in the molecule and based on the calculation of the pKa in the dissociation centers when the rest of the molecule

is neutral, respectively ^[91]. Table 18 summarizes predicted pKa values for each molecule of interest.

Table 18: Results from the calculation of the pKa.

	17	18	19	20	23	24	25	26
MarvinSketch	7.013	8.483	3.324	8.476	6.911	8.380	3.324	8.374
ACDLabs	9.40	11.40	3.40	11.40	9.40	11.40	3.40	11.40

The obtained pKa results are helpful to predict the ionization state of the molecule in a determined pH in the organism. The majority of the studied compounds synthesized have a pKa higher than 8, which means they will not be ionized at physiological pH. Therefore, it is reasonable to assume that these compounds will be mainly absorbed in human intestine and distributed in the blood at a non-ionized state. As previously discussed, compounds **19** and **23** will have a different profile.

4.2.3. Solubility

In a context of drug discovery, solubility is expressed by log S, which is the empirically derived general solubility equation of Yalkowsky and Banerjee based on lipophilicity and melting point ^[29].

In a similar way to log P prediction, several methodologies were involved for the prediction of log S, namely atom, fragment and property-based methods.

Similar to log P prediction, different methodologies, based on the individual contributions of atoms/fragments or based on the entire molecule contribution have been described ^[92, 93]. The following table represents the results obtained for the solubility prediction for each compound.

Table 19: Results from the calculation of the solubility in several softwares.

	Provider		17	18	19	20	23	24	25	26
Atom	ACDLabs	A/B	-2.95	-4.19	-4.69	-4.98	-2.97	-3.99	-4.48	-4.90
	KOWWIN		-3.45	-4.60	-5.89	-5.95	-2.88	-4.03	-5.32	-5.38
Fragment	SwissADME	SILICOS-IT	-4.17	-5.05	-4.59	-5.29	-3.79	-4.67	-4.21	-4.91
	ChemDraw		-3.64	-3.22	-3.73	-3.85	-3.27	-2.85	-3.36	-3.49
	PreADMET	Pure water	-3.90	-4.60	-4.74	-5.08	-3.40	-4.10	-4.23	-4.57
		Buffer	-3.33	-3.98	-3.31	-4.41	-2.71	-3.37	-2.70	-3.79
	MarvinSketch	Intrinsic	-2.96	-3.62	-4.18	-4.36	-2.47	-3.12	-3.67	-3.86
Property	SwissADME	Ali	-4.20	-3.94	-4.72	-4.83	-3.81	-3.55	-4.35	-4.45
		ESOL	-3.46	-3.62	-3.94	-4.15	-3.16	-3.33	-3.65	-3.85
	pkCSM	-3.28	-2.95	-3.14	-3.59	-3.00	-3.21	-2.79	-3.18	
	AquaSol*	-2.82	-2.78	-2.87	-3.15	-2.57	-2.50	-2.64	-2.90	
	Average*		-3.46 ± 0.49	-3.84 ± 0.77	-4.14 ± 0.92	-4.50 ± 0.84	-3.09 ± 0.45	-3.52 ± 0.63	-3.75 ± 0.88	-4.10 ± 0.81

The solubility data allows us to conclude that compounds **17**, **23** and **24** will probably be soluble in water because, according to a new classification method by Rutwijn and Marilyn^[94], they have $\log S > -3.5$. Among them, benzophenone will be the most soluble compound, highlight the role of highly pattern of substitution with hydroxyl groups and the role of the benzophenone scaffold. Indeed, the benzophenone cyclization leading to the xanthone scaffold, promote a decrease the solubility of the compounds, probably due to the increase planarity induced by the xanthone three aromatic rings scaffold. Even so, almost all drugs have a range of LogS between -6 and -1, which is in accordance with the prediction made ^[95].

4.2.4. Permeability

Tightly bounded to solubility, permeability is an important subject in the absorption of any compound. From a practical point of view, permeability is evaluated by measuring the permeability across a barrier of Caco 2 cells, a model to evaluate permeability across intestinal epithelial barrier, and it is expressed as the apparent permeability coefficient, known as P_{app} [96].

In this, three different approaches were used. pkCSM permeability prediction is based on the results of experimental data for a wide range of drug-like compounds [97]. PreADMET uses a MI-QSAR model of Caco-2 cell permeation obtained from a study involving 30 different drugs [98]. ACDLabs Percepta uses intrinsic attributes to the molecule (logP, pKa, H-bond donors) to calculate the permeability across jejunal epithelium [99]. Table 20 represents the results from the *in silico* predictions for the intestinal permeability in Caco-2 model and jejunum for the eight compounds of interest.

Table 20: Results from the calculation of intestinal permeability for the 8 compounds.

Provider		Units	17	18	19	20	23	24	25	26
pkCSM	Caco-2	P_{app} (10^{-6} cm/s)	2.40	11.75	2.82	12.30	2.09	11.48	2.45	12.02
PreADMET	Caco-2	P_{app} (10^{-6} cm/s)	1.486	0.892	0.841	1.098	1.471	0.330	0.234	0.629
ACDLabs	Jejunum	P_e (10^{-4} cm/s)	7.79	8.31	4.07	8.17	7.69	8.40	2.26	8.34

According to Hubatsch et al^[100], the permeability values obtained with pkCSM were consistent with a good permeation through Caco-2 cells, since it was reported that P_{app} values higher than $2 - 5 \times 10^{-6}$ cm/s indicate rapid transport and complete absorption in the human intestine. However, predictions made by PreADMET showed P_{app} values which are not consistent with good permeation, still considering the values provided by the protocol by Hubatsch et al^[100]. It is well known that due to culture-related conditions, experimental P_{app} values in Caco-2 cell lines varied greatly between different laboratories, which often make it extremely difficult to compare results in the literature ^[101]. Therefore, the discrepancy found on the prediction of the permeability of the studied compounds can be attributed to the variability in the dataset used for the permeability prediction.

4.2.5. Plasma protein binding

Plasma protein binding is a crucial pharmacokinetic parameter affecting all components of the drug ADMET profile [34]. Albumin is the most abundant plasma protein. Therefore, the $\log K_A^{\text{HSA}}$, which expresses the affinity constant of a drug to the human serum albumin, is often used in drug discovery as PK prediction parameter [102]. Table 21 presents the $\log K_A^{\text{HSA}}$ values and the percentage of plasma protein binding for each studied compound.

Table 21: Results from the prediction of plasma protein binding.

		17	18	19	20	23	24	25	26
PreADMET	%PPB	84.2	90.7	93.4	92.6	81.1	87.3	90.6	90.3
	$\log K_A^{\text{HSA}}$	4.8	5.28	5.48	5.48	4.77	5.23	5.43	5.37

%PPB – Percentage of plasma protein binding. $\log K_A^{\text{HSA}}$ - Affinity constant to human serum albumin.

According to the table, all the compounds will bind tightly to albumin. Consequently, a large compound percentage (> 85 %) will be distributed in the blood bound to albumin. This aspect will have implications on the drug ADMET profile and rises the need for the clearance study of this compounds in order to guarantee an effective plasmatic concentration.

4.2.1. Guidelines for the prediction of general drug-likeness for oral bioavailability

Inspired by the pivotal work Lipinski *et al*, several simple rules encoding physicochemical properties such as hydrogen bonding, size or lipophilicity, have been proposed to predict drug-likeness and oral bioavailability. Table 22 summarizes the physicochemical properties calculated for each compound as well as the requirements preconized by these guidelines.

Table 22: Calculated properties applied to three drug-like rules.

	Property	Value	17	18	19	20	23	24	25	26
Lipinski ^[103]	MW	<500	318.32	282.28	300.27	314.29	304.30	272.26	286.24	300.27
	H-bond donors	<5	3	2	2	1	3	2	2	1
	H-bond acceptors	<10	6	5	6	6	6	5	6	6
	LogP	<5	✓	✓	✓	✓	✓	✓	✓	✓
Veber ^[104]	Rotable bonds	<10	5	2	2	3	5	2	2	3
	tPSA	<140	96.22	75.99	93.06	82.06	96.22	75.99	95.06	82.06
	Total H-bonds	<12	9	7	8	7	9	7	8	7
Muegge ^[105]	MW	200 - 600	318.32	282.28	300.27	314.29	304.30	272.26	286.24	300.27
	Number rings	< 7	3	3	3	3	3	3	3	3
	Number carbons	> 4	17	16	16	17	16	15	15	16
	Number heteroatoms	> 1	6	5	6	6	6	5	6	6
	Rotable bonds	< 15	5	2	2	3	5	2	2	3
	H-bond donors	< 5	3	2	2	1	3	2	2	1
	H-bond acceptors	< 10	6	5	6	6	6	5	6	6
	LogP	-2 - 5	✓	✓	✓	✓	✓	✓	✓	✓
Egan ^[106]	LogP	< 5.88	✓	✓	✓	✓	✓	✓	✓	✓
	tPSA	< 131.6	96.22	75.99	93.06	82.06	96.22	75.99	95.06	82.06

Overall, all the compounds fit with the rules applied, making them drug-like compounds and in the good pathway on becoming a drug.

C
O
N
C
L
U
S
I
O
N
S

In this dissertation the total synthesis of two marine xanthenes, yicathins B and C, extracted from a fungus, is presented. A first approach to the total synthesis of these substances was previously performed in our group. In this work, we could confirm some of the already used synthetic paths and a tentative to get better yields and shorter reaction times were explored. As a result, yicathins B and C, as well as several intermediates and two yicathins analogues were obtained in quantities that could allow the biologic activity assays and the preparation of other compounds. The structure of all the synthesized compounds was elucidated by IR, EIMS, ¹H NMR, ¹³C NMR, HSQC and HMBC. All the new synthesized compounds were purified (>90 % RP-HPLC).

Eight synthesized compounds (yicathins B and C, two benzophenones intermediates and two yicathins analogues) were further explored, since their base structures are common to several natural bioactive substances. In this context, their biophysicochemical properties were *in silico* assessed and discussed. All compounds are in accordance with Lipinski rule of five, Weber, Muegge and Egan descriptors for oral bioavailability, exhibiting lipophilicity and other properties in accordance to the guidelines of drug-likeness in Medicinal Chemistry. From this study, it is also possible to say that these compounds might be moderate to highly soluble in water, that they might be permeable and might be bounded to the plasma proteins.

Next work will involve the study of the biological activities of the synthesized compounds and their experimental biophysicochemical properties.

R
E
F
E
R
E
N
C
E
S

1. Tanwar, J.; Das, S.; Fatima, Z.; Hameed, S., Multidrug Resistance: An Emerging Crisis. *Interdisciplinary Perspectives on Infectious Diseases* **2014**, *2014*, 7.
2. The top 10 causes of death. <http://www.who.int/mediacentre/factsheets/fs310/en/> (accessed May 7).
3. Chast, F., Chapter 1 - A History of Drug Discovery: From first steps of chemistry to achievements in molecular pharmacology A2 - Wermuth, Camille Georges. In *The Practice of Medicinal Chemistry (Third Edition)*, Academic Press: New York, 2008; pp 1-62.
4. Proudfoot, J. R., Chapter 7 - High-Throughput Screening and Drug Discovery A2 - Wermuth, Camille Georges. In *The Practice of Medicinal Chemistry (Third Edition)*, Academic Press: New York, 2008; pp 144-158.
5. Kumar, K.; Wetzel, S.; Waldmann, H., Chapter 9 - Biology Oriented Synthesis and Diversity Oriented Synthesis in Compound Collection Development A2 - Wermuth, Camille Georges. In *The Practice of Medicinal Chemistry (Third Edition)*, Academic Press: New York, 2008; pp 187-209.
6. Langer, T.; Bryant, S. D., Chapter 10 - In Silico Screening: Hit Finding from Database Mining A2 - Wermuth, Camille Georges. In *The Practice of Medicinal Chemistry (Third Edition)*, Academic Press: New York, 2008; pp 210-227.
7. Farmer, B. T.; Reitz, A. B., Chapter 11 - Fragment-Based Drug Discovery A2 - Wermuth, Camille Georges. In *The Practice of Medicinal Chemistry (Third Edition)*, Academic Press: New York, 2008; pp 228-243.
8. Polinsky, A., Chapter 12 - Lead-Likeness and Drug-Likeness A2 - Wermuth, Camille Georges. In *The Practice of Medicinal Chemistry (Third Edition)*, Academic Press: New York, 2008; pp 244-254.
9. Newman, D. J.; Cragg, G. M.; I. Kingston, D. G., Chapter 8 - Natural Products as Pharmaceuticals and Sources for Lead Structures A2 - Wermuth, Camille Georges. In *The Practice of Medicinal Chemistry (Third Edition)*, Academic Press: New York, 2008; pp 159-186.
10. Newman, D. J.; Cragg, G. M., Natural Products as Sources of New Drugs from 1981 to 2014. *Journal of Natural Products* **2016**, *79* (3), 629-661.
11. Cragg, G. M.; Newman, D. J.; Snader, K. M., Natural Products in Drug Discovery and Development. *Journal of Natural Products* **1997**, *60* (1), 52-60.
12. Hasan, S.; Ansari, M. I.; Ahmad, A.; Mishra, M., Major bioactive metabolites from marine fungi: A Review. *Bioinformation* **2015**, *11* (4), 176-81.
13. NASA The Water Planet. https://www.nasa.gov/multimedia/imagegallery/image_feature_1925.html (accessed June 25).
14. Méndez-Vilas, A., *Science Against Microbial Pathogens: Communicating Current Research and Technological Advances*. Formatex Research Center: 2011.
15. Shukla, S., Secondary metabolites from marine microorganisms and therapeutic efficacy: A mini review. *Indian Journal of Geo-Marine Sciences* **2016**, *45* (10), 1245-1254.
16. Tchamo Diderot, N.; Silvere, N.; Etienne, T., Xanthones as therapeutic agents: chemistry and pharmacology. In *Advances in Phytomedicine*, 2006; Vol. 2, pp 273-298.

17. Pinto, M. M. M.; Castanheiro, R. A. P.; Kijjoo, A., Xanthonones from Marine-Derived Microorganisms: Isolation, Structure Elucidation and Biological Activities. In *Encyclopedia of Analytical Chemistry*, John Wiley & Sons, Ltd: 2006.
18. Sun, R. R.; Miao, F. P.; Zhang, J.; Wang, G.; Yin, X. L.; Ji, N. Y., Three new xanthone derivatives from an algicolous isolate of *Aspergillus wentii*. *Magnetic Resonance in Chemistry* **2013**, *51* (1), 65-68.
19. König, G. M.; Kehraus, S.; Seibert, S. F.; Abdel-Lateff, A.; Müller, D., Natural Products from Marine Organisms and Their Associated Microbes. *ChemBioChem* **2006**, *7* (2), 229-238.
20. Ryzdewski, R. M., Chapter 3 - Industrial considerations. In *Real world drug discovery*, Elsevier: Amsterdam, 2008; pp 113-150.
21. The Sustainable Pipeline Myth. <http://www.discoverymanagementsolutions.com/the-organization-of-biopharmaceutical-rd/the-sustainable-pipeline-myth/> (accessed December 15).
22. Stevens, E., *Medicinal Chemistry: The Modern Drug Discovery Process*. Pearson Education, Limited: 2013.
23. Process Development and Scale-up Program. <https://www.anl.gov/energy-systems/project/process-development-and-scale-program> (accessed December 15).
24. Kerns, E. H.; Di, L., Pharmaceutical profiling in drug discovery. *Drug Discovery Today* **2003**, *8* (7), 316-323.
25. Azevedo, C. Synthesis and multidimensional optimization of antitumor xanthonones. FFUP, Porto, 2012.
26. Physicochemistry. In *Pharmacokinetics and metabolism in drug design*, Wiley-VCH Verlag GmbH & Co. KGaA: 2012; pp 1-17.
27. Liu, X.; Testa, B.; Fahr, A., Lipophilicity and its relationship with passive drug permeation. *Pharm Res* **2010**, *28* (5), 962-977.
28. Pliška, V.; Testa, B.; van de Waterbeemd, H., Lipophilicity: The empirical tool and the fundamental objective. An introduction. In *Lipophilicity in drug action and toxicology*, Wiley-VCH Verlag GmbH: 2008; pp 1-6.
29. Kerns, E. H.; Di, L., Chapter 7 - Solubility. In *Drug-like properties: Concepts, structure design and methods*, Academic Press: San Diego, 2008; pp 56-85.
30. Di, L.; Fish, P. V.; Mano, T., Bridging solubility between drug discovery and development. *Drug Discov Today* **2012**, *17* (9-10), 486-495.
31. Kerns, E. H.; Di, L., Chapter 6 - pKa. In *Drug-like properties: Concepts, structure design and methods*, Academic Press: San Diego, 2008; pp 48-55.
32. Manallack, D. T., The pK(a) distribution of drugs: Application to drug discovery. *Perspect Medicin Chem* **2007**, *1*, 25-38.
33. Kerns, E. H.; Di, L., Chapter 8 - Permeability. In *Drug-like properties: Concepts, structure design and methods*, Academic Press: San Diego, 2008; pp 86-99.
34. Kerns, E. H.; Di, L., Chapter 14 - Plasma protein binding. In *Drug-like properties: Concepts, structure design and methods*, Academic Press: San Diego, 2008; pp 187-196.
35. Mannhold, R.; Kubinyi, H.; Folkers, G., *Molecular drug properties: Measurement and prediction*. Wiley: 2008.

36. Azevedo, C. M. G.; Afonso, C. M. M.; Pinto, M. M. M., Routes to xanthenes: An update on the synthetic approaches. *Curr Org Chem* **2012**, *16* (23), 2818-2867.
37. Sousa, M. E.; Pinto, M. M. M., Synthesis of xanthenes: An overview. *Curr Med Chem* **2005**, *12* (21), 2447-2479.
38. Grover, P. K.; Shah, G. D.; Shah, R. C., Xanthenes. Part IV. A new synthesis of hydroxyxanthenes and hydroxybenzophenones. *J Chem Soc* **1955**, 3982-3985.
39. Zhao, J.; Larock, R. C., One-pot synthesis of xanthenes and thioxanthenes by the tandem coupling-cyclization of arynes and salicylates. *Org Lett* **2005**, *7* (19), 4273-5.
40. Zhao, J.; Larock, R. C., Synthesis of xanthenes, thioxanthenes, and acridones by the coupling of arynes and substituted benzoates. *J Org Chem* **2007**, *72* (2), 583-8.
41. Wang, S.; Xie, K.; Tan, Z.; An, X.; Zhou, X.; Guo, C.-C.; Peng, Z., One-step preparation of xanthenes via Pd-catalyzed annulation of 1,2-dibromoarenes and salicylaldehydes. *Chem Commun* **2009**, (42), 6469-6471.
42. Quillinan, A. J.; Scheinmann, F., Studies in the xanthone series. Part XII. A general synthesis of polyoxygenated xanthenes from benzophenone precursors. *J Chem Soc, Perkin Trans 1* **1973**, (0), 1329-1337.
43. Clayden, J., *Organolithiums: Selectivity for Synthesis*. Elsevier Science: Oxford, 2002.
44. Suzuki, Y.; Toyota, T.; Miyashita, A.; Sato, M., Synthesis of heterocyclic compounds via nucleophilic arylation catalyzed by imidazolidenyl carbene. *Chem Pharm Bull* **2006**, *54* (12), 1653-1658.
45. Kraus, G.; Mengwasser, J., Quinones as key intermediates in natural products synthesis. Syntheses of bioactive xanthenes from *Hypericum perforatum*. *Molecules* **2009**, *14* (8), 2857.
46. Barton, D. H. R.; Scott, A. I., 363. The constitutions of geodin and erdin. *J Chem Soc* **1958**, (0), 1767-1772.
47. Afzal, M.; Al-Hassan, J. M., Synthesis and biosynthesis of phytoxanthenes. *Heterocycles* **1980**, *14* (8), 1173-1205.
48. Dean, F. M., The total synthesis of naturally occurring oxygen ring compounds. In *Total synthesis of natural products*, John Wiley & Sons, Inc.: 2007; pp 467-562.
49. Barbero, N.; SanMartin, R.; Dominguez, E., An efficient copper-catalytic system for performing intramolecular O-arylation reactions in aqueous media. New synthesis of xanthenes. *Green Chem* **2009**, *11* (6), 830-836.
50. Ellis, R. C.; Whalley, W. B.; Ball, K., Biogenetic-type syntheses of xanthenes. *Chem Commun (London)* **1967**, (16), 803-804.
51. Tisdale, E. J.; Kochman, D. A.; Theodorakis, E. A., Total synthesis of atroviridin. *Tetrahedron Lett.* **2003**, *44* (16), 3281-3284.
52. Ullmann, F.; Sponagel, P., Ueber die Phenylirung von Phenolen. *Ber Dtsch Chem Ges* **1905**, *38* (2), 2211-2212.
53. Müller, P.; Venakis, T.; Eugster, C. H., Aktivierte chinone: O- versus C-addition von phenolen; eine neue, regiospezifische Synthese von xanthenen, thioxanthenen und N-methyl-9-acridonen. *Helv Chim Acta* **1979**, *62* (7), 2350-2360.

54. Simoneau, B.; Brassard, P., A new regiospecific synthesis of 1,4-dihydroxyxanthenes. *J Chem Soc, Perkin Trans 1* **1984**, (0), 1507-1510.
55. Azevedo, C. M. G.; Afonso, C. M. M.; Pinto, M. M. M., Routes to xanthenes: An update on the synthetic approaches. *Current Organic Chemistry* **2012**, 16 (23), 2818-2867.
56. Loureiro, D. Synthesis of marine xanthenes: tracking yicathins B and C. Universidade de Coimbra, Coimbra, 2016.
57. Perrin, D. D.; Armarego, W. L. F., *Purification of Laboratory Chemicals*. 4th ed.; Elsevier Science: 2017.
58. Tan, J. S.; Ciufolini, M. A., Total Synthesis of Topopyrones B and D. *Organic Letters* **2006**, 8 (21), 4771-4774.
59. Ohta, S.; Nozaki, A.; Ohashi, N.; Matsukawa, M.; Okamoto, M., A Total Synthesis of Grifolin. *Chemical & Pharmaceutical Bulletin* **1988**, 36 (6), 2239-2243.
60. Townsend, C. A.; Davis, S. G.; Christensen, S. B.; Link, J. C.; Lewis, C. P., Methoxymethyl-directed aryl metalation. Total synthesis of (+-)-averufin. *Journal of the American Chemical Society* **1981**, 103 (23), 6885-6888.
61. Carta, F.; Vullo, D.; Maresca, A.; Scozzafava, A.; Supuran, C. T., Mono-/dihydroxybenzoic acid esters and phenol pyridinium derivatives as inhibitors of the mammalian carbonic anhydrase isoforms I, II, VII, IX, XII and XIV. *Bioorganic & Medicinal Chemistry* **2013**, 21 (6), 1564-1569.
62. Clayden, J.; Greeves, N.; Warren, S., *Organic Chemistry*. Oxford University Press Inc.: New York, 2012.
63. Burkhardt, E. R.; Matos, K., Boron Reagents in Process Chemistry: Excellent Tools for Selective Reductions. *Chemical Reviews* **2006**, 106 (7), 2617-2650.
64. McMurry, J., *Organic Chemistry*. Cengage Learning: United States of America, 2016.
65. Brown, J. D.; Haddenham, D., Sodium Borohydride and Iodine. In *Encyclopedia of Reagents for Organic Synthesis*, John Wiley & Sons, Ltd: 2001.
66. Wuts, P. G. M.; Greene, T. W., Protection for the Hydroxyl Group, Including 1,2- and 1,3-Diols. In *Greene's Protective Groups in Organic Synthesis*, John Wiley & Sons, Inc.: 2006; pp 16-366.
67. Wuts, P. G. M., *Greene's Protective Groups in Organic Synthesis*. Wiley: 2014.
68. Corey, E. J.; Venkateswarlu, A., Protection of hydroxyl groups as tert-butyldimethylsilyl derivatives. *Journal of the American Chemical Society* **1972**, 94 (17), 6190-6191.
69. Banwell, M. G.; Chand, S., Exploitation of Co-operative Directed ortho-Metallation (DoM) by 1,3-related -OMOM Groups in the Development of a Fully Regio-controlled Synthesis of Atranol from Orcinol. *Organic Preparations and Procedures International* **2005**, 37 (3), 275-279.
70. Rappoport, Z.; Marek, I., *The Chemistry of Organolithium Compounds*. Wiley: 2004.
71. Snieckus, V., Directed ortho metalation. Tertiary amide and O-carbamate directors in synthetic strategies for polysubstituted aromatics. *Chemical Reviews* **1990**, 90 (6), 879-933.
72. Merriman, G., Dimethyl Sulfate. In *Encyclopedia of Reagents for Organic Synthesis*, John Wiley & Sons, Ltd: 2001.
73. Stodola, F. H., Base-Catalyzed Preparation of Methyl and Ethyl Esters of Carboxylic Acids. *The Journal of Organic Chemistry* **1964**, 29 (8), 2490-2491.

74. Henry, K. M.; Townsend, C. A., Synthesis and Fate of o-Carboxybenzophenones in the Biosynthesis of Aflatoxin. *Journal of the American Chemical Society* **2005**, *127* (10), 3300-3309.
75. Williams, D. B. G.; Lawton, M., Drying of Organic Solvents: Quantitative Evaluation of the Efficiency of Several Desiccants. *The Journal of Organic Chemistry* **2010**, *75* (24), 8351-8354.
76. Lou, J.-D.; Xu, Z.-N., Solvent free oxidation of alcohols with manganese dioxide. *Tetrahedron Letters* **2002**, *43* (35), 6149-6150.
77. Wirth, T., IBX - New reactions with an old reagent. *Angewandte Chemie - International Edition* **2001**, *40* (15), 2812-2814.
78. Yadav, J. S.; Ganganna, B.; Bhunia, D. C.; Srihari, P., NbCl₅ mediated deprotection of methoxy methyl ether. *Tetrahedron Letters* **2009**, *50* (30), 4318-4320.
79. Little, A.; Porco, J. A., Total Syntheses of Graphisin A and Sydowinin B. *Organic Letters* **2012**, *14* (11), 2862-2865.
80. Fernandes, C.; Masawang, K.; Tiritan, M. E.; Sousa, E.; de Lima, V.; Afonso, C.; Bousbaa, H.; Sudprasert, W.; Pedro, M.; Pinto, M. M., New chiral derivatives of xanthenes: Synthesis and investigation of enantioselectivity as inhibitors of growth of human tumor cell lines. *Bioorganic & Medicinal Chemistry* **2014**, *22* (3), 1049-1062.
81. Tojo, G.; Fernandez, M. I., *Oxidation of Primary Alcohols to Carboxylic Acids: A Guide to Current Common Practice*. Springer: 2007.
82. Chromium-based Reagents. In *Oxidation of Alcohols to Aldehydes and Ketones: A Guide to Current Common Practice*, Springer US: Boston, MA, 2006; pp 1-95.
83. Zhao, M.; Li, J.; Song, Z.; Desmond, R.; Tschäen, D. M.; Grabowski, E. J. J.; Reider, P. J., A novel chromium trioxide catalyzed oxidation of primary alcohols to the carboxylic acids. *Tetrahedron Letters* **1998**, *39* (30), 5323-5326.
84. Orlek, B. S.; Thompson, M.; Ward, R. W., Novel compounds. Google Patents: 1999.
85. Bogda, D.; ukasiewicz, M., Microwave-Assisted Oxidation of Alcohols Using Aqueous Hydrogen Peroxide. *Synlett* **2000**, *2000* (01), 143-145.
86. Li, J., Carboxylic Acid Derivatives Synthesis: Fischer-Speier Esterification. In *Name Reactions for Functional Group Transformations*, 2010; pp 458-461.
87. Borchardt, R.; Kerns, E.; Lipinski, C.; Thakker, D.; Wang, B., *Pharmaceutical Profiling in Drug Discovery for Lead Selection*. American Assoc. of Pharm. Scientists: 2005.
88. Kerns, E. H.; Di, L., Chapter 1 - Introduction. In *Drug-like Properties: Concepts, Structure Design and Methods*, Academic Press: San Diego, 2008; pp 3-5.
89. Bernan, V. S.; Greenstein, M.; Carter, G. T., Mining marine microorganisms as a source of new antimicrobials and antifungals. *Current Medicinal Chemistry: Anti-Infective Agents* **2004**, *3* (3), 181-195.
90. pH Values of the Human body. <http://www.phreshproducts.com/wp-content/gallery/charts/human-body-ph-wm.jpg> (accessed July 11).
91. Toure, O.; Dussap, C.-G.; Lebert, A., Comparison of Predicted pKa Values for Some Amino-Acids, Dipeptides and Tripeptides, Using COSMO-RS, ChemAxon and ACD/Labs Methods. *Oil Gas Sci. Technol. – Rev. IFP Energies nouvelles* **2013**, *68* (2), 281-297.

92. Delaney, J. S., ESOL: Estimating Aqueous Solubility Directly from Molecular Structure. *Journal of Chemical Information and Computer Sciences* **2004**, *44* (3), 1000-1005.
93. Lusci, A.; Pollastri, G.; Baldi, P., Deep Architectures and Deep Learning in Chemoinformatics: The Prediction of Aqueous Solubility for Drug-Like Molecules. *Journal of Chemical Information and Modeling* **2013**, *53* (7), 1563-1575.
94. Dave, R. A.; Morris, M. E., Novel high/low solubility classification methods for new molecular entities. *International journal of pharmaceutics* **2016**, *511* (1), 111-26.
95. Klamt, A.; Smith, B. J., Challenge of Drug Solubility Prediction. In *Molecular Drug Properties*, Wiley-VCH Verlag GmbH & Co. KGaA: 2008; pp 283-311.
96. Lea, T., Caco-2 Cell Line. In *The Impact of Food Bioactives on Health: in vitro and ex vivo models*, Verhoeckx, K.; Cotter, P.; López-Expósito, I.; Kleiveland, C.; Lea, T.; Mackie, A.; Requena, T.; Swiatecka, D.; Wichers, H., Eds. Springer International Publishing: Cham, 2015; pp 103-111.
97. Pires, D. E. V.; Blundell, T. L.; Ascher, D. B., pkCSM: Predicting Small-Molecule Pharmacokinetic and Toxicity Properties Using Graph-Based Signatures. *Journal of Medicinal Chemistry* **2015**, *58* (9), 4066-4072.
98. Kulkarni, A.; Han, Y.; Hopfinger, A. J., Predicting Caco-2 Cell Permeation Coefficients of Organic Molecules Using Membrane-Interaction QSAR Analysis. *Journal of Chemical Information and Computer Sciences* **2002**, *42* (2), 331-342.
99. Reynolds, D. P.; Lanevskij, K.; Japertas, P.; Didziapetris, R.; Petrauskas, A., Ionization-specific analysis of human intestinal absorption. *Journal of Pharmaceutical Sciences* **2009**, *98* (11), 4039-4054.
100. Hubatsch, I.; Ragnarsson, E. G. E.; Artursson, P., Determination of drug permeability and prediction of drug absorption in Caco-2 monolayers. *Nat. Protocols* **2007**, *2* (9), 2111-2119.
101. Sambuy, Y.; De Angelis, I.; Ranaldi, G.; Scarino, M. L.; Stamatii, A.; Zucco, F., The Caco-2 cell line as a model of the intestinal barrier: influence of cell and culture-related factors on Caco-2 cell functional characteristics. *Cell biology and toxicology* **2005**, *21* (1), 1-26.
102. Petrauskas, A.; Japertas, R.; Lanevskij, K. In *Modeling plasma protein binding and volume of distribution*.
103. Lipinski, C. A.; Lombardo, F.; Dominy, B. W.; Feeney, P. J., Experimental and computational approaches to estimate solubility and permeability in drug discovery and development settings. *Advanced drug delivery reviews* **2001**, *46* (1-3), 3-26.
104. Veber, D. F.; Johnson, S. R.; Cheng, H.-Y.; Smith, B. R.; Ward, K. W.; Kopple, K. D., Molecular Properties That Influence the Oral Bioavailability of Drug Candidates. *Journal of Medicinal Chemistry* **2002**, *45* (12), 2615-2623.
105. Muegge, I.; Heald, S. L.; Brittelli, D., Simple Selection Criteria for Drug-like Chemical Matter. *Journal of Medicinal Chemistry* **2001**, *44* (12), 1841-1846.
106. Egan, W. J.; Merz, K. M., Jr.; Baldwin, J. J., Prediction of drug absorption using multivariate statistics. *J Med Chem* **2000**, *43* (21), 3867-77.

A
P
P
E
N
D
I
X

7.1. Appendix 1: NMR spectra for compounds **8** and **14** – **26**.

NMR spectra (^1H and ^{13}C) of compound **8**.

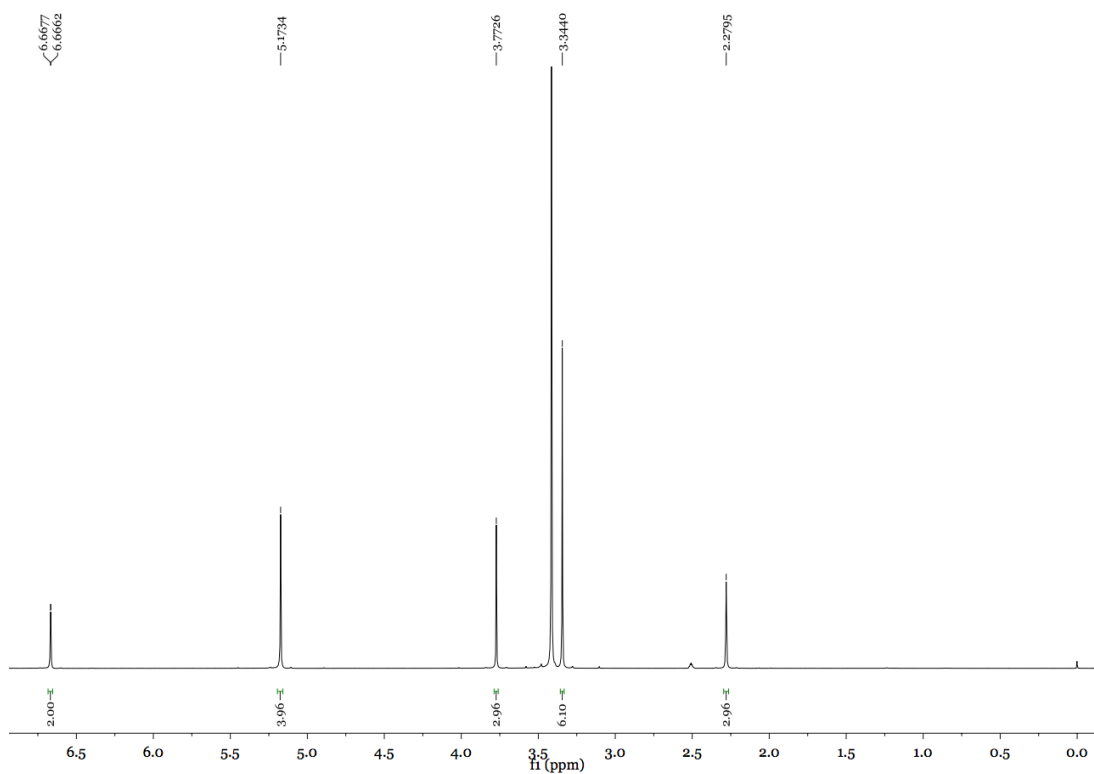


Figure 25: ^1H NMR of compound **8**.

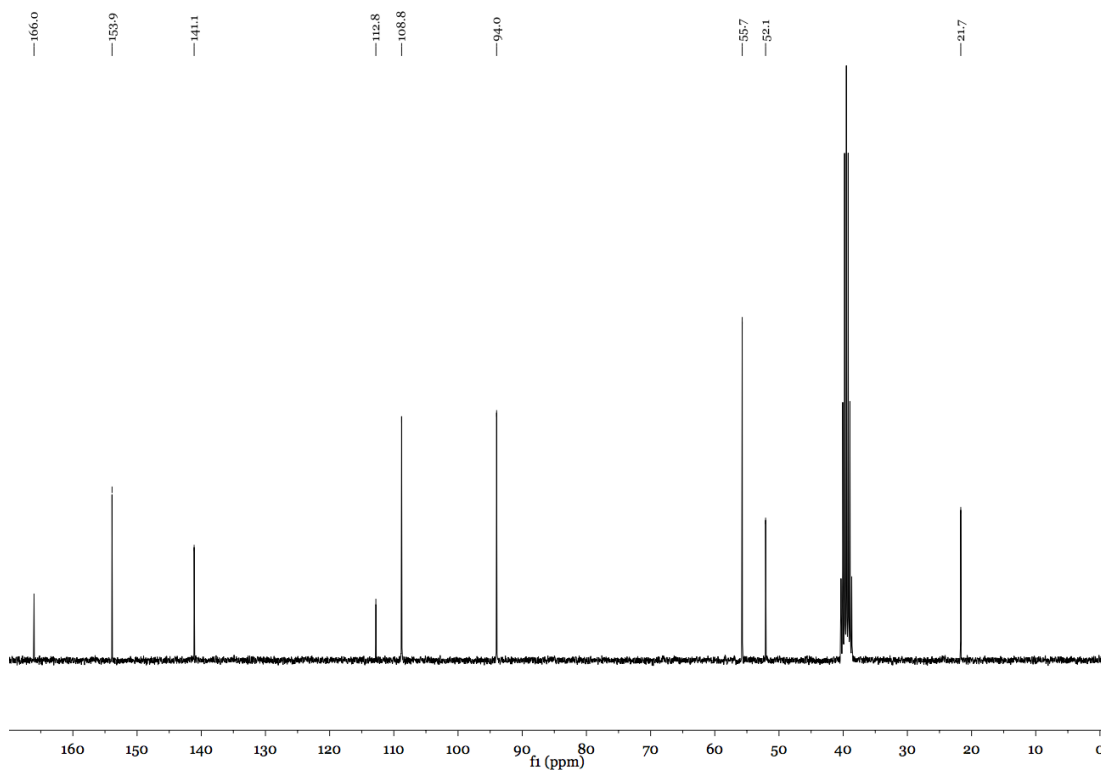


Figure 26: ^{13}C NMR of compound **8**.

NMR spectra (^1H and ^{13}C) of compound **14**.

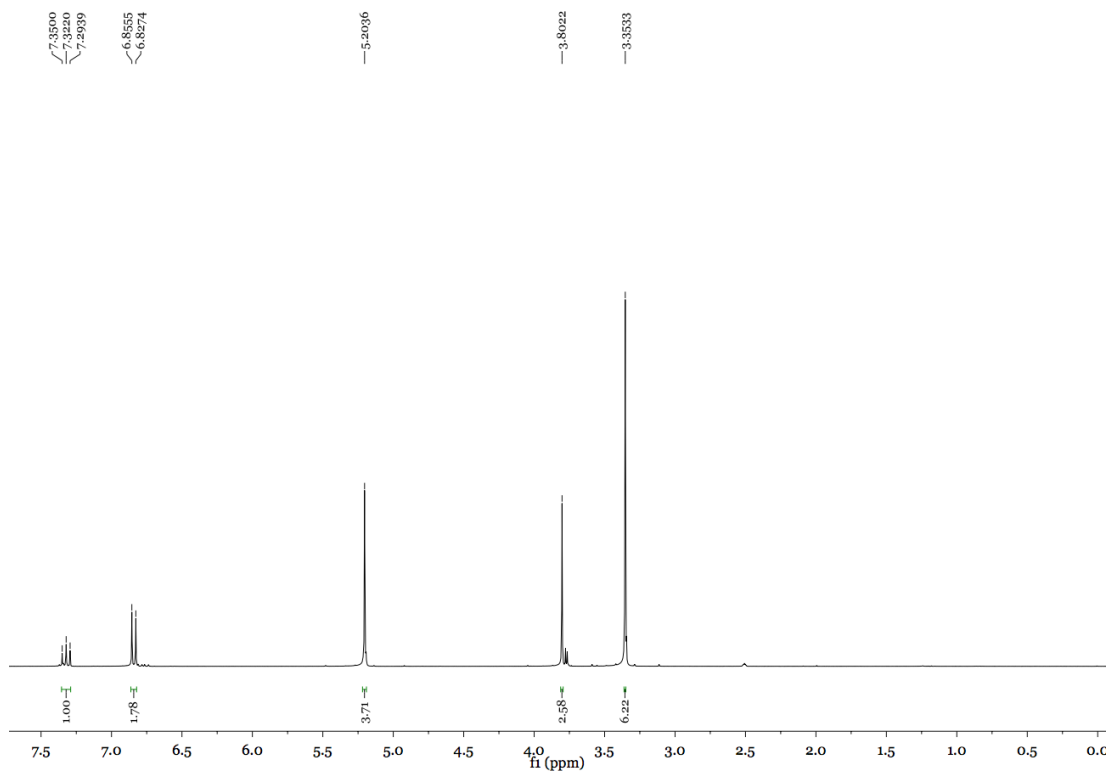


Figure 27: ^1H NMR of compound **14**.

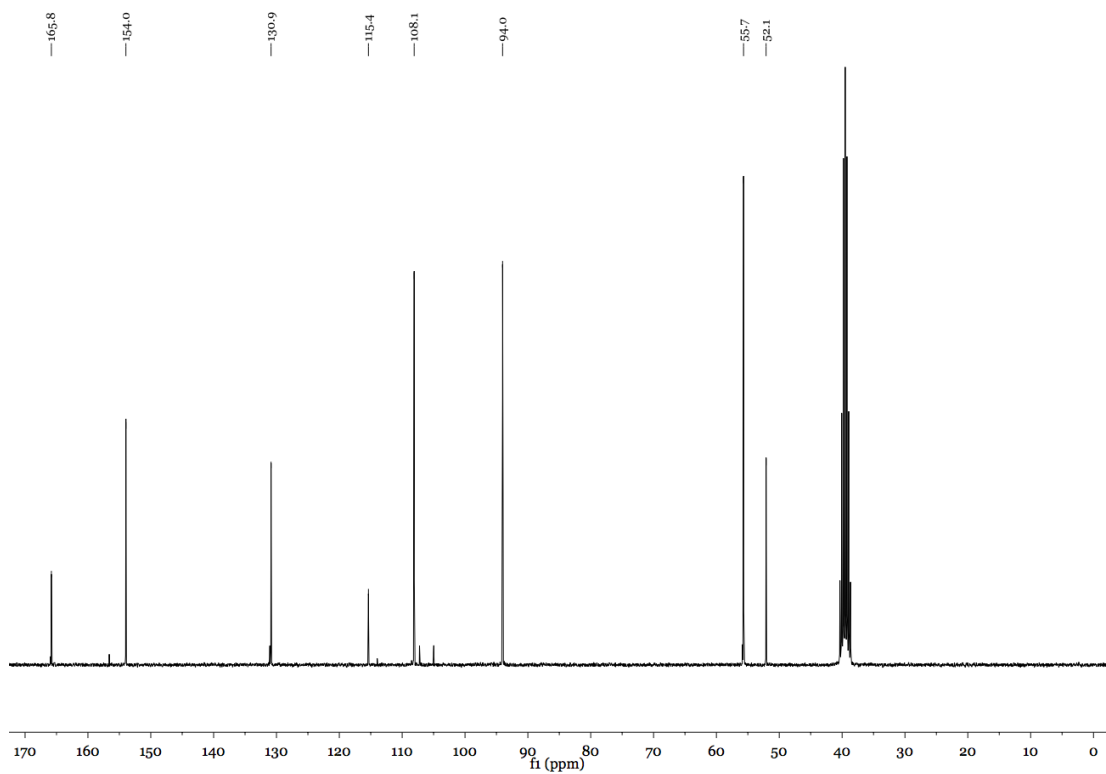


Figure 28: ^{13}C NMR of compound **14**.

NMR spectra (^1H and ^{13}C) of compound **15**.

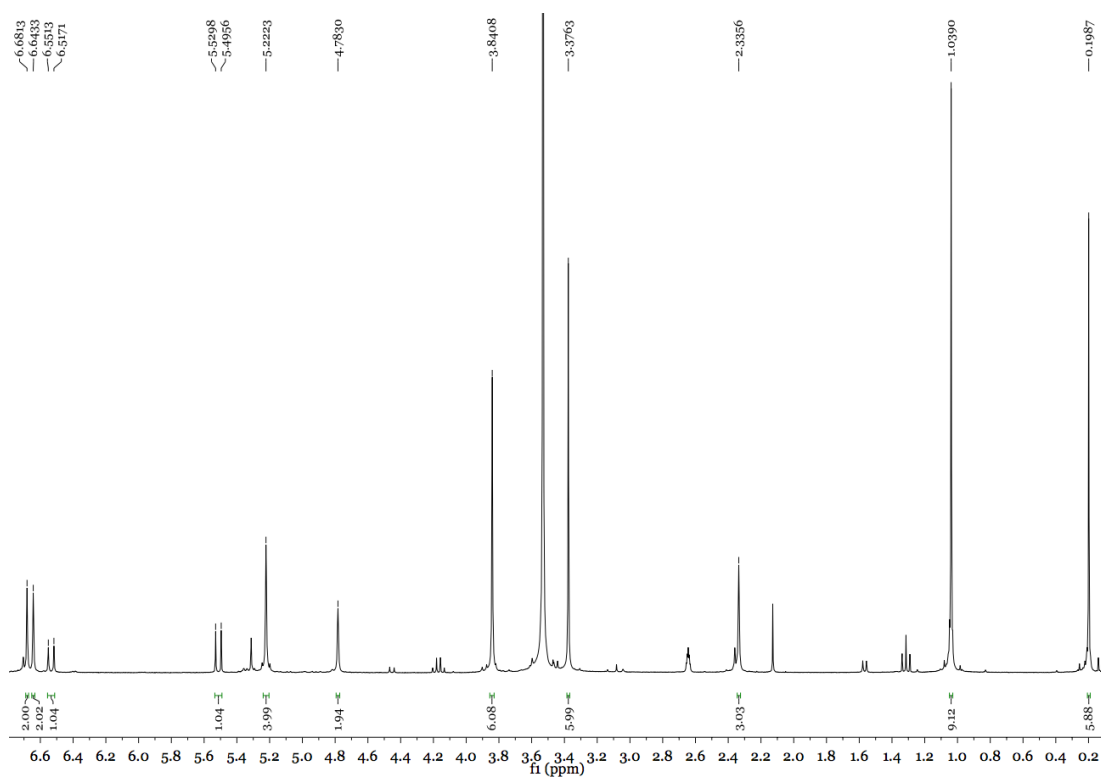


Figure 29: ^1H NMR of compound **15**.

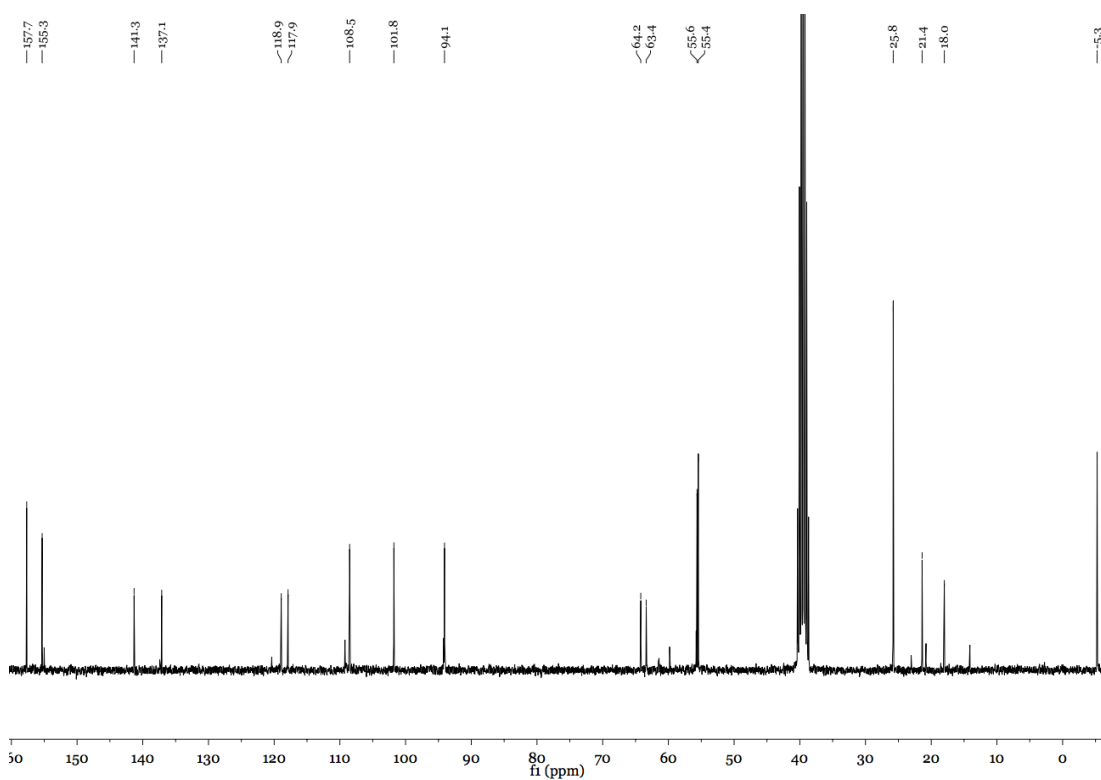


Figure 30: ^{13}C NMR of compound **15**.

NMR spectra (^1H and ^{13}C) of compound **16**.

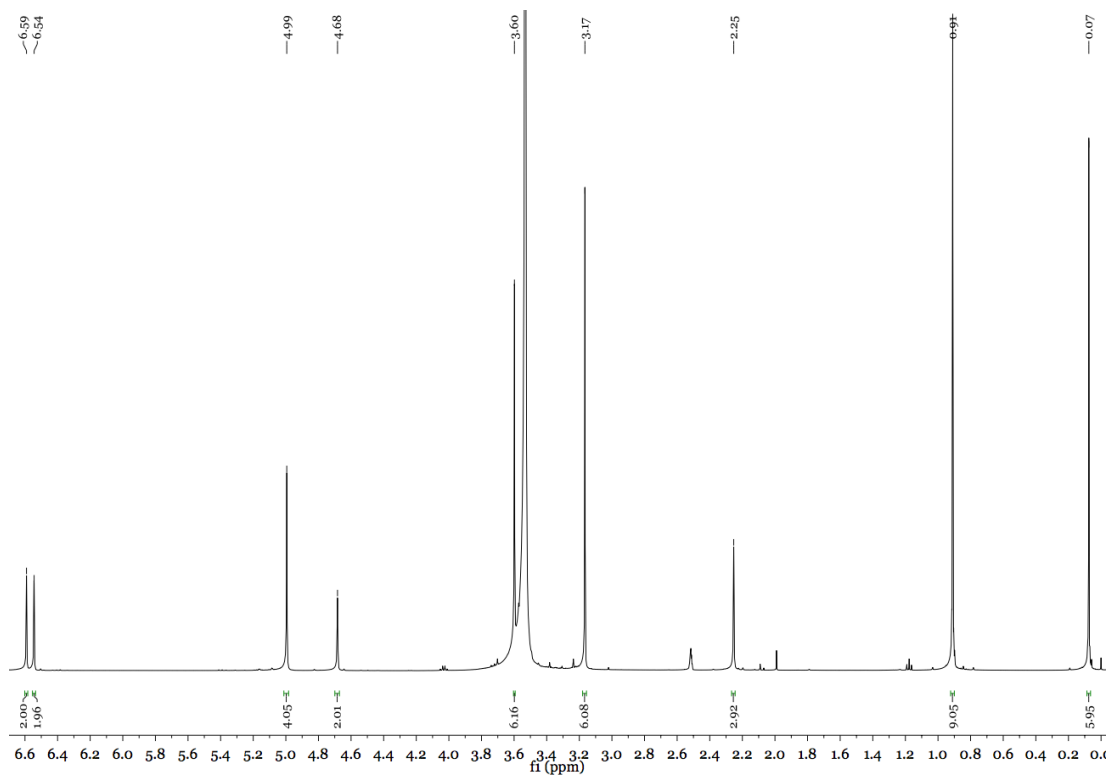


Figure 31: ^1H NMR of compound **16**.

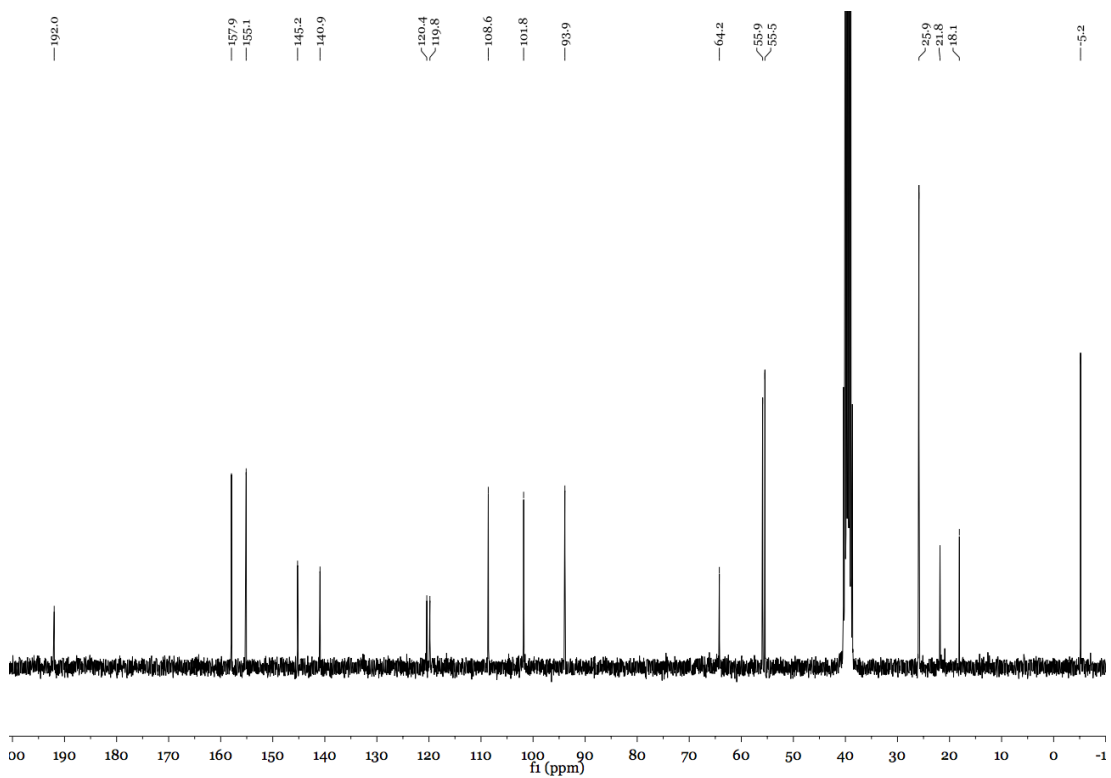


Figure 32: ^{13}C NMR of compound **16**.

NMR spectra (^1H and ^{13}C) of compound **17**.

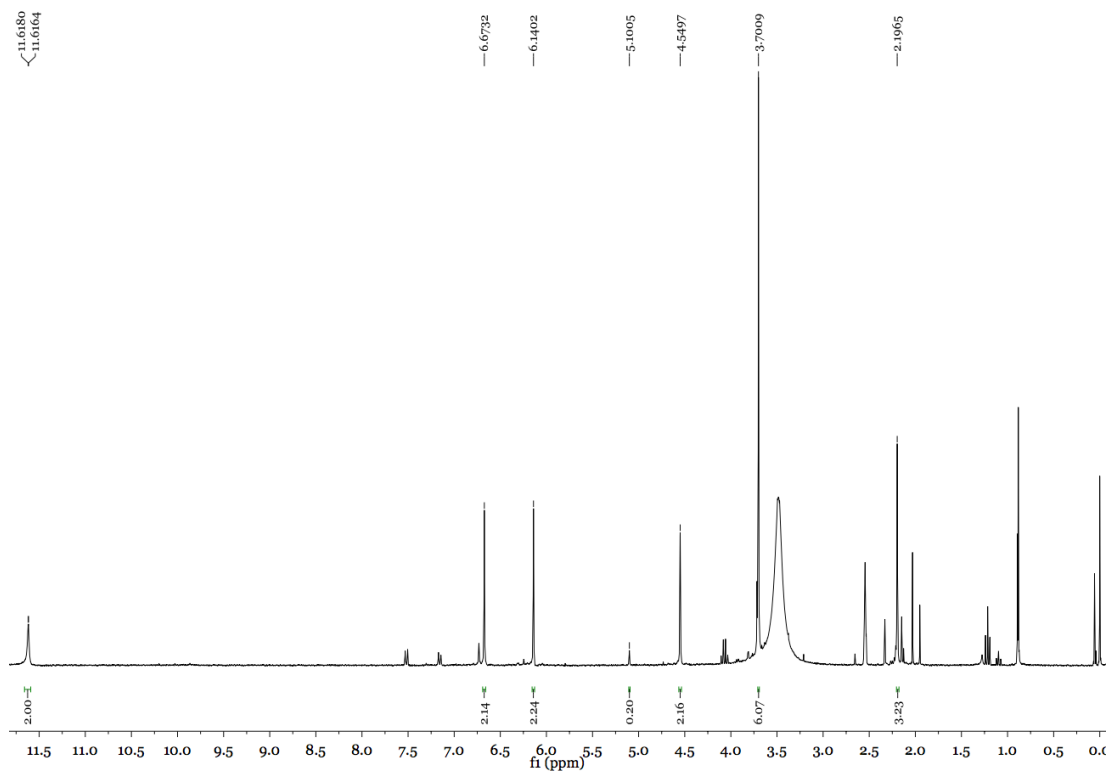


Figure 33: ^1H NMR of compound **17**.

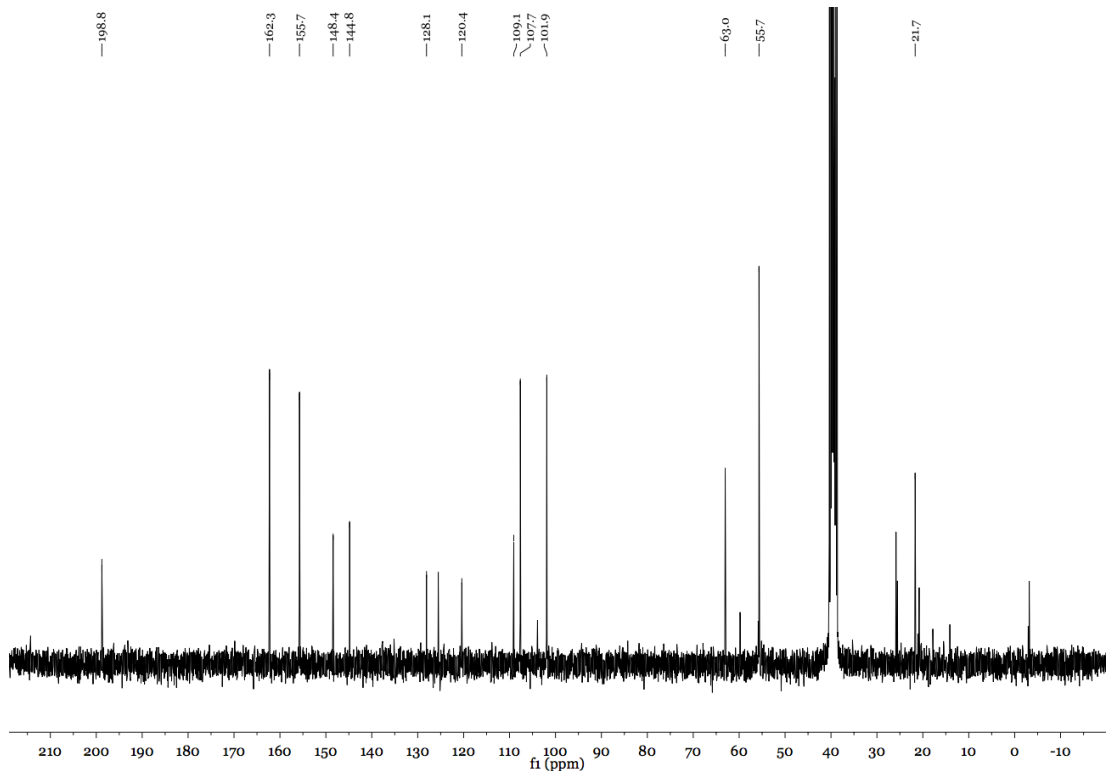


Figure 34: ^{13}C NMR of compound **17**.

NMR spectra (^1H and ^{13}C) of compound **18**.

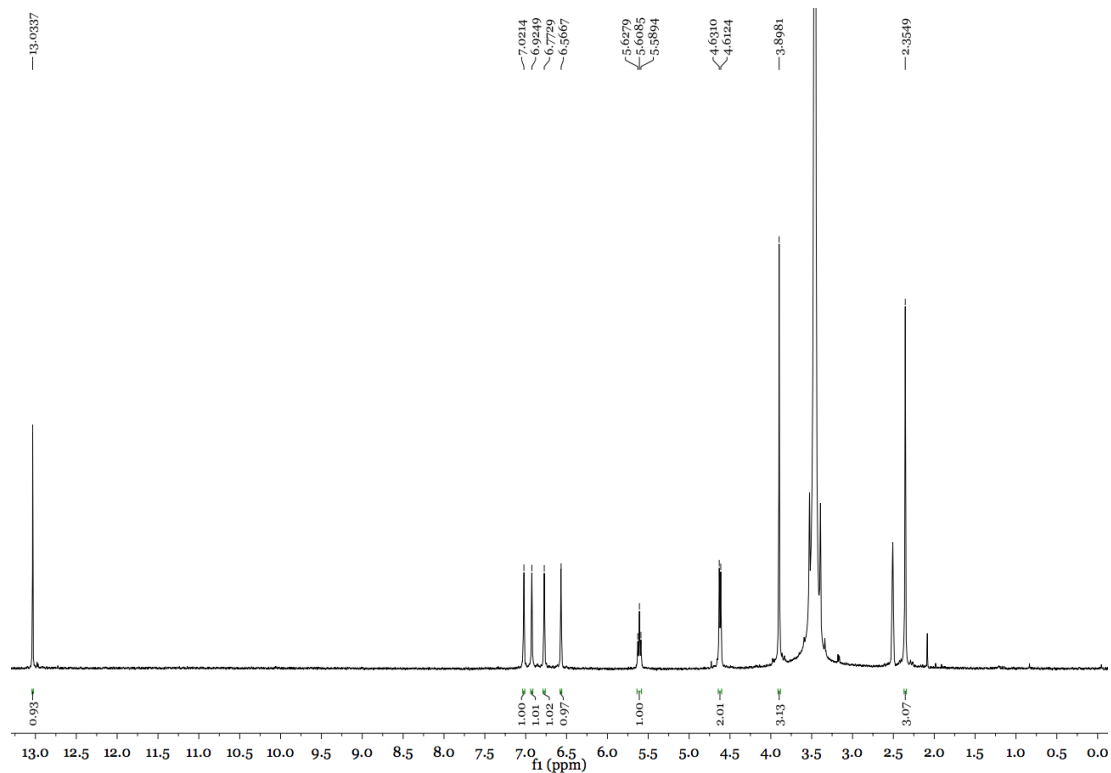


Figure 35: ^1H NMR of compound **18**.

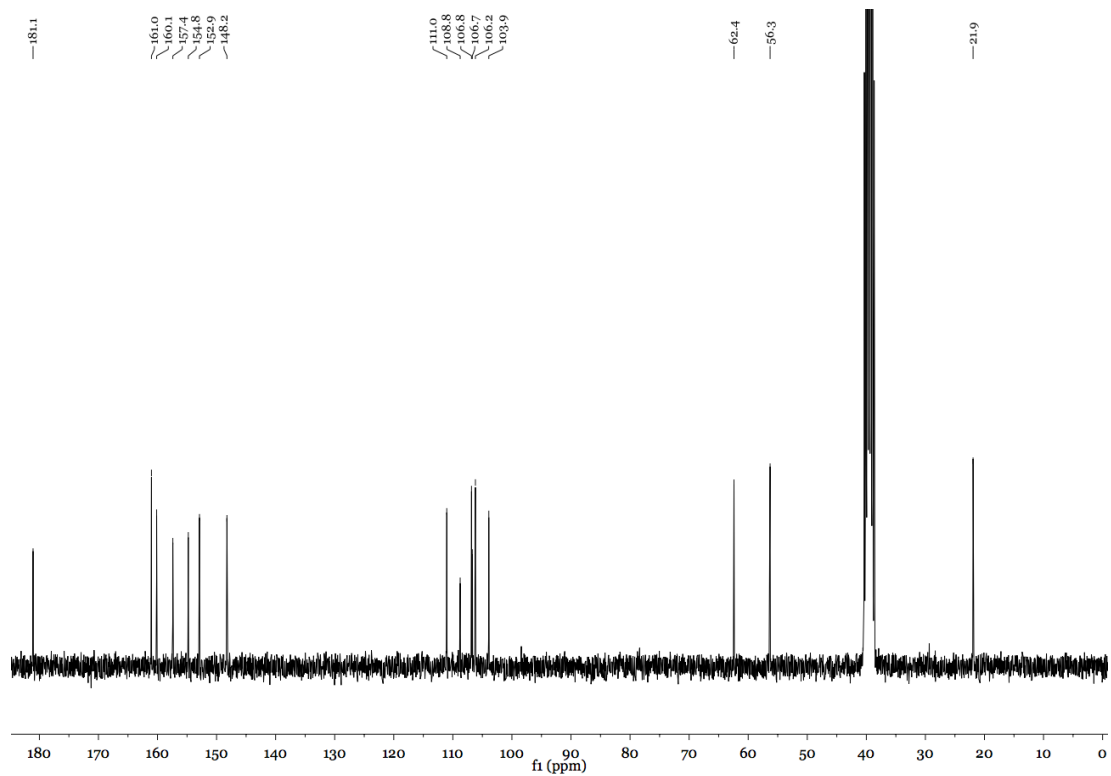


Figure 36: ^{13}C NMR of compound **18**.

NMR spectra (^1H and ^{13}C) of compound **19**.

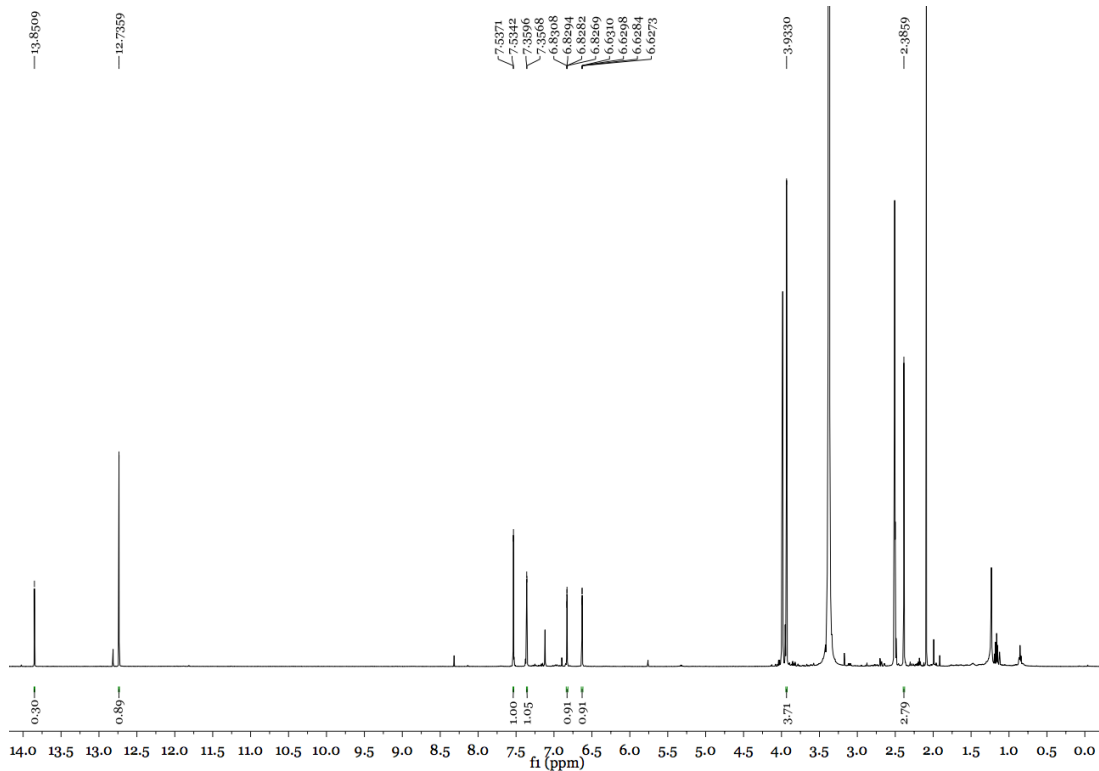


Figure 37: ^1H NMR of compound **19**.

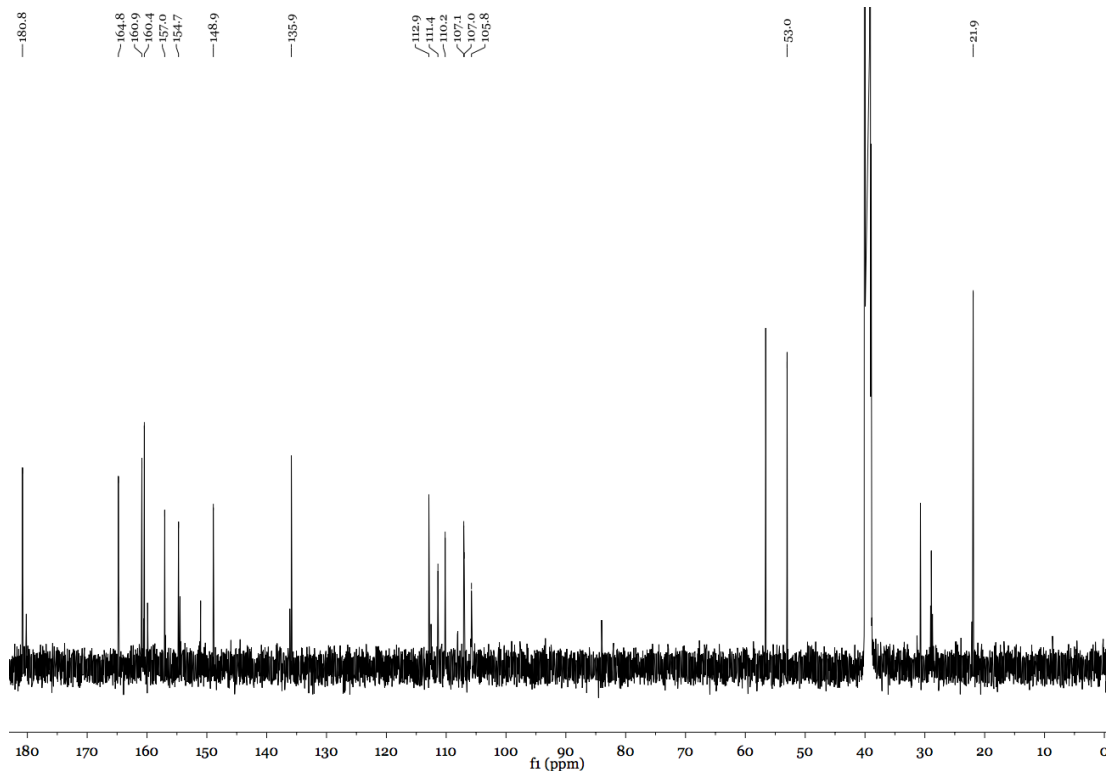


Figure 38: ^{13}C NMR of compound **19**.

NMR spectra (^1H and ^{13}C) of compound **20**.

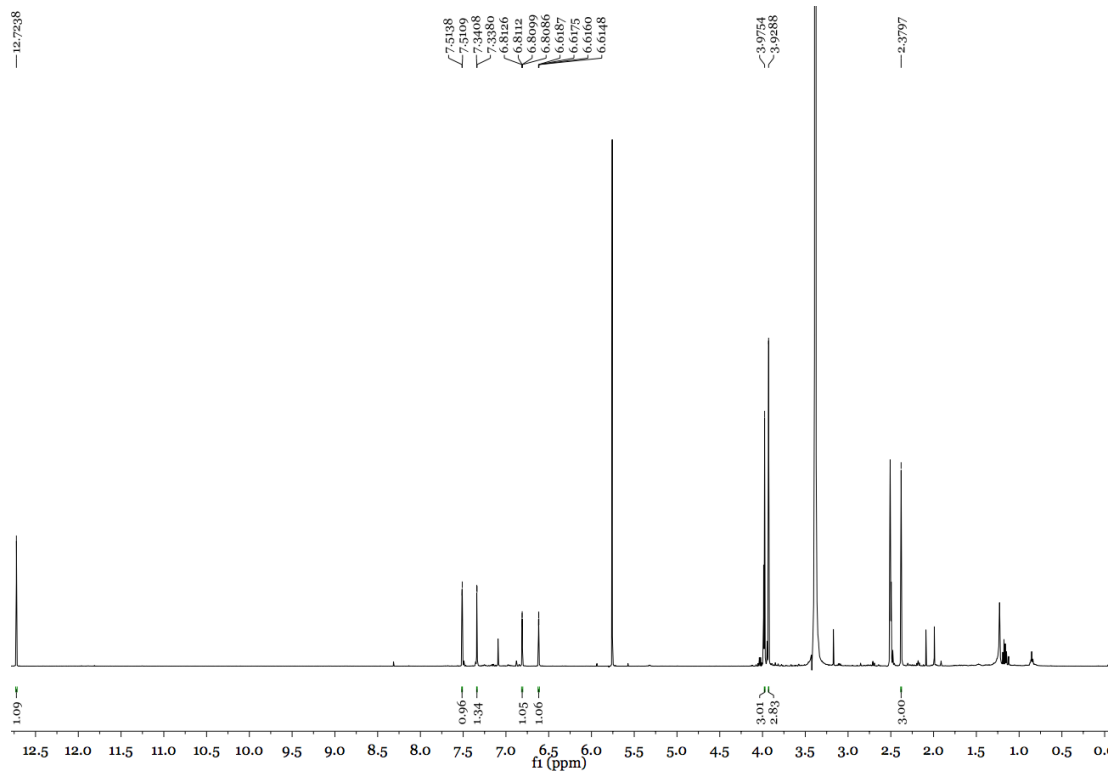


Figure 39: ^1H NMR of compound **20**.

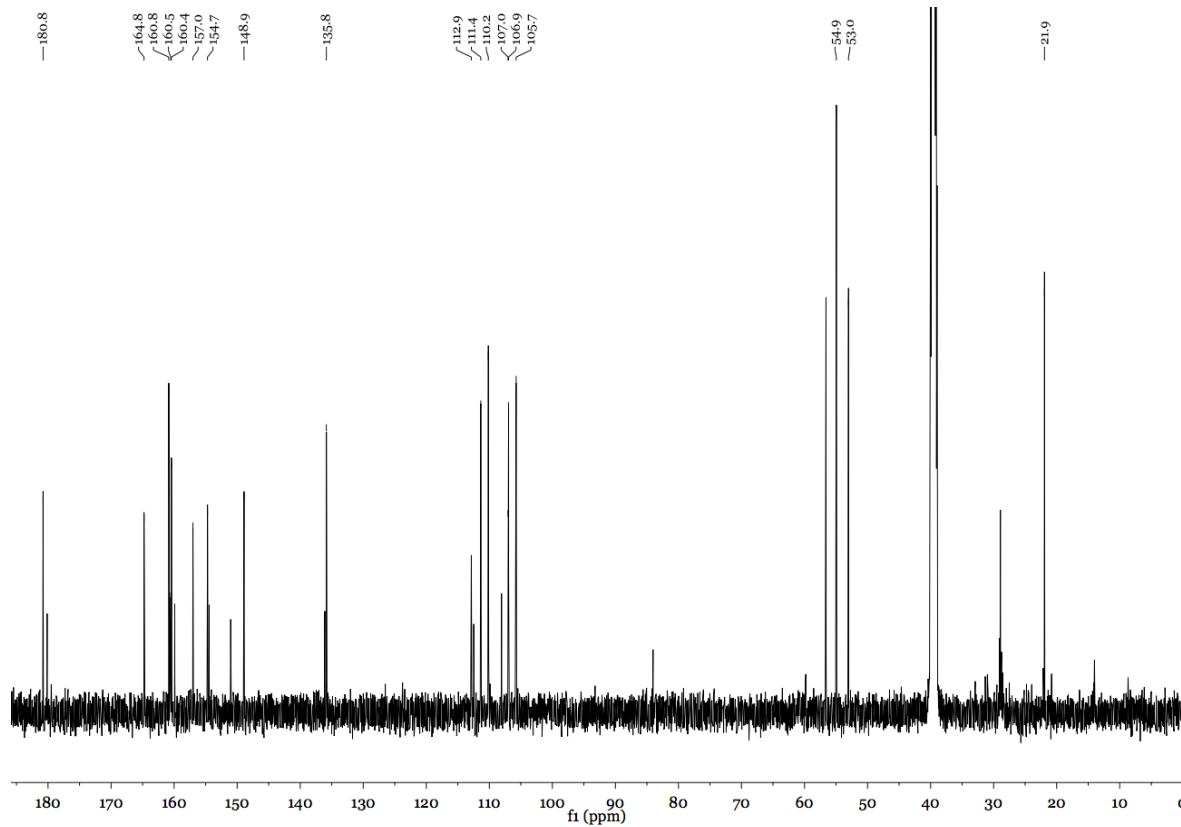


Figure 40: ^{13}C NMR of compound **20**.

NMR spectra (^1H and ^{13}C) of compound **21**.

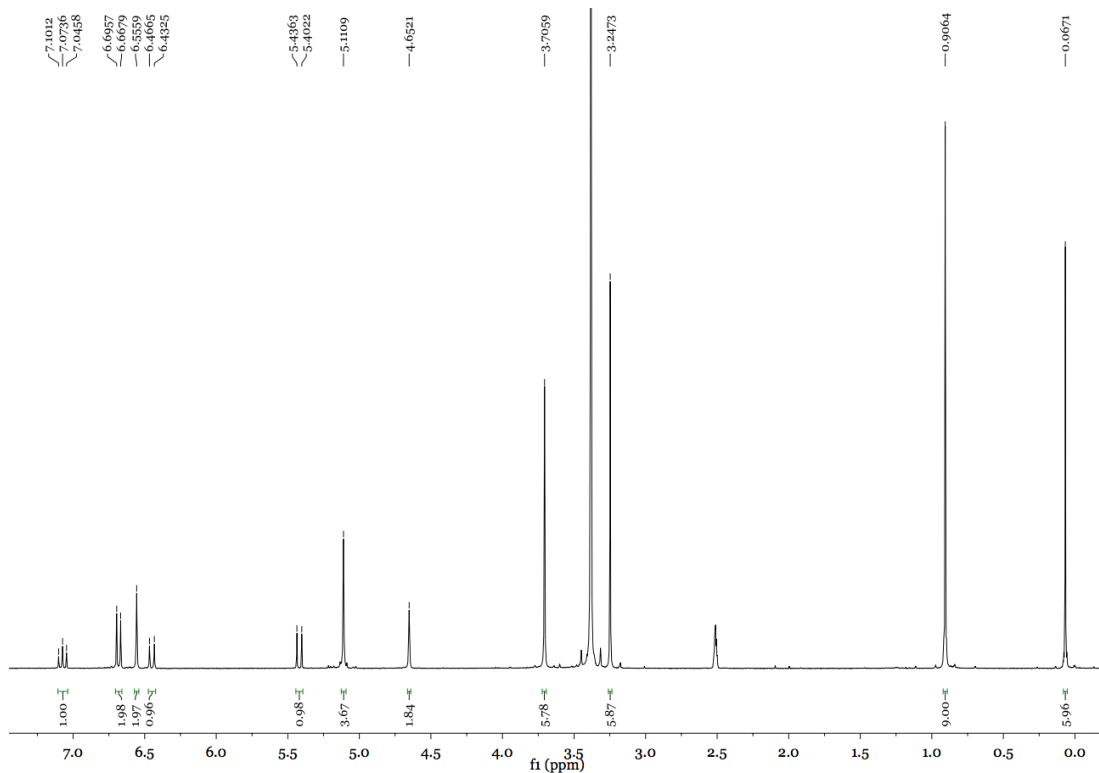


Figure 41: ^1H NMR of compound **21**.

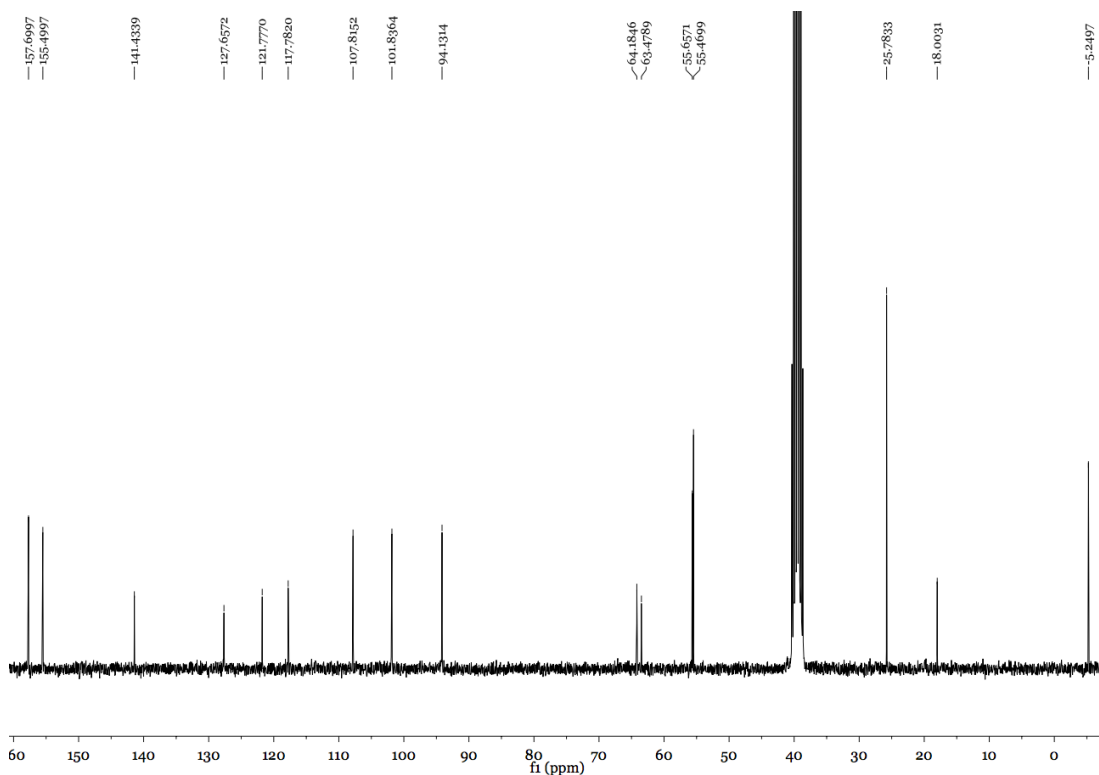


Figure 42: ^{13}C NMR of compound **21**.

NMR spectra (^1H and ^{13}C) of compound **22**.

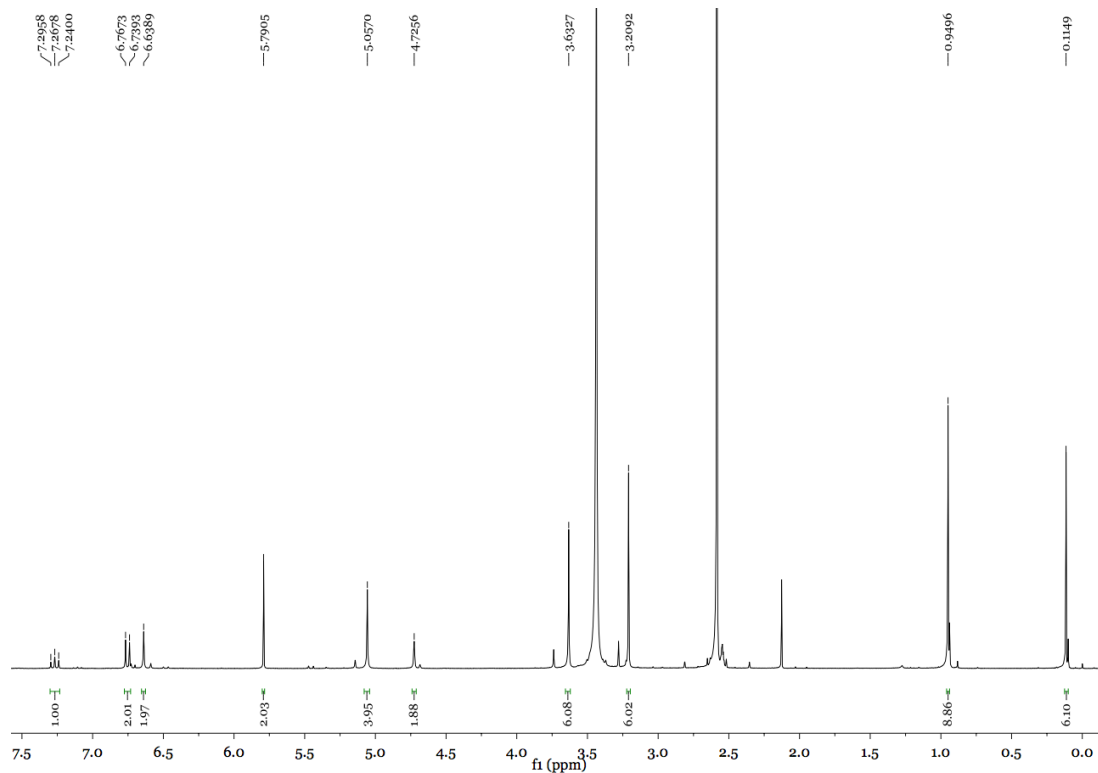


Figure 43: ^1H NMR of compound **22**.

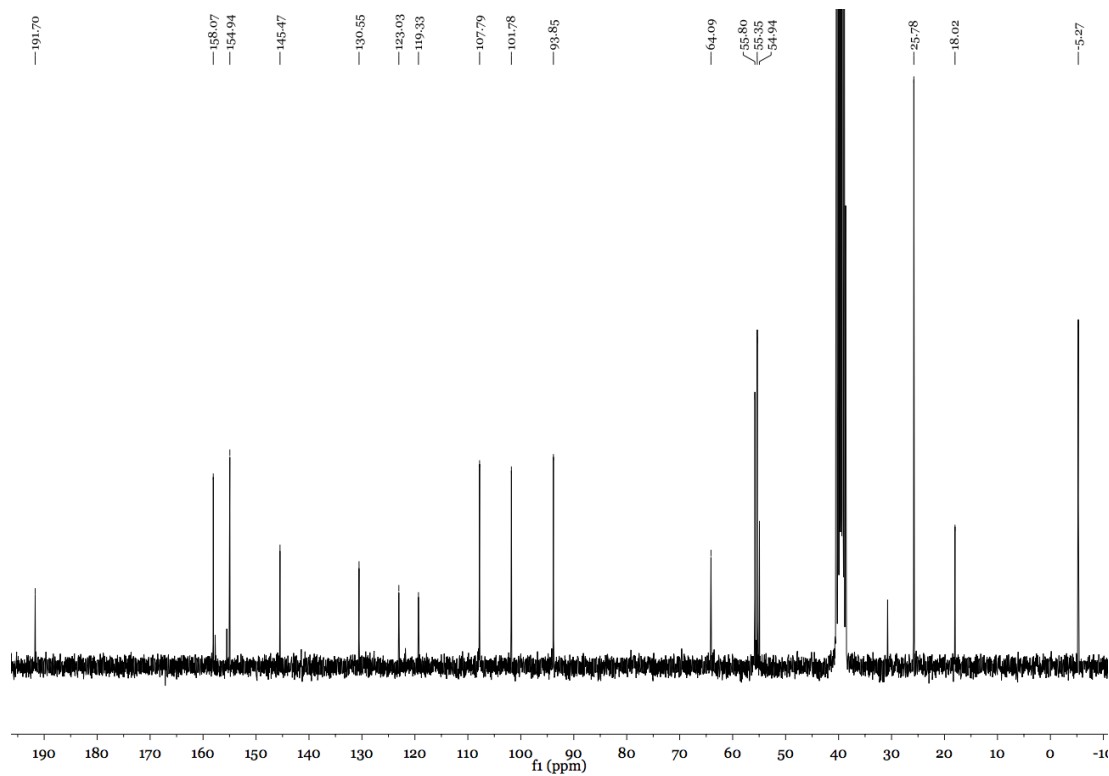


Figure 44: ^{13}C NMR of compound **22**.

NMR spectra (^1H and ^{13}C) of compound **23**.

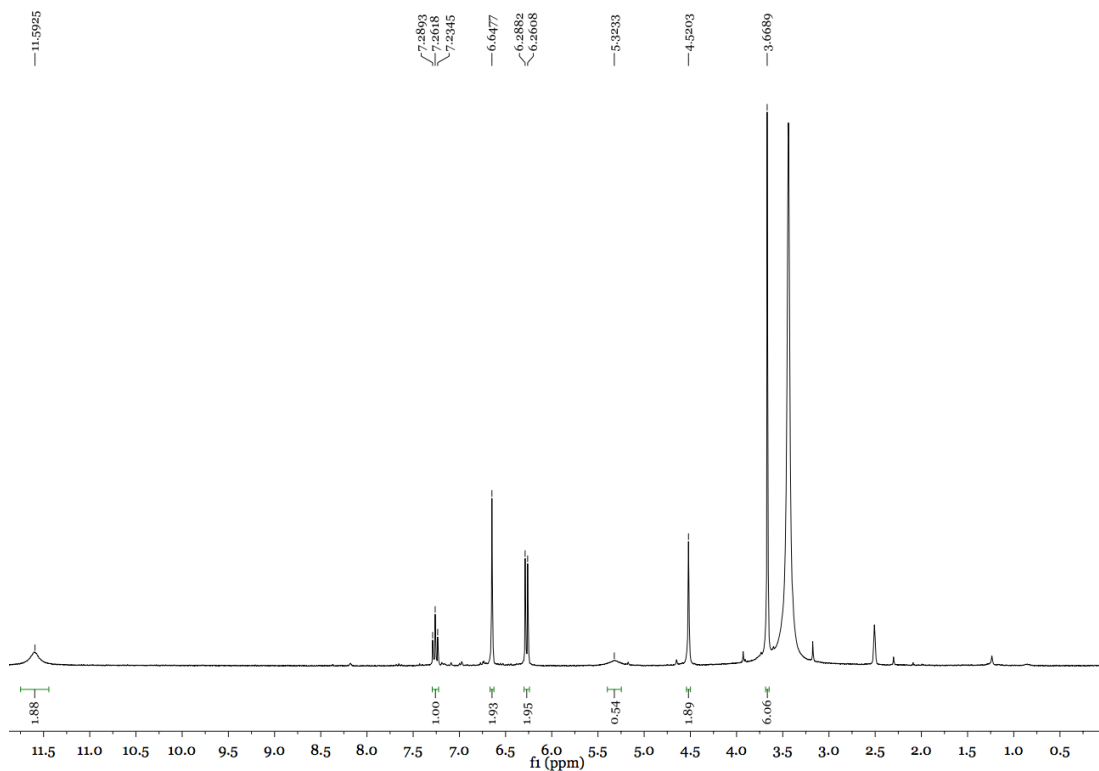


Figure 45: ^1H NMR of compound **23**.

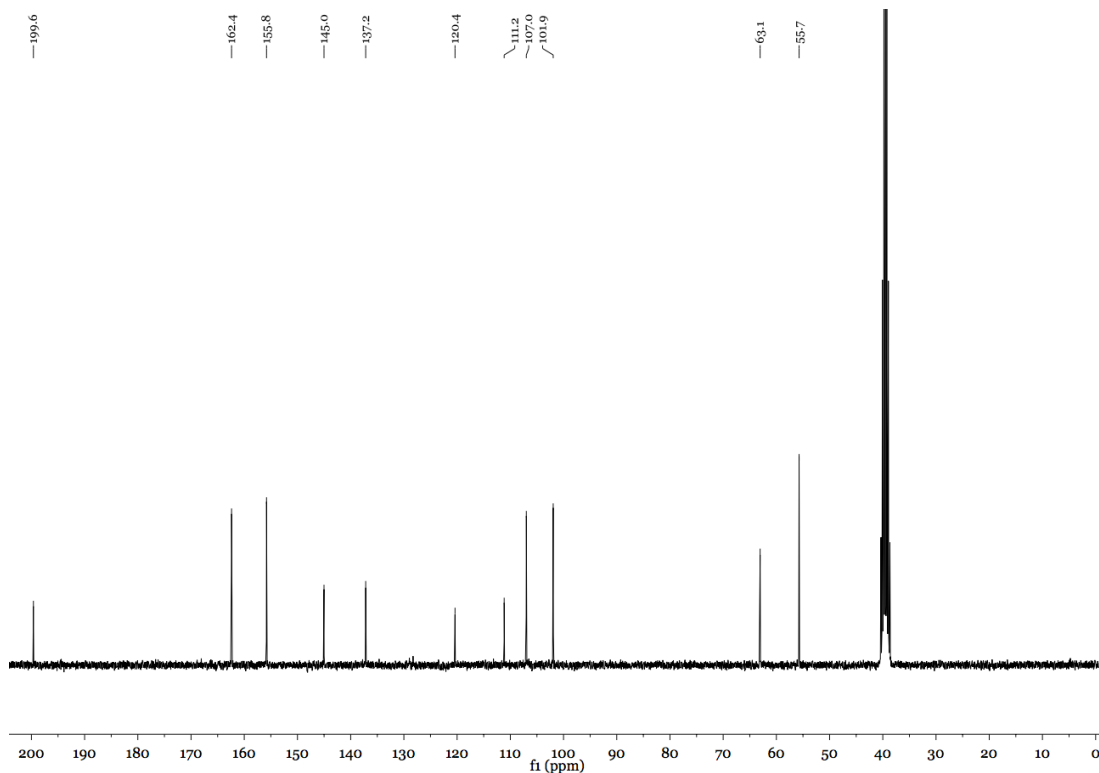


Figure 46: ^{13}C NMR of compound **23**.

NMR spectra (¹H and ¹³C) of compound **24**.

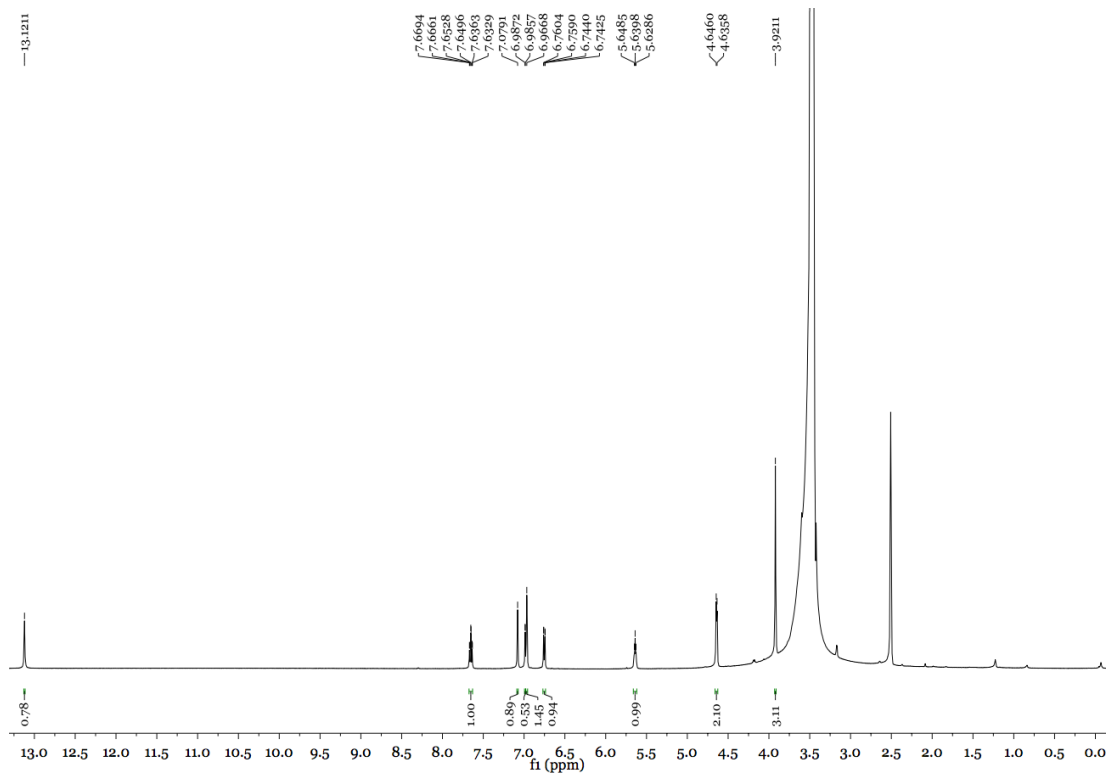


Figure 47: ¹H NMR of compound **24**.

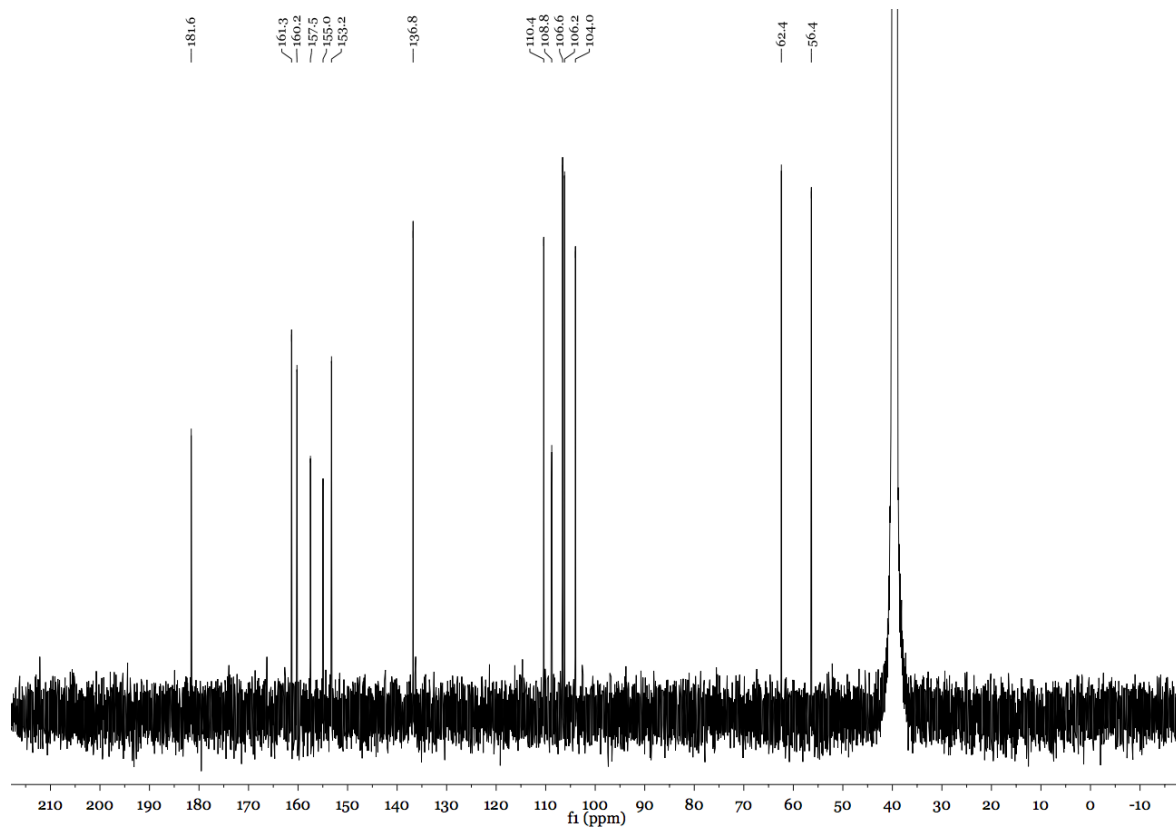


Figure 48: ¹³C NMR of compound **24**.

NMR spectra (^1H and ^{13}C) of compound **25**.

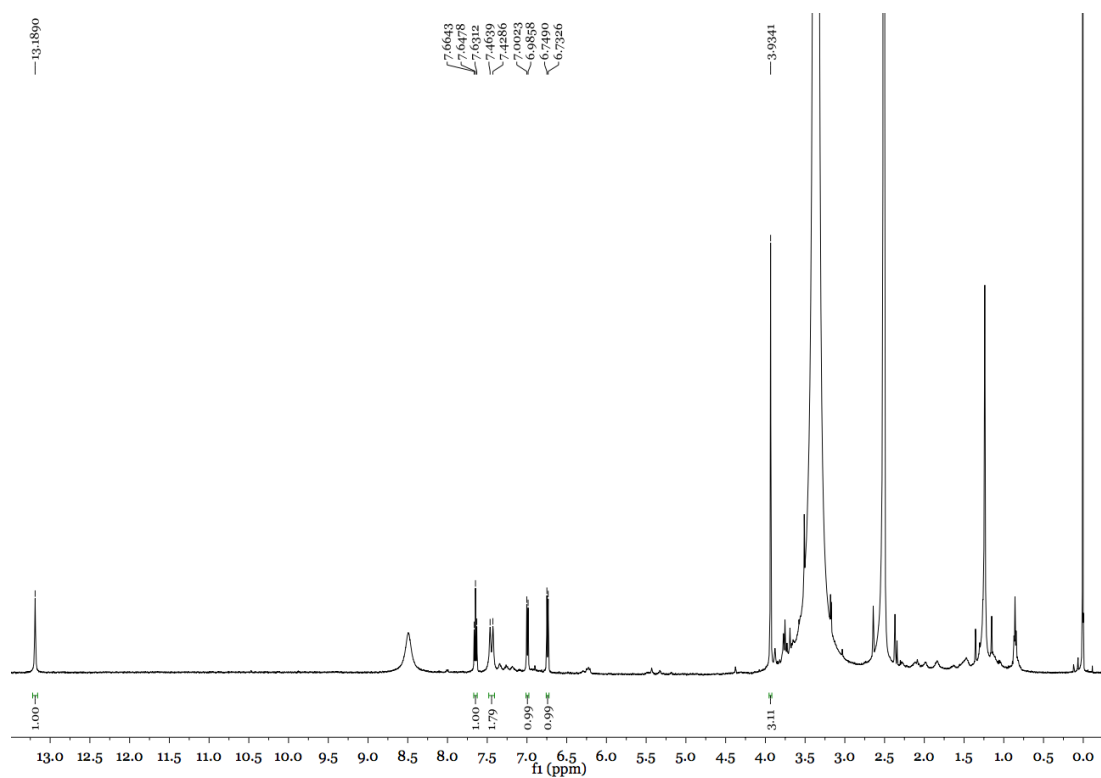


Figure 49: ^1H NMR of compound **25**.

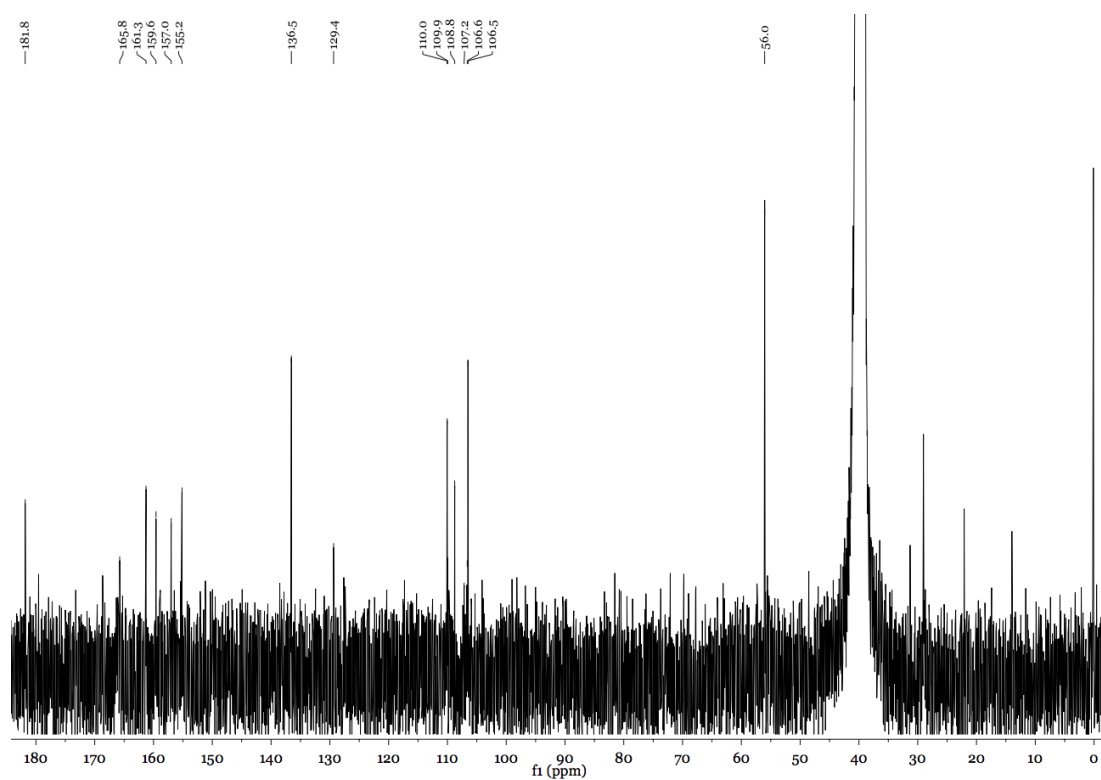


Figure 50: ^{13}C NMR of compound **25**.

NMR spectra (^1H and ^{13}C) of compound **26**.

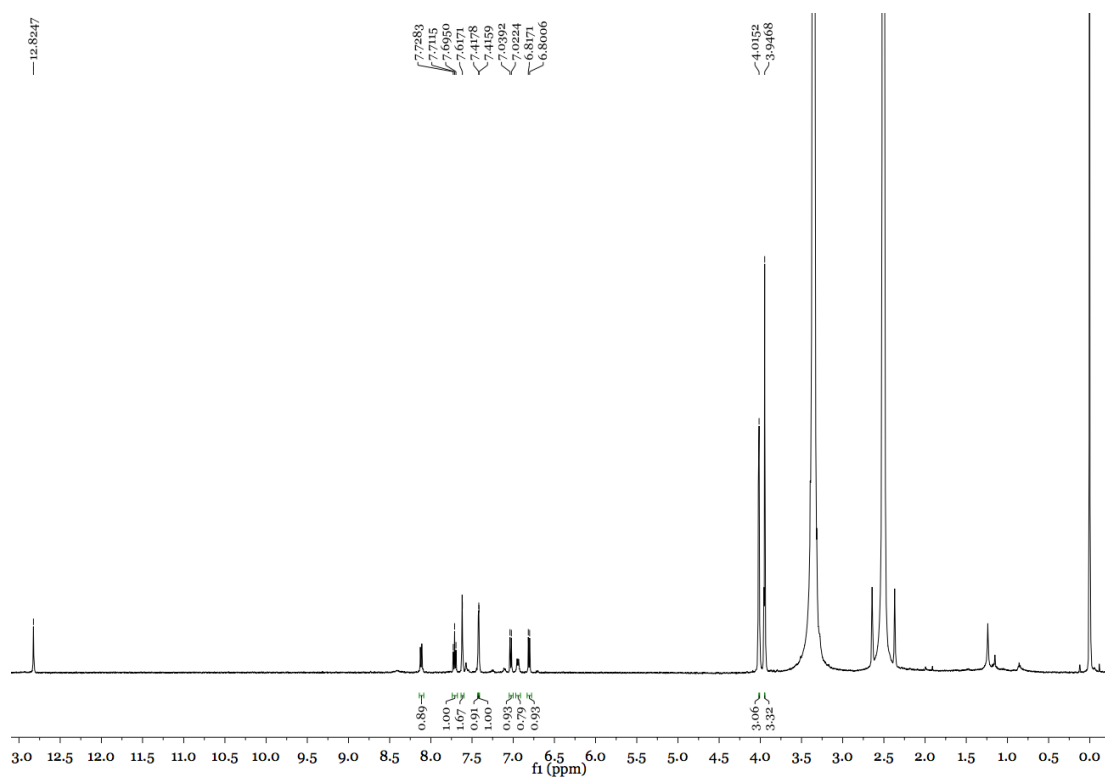


Figure 51: ^1H NMR of compound **26**.

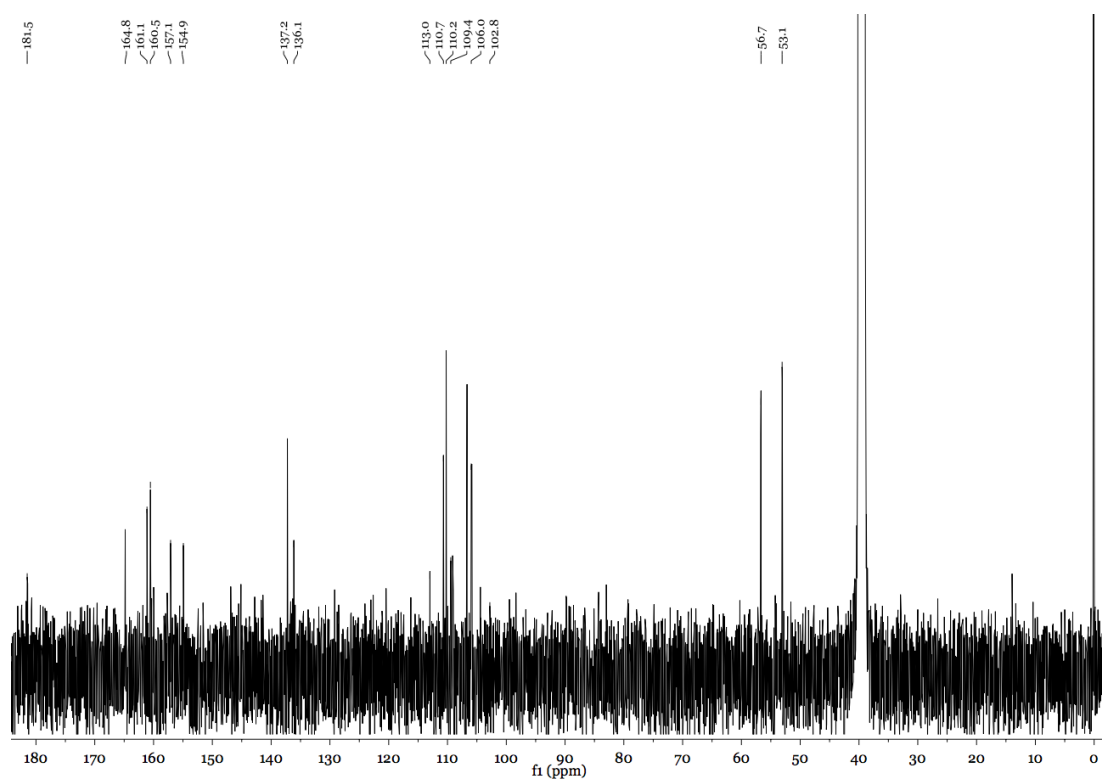
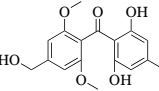
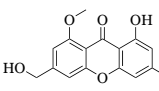
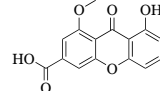
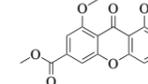
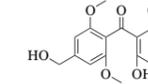
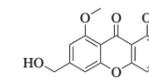
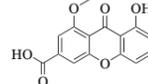
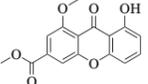


Figure 52: ^{13}C NMR of compound **26**.

Appendix 2: General table with *in silico* acquired biophysicochemical properties of the eight compounds of interest.

Table 1: Data obtained with the study of *in silico* biophysicochemical properties of the compounds of interest.

											
		17	18	19	20	23	24	25	26		
General properties	Molecular weight	318.32	282.28	300.27	314.29	304.30	272.26	286.24	300.27		
	Rotable bonds	5	2	2	3	5	2	2	3		
	H-bond donors	3	2	2	1	3	2	2	1		
	H-bond acceptors	6	5	6	6	6	5	6	6		
Lipophilicity	tPSA	96.22	75.99	93.06	82.06	96.22	75.99	95.06	82.06		
	Log P	MarvinSketch	3.13	2.40	2.75	3.38	2.66	1.93	2.28	2.91	
		PreADMET	2.54	2.54	2.96	2.99	1.97	1.98	2.40	2.43	
		WLogP	1.99	2.31	2.67	2.76	1.69	2.00	2.36	2.45	
		XLogP ₃	2.53	2.61	3.02	3.35	2.16	2.24	2.66	2.98	
		Broto's	1.76	2.23	2.33	2.80	1.35	1.81	1.92	2.39	
		EPI Suite	3.53	3.85	4.65	4.60	2.98	3.30	4.10	4.06	
		Molinspiration	2.98	3.00	3.58	3.83	2.58	2.60	3.17	3.43	
		Crippen's	2.12	2.14	2.27	2.54	1.64	1.66	1.79	2.05	
		Viswanadhan's	2.13	2.05	2.28	2.31	1.66	1.58	1.81	1.84	
		CLogP	2.42	2.59	3.92	4.29	1.92	2.56	3.42	3.79	
		Silicos-IT LogP	2.90	3.35	2.90	3.43	2.38	2.85	2.39	2.92	
		AB/LogP	3.08	3.15	3.48	3.69	2.59	2.65	2.89	3.26	
		ACDLogP	2.88	1.85	3.17	3.23	2.42	1.39	2.71	2.77	
	MLogP	0.78	0.81	1.00	1.24	0.54	0.56	0.75	1.00		
	iLogP	2.25	2.55	2.28	2.41	2.03	2.46	1.42	2.78		
	Log D	MarvinSketch	pH 1.5	3.13	2.40	2.74	3.38	2.66	1.93	2.27	2.91
			pH 5.0	3.12	2.40	1.07	3.38	2.65	1.93	0.6	2.91
			pH 6.5	3.01	2.39	-0.32	3.37	2.52	1.92	-0.78	2.91
PreADMET		pH 7.4	2.57	2.39	-0.82	3.34	2.02	1.88	-1.30	2.87	
		pH 7.4	2.54	2.54	1.71	2.99	1.97	1.98	1.15	2.43	
		pH 1.5	3.08	3.14	3.45	3.68	2.59	2.64	2.86	3.25	
ACDLabs		pH 5.0	3.08	3.15	1.83	3.69	2.59	2.65	1.24	3.26	
		pH 6.5	3.08	3.15	0.38	3.69	2.59	2.65	-0.20	3.26	
		pH 7.4	3.08	3.15	-0.29	3.69	2.58	2.65	-0.88	3.26	
Solubility	Log S	ACDLabs (A/B)	-2.95	-4.19	-4.69	-4.98	-2.97	-3.99	-4.48	-4.90	
		EPI Suite	-3.45	-4.60	-5.89	-5.95	-2.88	-4.03	-5.32	-5.38	
		SILICOS-IT	-4.17	-5.05	-4.59	-5.29	-3.79	-4.67	-4.21	-4.91	
		ChemDraw	-3.64	-3.22	-3.73	-3.85	-3.27	-2.85	-3.36	-3.49	
		PreADMET	Pure Water	-3.90	-4.60	-4.74	-5.08	-3.40	-4.10	-4.23	-4.57
			Buffer	-3.33	-3.98	-3.31	-4.41	-2.71	-3.37	-2.70	-3.79
		MarvinSketch	-2.96	-3.62	-4.18	-4.36	-2.47	-3.12	-3.67	-3.86	
		Ali	-4.20	-3.94	-4.72	-4.83	-3.81	-3.55	-4.35	-4.45	
		ESOL	-3.46	-3.62	-3.94	-4.15	-3.16	-3.33	-3.65	-3.85	
		pkCSM	-3.28	-2.95	-3.14	-3.59	-3.00	-3.21	-2.79	-3.18	
		AquaSol	-2.82	-2.78	-2.87	-3.15	-2.57	-2.50	-2.64	-2.90	
pKa	MarvinSketch	7.013	8.483	3.324	8.476	6.911	8.380	3.324	8.374		
	ACDLabs	9.40	11.40	3.40	11.40	9.40	11.40	3.40	11.40		
Perm.	P_{app}	pkCSM	2.40	11.75	2.82	12.30	2.09	11.48	2.45	12.02	
		PreADMET	1.486	0.892	0.841	1.098	1.471	0.330	0.234	0.629	
PPB	P_e	ACDLabs	7.79	8.31	4.07	8.17	7.69	8.40	2.26	8.34	
		PreADMET	84.2	90.7	93.4	92.6	81.1	87.3	90.6	90.3	
		ACDLabs	89.4	87.7	97.7	97.7	86.3	90.2	97.3	97.0	
	LogKa HSA	4.8	5.28	5.48	5.48	4.77	5.23	5.43	5.37		